Blended Drought Indices for Agricultural Drought Risk Assessment on the Canadian Prairies

By

Liu Sun

A thesis submitted to the Faculty of Graduate Studies and Research

In partial fulfillment of the requirements for the degree of

Master of Science

Department of Geography and Environmental Studies
Carleton University
Ottawa, Ontario
July, 2009

Your file Votre référence
ISBN: 978-0-494-60193-8
Our file Notre référence
ISBN: 978-0-494-60193-8

ABSTRACT

The development of new tools that provide timely agricultural drought risk assessment is essential for improving drought preparedness and response. This thesis developed an operational model framework to assess real-time agricultural drought risk on the Canadian prairies, as related to spring wheat crop yield. The agricultural drought risk assessment (ADRA) model integrates multiple drought indices including the Standardized Precipitation Index, the Palmer Drought Severity Index and the Palmer Moisture Anomaly Index. Drought risk is assessed at the beginning of each month before and during the growing season using principal component analysis and multiple regression analysis. The performance of the model was validated by cross-validation. The results showed that drought risk can be detected at pre-planting; the assessment accuracy improves as the crop develops, and the most accurate assessment can be achieved at the beginning of August (average $R^2 = 0.61$). The model performed best in regions that have a more southerly location, a low and highly variable growing season precipitation regime. The risk-assessment maps for the three representative years (i.e. two drought years and one non-drought year) provided a better visualization of the assessment results and illustrated the utility of the ADRA model. The framework developed in this study can be applied to other crops and regions, supporting decision making at the farm level.

ACKNOWLEDGEMENTS

This study would not have been possible without the help and support of many people. I would like to thank my supervisor, Scott Mitchell, who provided an excellent learning opportunity and guided me throughout this study. Great thanks to my co-supervisor, Andrew Davidson, for his valuable advice and support in this study, and for providing a wide range of research opportunities. He also provided the climate gridded dataset and technical help with data processing. Their help and encouragement meant more to me than they could ever know and were greatly appreciated.

I am also grateful to the contributions of other people: Richard Warren provided the source code of the computer program to generate drought indices and helped me modify the program for my study. Frédéric Bédard provided the spring wheat yield data, Census Agricultural Region boundary data and clarified related issues. Many thanks to Andrew Bootsma, Zhirong Yang, Nathaniel Newlands, Allan Howard, Aston Chipanshi, Xiaoyuan Geng, Daniel McKenney, Michael Hutchinson, Jesslyn Brown, Anne Steinemann, Richard Heim, Mark Svoboda and Elham Rahmani, for their help in sharing ideas/materials and giving me valuable advice at various stages during this process. Also, thank you Budong Qian for giving excellent advice as an external examiner.

I acknowledge the financial support for this study provided by Government Related Initiatives Program (GRIP) – "Integrating remote sensing data into selected models to enhance operational decision support for crops, drought and agricultural water management" of Agriculture and Agri-Food Canada, and the Department of Geography and the Environmental Studies of Carleton University.

Special thanks to my parents, for their love and encouragement. Finally, I would like to thank my husband, Haining Yang, for his love and support throughout this journey.

TABLE OF CONTENTS

LIST OF TABLES

LIST OF FIGURES

LIST OF APPENDICES

LIST OF ABBREVIATIONS

AAFC	Agriculture and Agri-Food Canada
ADRA	Agricultural drought risk assessment
AI	Aggregation-Interpolation
AWHC	Available water holding capacity
CanSIS	Canadian Soil Information System
CAR	Census Agricultural Region
CMI	Crop Moisture Index
CSDI	Crop-specific Drought Index
CV	Coefficient of variation
ECDF	Empirical cumulative distribution function
ESS	Error sum of squares
ET	Evapotranspiration
GCV	Generalized cross validation
IA	Interpolation-Aggregation
MBE	Mean bias error
MSC	Meteorological Service of Canada
NAIS	National Agroclimate Information Service
NDMC	National Drought Mitigation Center
OBDI	Objective Blend of Drought Indicator
PASG	Percent average seasonal greenness
PC	Principal component
PCA	Principal component analysis
PDSI	Palmer Drought Severity Index
PET	Potential evapotranspiration
PHDI	Palmer Hydrologic Drought Index
R^2	Coefficient of determination

RCS	Reference climate station
RDI	Reclamation Drought Index
RMSE	Root mean square error
SLC	Soil Landscapes of Canada
SOSA	Start of season anomaly
SPI	Standardized Precipitation Index
SWSI	Surface Water Supply Index
Tmax	Maximum temperature
Tmin	Minimum temperature
TotPrec	Total precipitation
USDM	U.S. Drought Monitor
VegDRI	Vegetation Drought Response Index
VSMB	Versatile Soil Moisture Budget
Z-index	Palmer Moisture Anomaly Index

Chapter 1: Introduction

1.1 Statement of the Research Problem

Drought is a slow-onset phenomenon that occurs in virtually all climate regimes, but its characteristics and impacts vary significantly from one region to another (Wilhite, 1992). The less predictable characteristics of droughts include their initiation, termination, frequency and severity (Paulo and Pereira, 2007). The variability of these characteristics makes drought both a hazard and a disaster. Drought is a hazard because it is a natural event of unpredictable occurrence but of recognizable recurrence, and it is a disaster because it corresponds to the deficits of precipitation, causing the shortage of water supply to natural ecosystems and resulting in serious economic, environmental and social impacts (Pereira *et al.*, 2002; Moreira *et al.*, 2006).

Droughts are frequent on the Canadian prairies (hereafter referred to as the prairies). More than half of the years in three 20th century decades (1910-1919, 1930-1939, and 1980-1989) experienced drought (Nkemdirim and Weber, 1999) and the recent drought of 1999-2004 was the most severe on record in parts of the prairies (Bonsal and Wheaton, 2005). Drought has a major economic impact on the prairies owing to the vulnerability of the region's agricultural sector to weather variability (Kumar, 1999). Recent growing season droughts in the prairies during 2001 and 2002 resulted in an estimated $3.6 billion loss in agricultural production (Wheaton *et al.*, 2005).

Drought indices are commonly used to detect the onset and severity of drought, and to study its spatial and temporal patterns. Many drought indices have been developed over the years, and their suitability and effectiveness in characterizing and detecting drought in specific regions have been widely studied. Although these studies have provided valuable recommendations for using drought indices in a drought plan, they are limited in two main respects. First, many studies have focused on using one single well-developed drought index to quantify and predict droughts in a specific geographic region (e.g. Briffa *et al.*, 1994; Tsakiris and Vangelis, 2004; Quiring and Papakryiskou, 2005; Cancelliere *et al.*, 2007). However, because each drought index provides a somewhat different measure of drought (Heim, 2002), a single drought index has often been demonstrated to be inadequate for completely representing this complex phenomena (Steinemann *et al.*, 2005). Second, many studies have focused on measuring and predicting droughts on seasonal or longer time scales (e.g. Kumar and Panu, 1997; Dietz *et al.*, 1998; Kumar, 1999; Chopra, 2006). This limits the opportunity to mitigate the impact of short-term droughts. Finer-scale drought risk assessment is useful to better match crop phenological stages and to detect short-term drought events.

Therefore, employing multiple drought indices for drought risk assessment is meaningful, and may provide a more comprehensive assessment of drought conditions than single-index studies. It is also important to detect potential agricultural drought risk in a timely manner, especially at pre-planting and early crop growth stages, when policy makers have sufficient time to set out drought mitigation strategies in advance (Wu *et al.*, 2004).

In light of these limitations, the purpose of this thesis is to integrate multiple drought indices to assess real-time agricultural drought risk before and during the growing season in the Canadian prairies.

1.2 Research Objectives

The following research objectives have been identified:

1) to establish a classification of drought intensity on the prairies based on the cumulative frequency of historical crop yield;
2) to define an appropriate scale of analysis for drought risk assessment on the prairies;
3) to develop an operational model framework to assess real-time agricultural drought risk by establishing a predictable relationship between blended drought indices and crop yield for the prairies.

Chapter 2: Literature Review

This chapter reviews literature pertaining to the study of agricultural drought on the prairies. It is presented in five sections. The first section explains the concept and the classification of drought. The second section provides an overview of the climate and drought history of the prairies. The third section discusses the relationship between agricultural drought and crop yield. The fourth section provides an introduction of drought indices used in this study, and is followed by the last section which further discusses the advantages of blending multiple drought indices for drought risk assessment.

2.1 The Geographic Concept of Drought

2.1.1 A Definition of Drought

A proper definition of drought is essential for better understanding and further analyzing this complex phenomenon. However, drought lacks a single, all-inclusive definition, because its description is often spatially variant and context dependent (Loukas and Vasiliades, 2004). Scientists and policy makers are apt to have their own differing concepts of drought, and their own criteria for measuring its severity. As a result, there are many definitions of drought in the literature, depending on the duration, spatial extension and impacts on human activities. Although the concepts and criteria of drought are relative rather than absolute, it is generally agreed that "drought results from a deficiency of precipitation from expected or 'normal' that, when extended over a season

or longer period of time, is insufficient to meet the demands of human activities and the environment" (Wilhite and Buchanan-Smith, 2005).

2.1.2 Types of Drought

Within this basic definition, the magnitude of droughts and which economic sectors and natural resources are most affected are still ambiguous. To deal with this, different types of drought categories are defined. The most well known classification of drought was proposed by Dracup *et al.* (1980) – and subsequently adopted by the American Meteorological Society (1997) – that defines drought as being: meteorological, agricultural, hydrological, and socioeconomic.

Meteorological drought is usually defined as the lack of precipitation for a sufficiently long period to cause severe hydrology imbalance in the affected area (Dracup *et al.*, 1980; Wilhite and Glantz, 1985). Since meteorological drought refers to any significant negative departure from "normal" precipitation over a period of time, it depends on the area under examination and on what the "normal" climatic conditions of that region are (Cacciamani *et al.*, 2007).

Agricultural drought occurs when the moisture supply of a region consistently fails to meet the needs of a particular crop at a particular time, such that the crop production or range productivity is significantly affected (Bordi and Sutera, 2007; Rosenberg, 1978). Agricultural drought links various characteristics of meteorological drought to agricultural impacts, mainly focusing on precipitation shortages, differences between

actual and potential evapotranspiration, soil water deficits, and reduced ground water or reservoir levels (Wilhite and Glantz, 1985). As a result, crop yield (production per unit of area) is significantly reduced.

Hydrological drought relates to deficiencies in surface and subsurface water (e.g. stream flow, groundwater and reservoir levels) supplies due to precipitation reduction over an extended period of time (Bordi and Sutera, 2007). Hydrological droughts usually occur after the occurrence of meteorological and agricultural droughts, because it takes longer for precipitation deficiencies to appear in components of the hydrological system.

Figure 2-1 illustrates the relationship between meteorological, agricultural and hydrological drought. In the occurrence of a meteorological drought, the agricultural sector is usually the first to be affected, particularly in areas that rely heavily on stored soil moisture rather than irrigation (Harwood, 1999). If precipitation deficits continue (e.g. for period of three to six months), hydrological drought may become apparent.

Socioeconomic drought correlates the supply and demand of economic goods with the three above-mentioned types of drought (Wilhite and Buchanan-Smith, 2005). Many economic goods (e.g. water, food grains, grazing, and hydroelectric power) have their supplies greatly dependent on precipitation. A socioeconomic drought takes place when the supply of an economic good cannot meet the demand for that product, and the primary cause of this shortfall is precipitation deficit (Wilhite and Glantz, 1985).

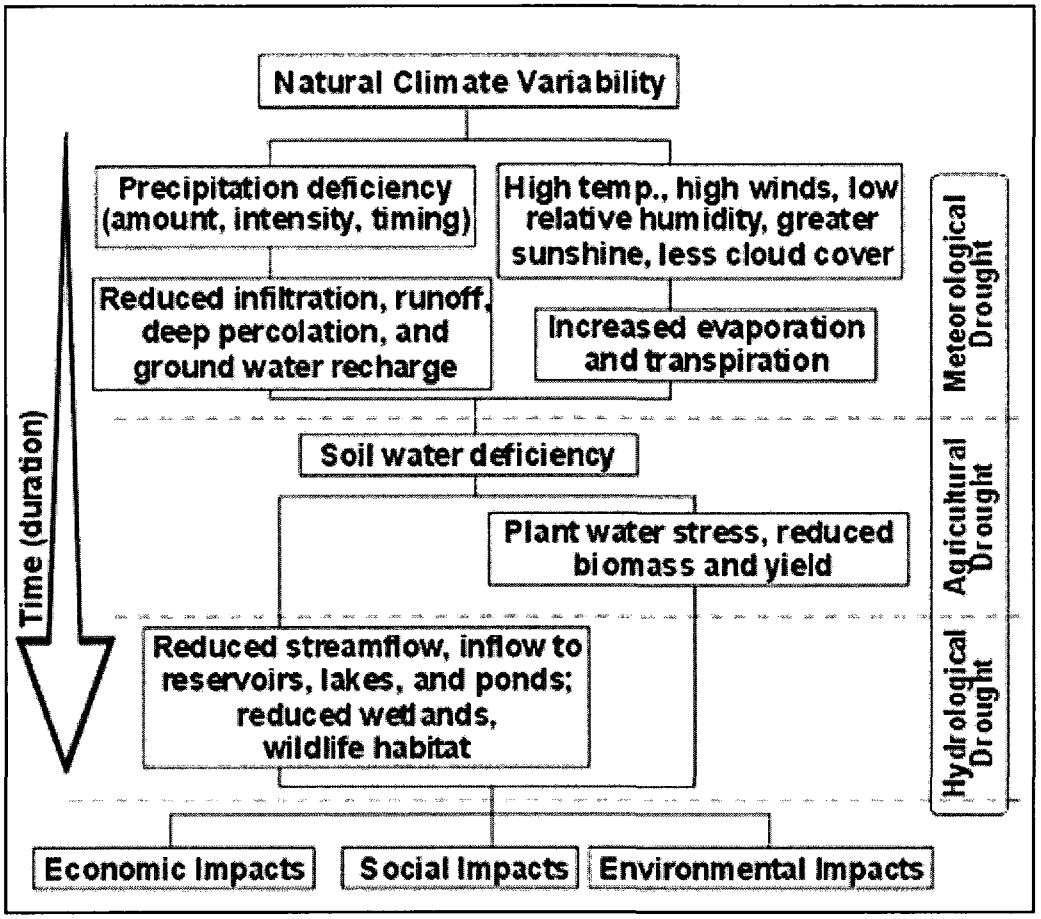

Figure 2-1 Relationship between meteorological, agricultural and hydrological drought (NDMC, 2006)

The significance of each type of drought to a given region mainly depends on its agro-climatic features and socioeconomic characteristics. This study will focus on agricultural drought, as agriculture is the primary economic sector affected by drought in the prairies. The vulnerability of the prairies to drought is discussed in detail in the next section.

2.2 Drought Vulnerability of the Canadian Prairies

The prairies are vulnerable to droughts due to the susceptibility of the region's agricultural sector to weather variability (Kumar, 1999). Droughts on the prairies feature a lack of precipitation, above normal temperature, low soil moisture, and insufficient surface water supply (Wheaton *et al.*, 1992; Nkemdirim and Weber, 1999). Severe drought occurs most often in the southern prairies – especially in southern Alberta and southern Saskatchewan – although the province of Manitoba experienced fewer and less severe droughts during the 20th century (Khandekar, 2004). The most drought-prone regions are coincident with the "Palliser Triangle", a triangular region that extends from the eastern slopes of the Rocky Mountains to the southwest corner of Manitoba (Figure 2-2), and is named after its description in John Palliser's 1863 report on conditions in British North America's north-west (Bumsted, 1999). The Palliser Triangle is characterized by dry conditions in the winter, especially in the western part, due to atmospheric blocking imposed by the Rocky Mountains (Fang and Pomeroy, 2007).

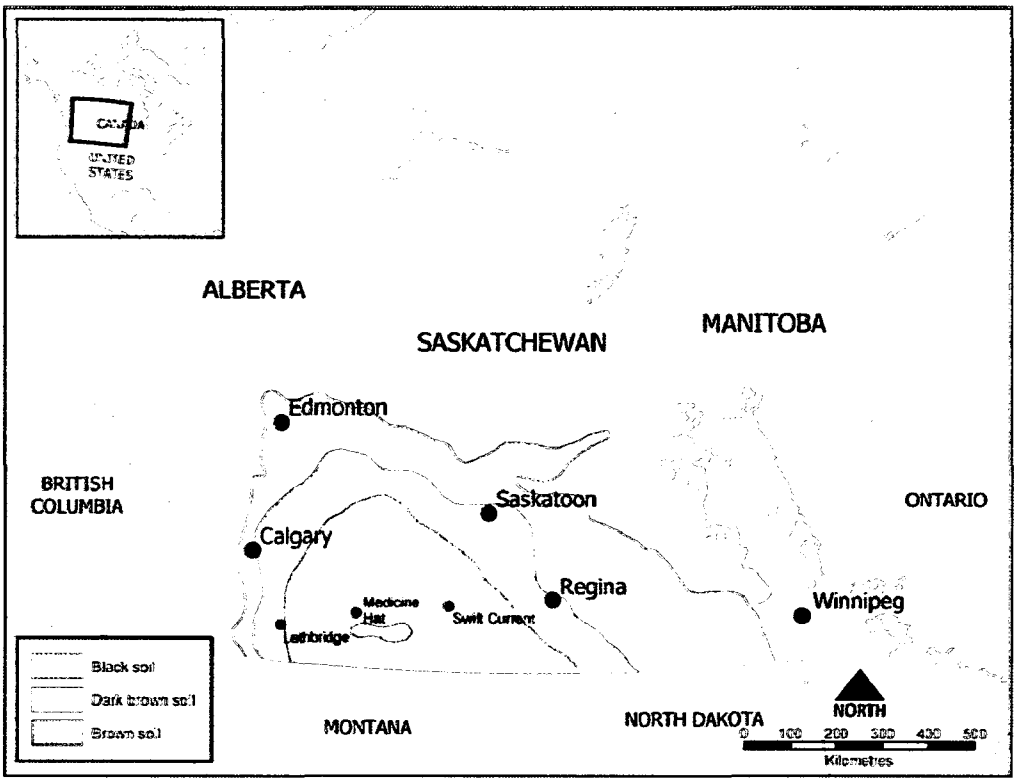

Figure 2-2 Palliser's triangle is usually shown as corresponding to the Brown soil region shown here (Einstein, 2005)

In the past 100 years, severe droughts occurred on the prairies in 1929-1933, 1936-1937, 1961, 1976-1977, 1984, 1988 and 2001-2002 (Maybank *et al.*, 1995; Wheaton *et al.*, 2005), while minor droughts occurred in 1910, 1917-1921, 1980, and 1989 (Kemp, 1982; Maybank *et al.*, 1995). The lengths of these droughts vary from one year to four years. To illustrate the general occurrence and evolvement of droughts, two of the most significant drought events, 1961 and 2001-2002, are described here.

The 1961 drought was considered the most extensive single year prairie drought in the 20th century, spreading across the entire southern agricultural region (Fang and Pomeroy,

2007). Lack of precipitation in fall 1960 depleted soil moisture, and there was very little water recharged during the following spring. Extremely high temperatures together with lack of precipitation in June and July, intensified the dry conditions in 1961, and led to a complete crop failure and more than $300 million in economic losses (Maybank *et al.*, 1995; Bonsal *et al.*, 1999).

The most recent drought of 2001-2002 was identified as the most severe multi-year drought on record in parts of the prairies (Bonsal and Wheaton, 2005). Preceding low precipitation in winter, coupled with a dry spring, set the stage for the 2001 drought and aggravated the dry conditions in 2002. Low precipitation and high temperature in summer and fall were the other common features of 2001 and 2002 droughts. Although in 2002 southern Alberta and south-western Saskatchewan received more than 50% above normal precipitation in the summer, some of the rainfall was too late for agricultural production (Wheaton *et al.*, 2005). The impacts of the drought of 2001 to 2002 on the agricultural sector were devastating. Crop production dropped an estimated $3.6 billion for the 2001 and 2002 drought years, with the largest loss in 2002 at more than $2 billion (Wheaton *et al.*, 2005).

Although drought evolves slowly through time and takes a long time to impact socioeconomic systems, the main factors have been identified in the scientific literature. These include a) the occurrence of low precipitation, b) high temperatures and c) low initial soil moisture. The latter factor c) not only induces drought, but also further affects

its frequency, duration and intensity (Maybank *et al.*, 1995; Quiring, 2001). These factors do not operate independently, and each links with others through a complex series of feedback loops.

2.3 Agricultural Drought and Crop Yield

The occurrence of agricultural drought is associated with seasonal rainfall variability and can be reflected by seasonal soil moisture deficits that significantly affect crop growth and yield (Bordi and Sutera, 2007). The impacts of agricultural drought on crop yield not only depend on the magnitude, timing and duration of precipitation deficits, but also on the different responses of various crops and soils to water stress (Whitmore, 2000). Water stress is the difference between the crop water demand and the amount it actually receives during the growing season (Ash and Shaykewich, 2005). Crop water demand refers to the amount of moisture a crop would use given an unlimited supply of water (Manitoba Ag-Weather Program, 2001). Even for the same crop planted on the same soil, the relationship between seasonal rainfall and yield is complex (Smart, 1983), since crop water demand is not consistent throughout the growing season, resulting in a dynamic link between rainfall and yield as the crop passes through its various growth stages.

2.3.1 Growing Season Crop Water Demand

A crop requires a specific amount of water during the growing season (defined as the period from planting to maturity). During the growing season, crop water demands are different for each growth stage. For example, the water demands of spring wheat are

different through the four broad growth stages of its growing season (Figure 2-3): tillering, stem extension, heading and ripening.

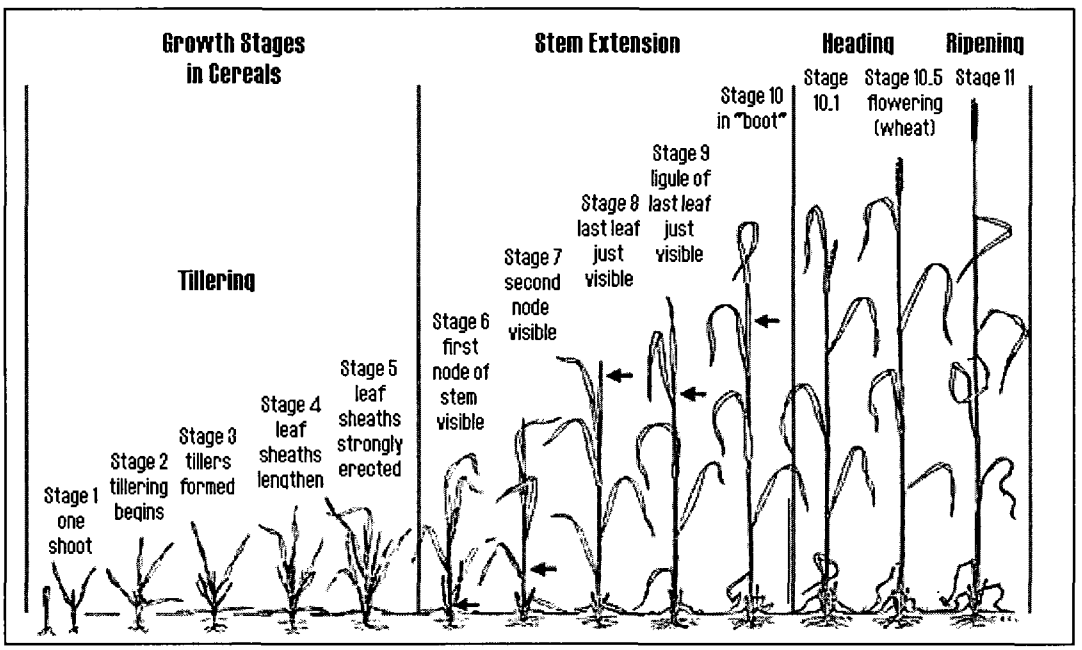

Figure 2-3 Cereal growth stages (Large, 1954)

At the beginning of the growing season, soil moisture conditions for tiller initiation and development, usually occurring during May, are important. Sufficient soil moisture conditions encourage good germination and early root growth, and also determine the number of heads the wheat will formed (King, 1987; Whitmore, 2000). The moisture condition at this stage is largely attributed to the precipitation during fall, winter, and spring months prior to planting.

The highest water demand occurs in the stages of stem extension and heading, usually from June to July, coincident with the period of highest precipitation (Bonsal *et al.*,

1999). Adequate soil moisture is needed at early heading to produce long, strong stalks and a good number of flowers per spikelet (Whitmore, 2000). At late heading, the number of kernels in each head is also determined by the moisture conditions (King, 1987). Drought at these stages can reduce the number of flower-bearing spikes, damage pollen and ovaries, and also cause the kernel size shrink (Whitmore, 2000). Even a moderate drought may decrease the number of wheat grains formed in an ear. Drought has little further detrimental effect on the wheat from the hard dough stage up to ripening (Whitmore, 2000).

Sufficient precipitation before and during the growing season is vital to crop growth. However, an excess of precipitation (e.g. flood) can also be detrimental to crop yields. If too much rain falls prior to planting, it may prevent the seedlings from establishing deep root systems, making them more susceptible to moisture stress later in the growing season (Quiring, 2001). Too much moisture during the growing season may lead to water logging, which reduces crop yield by prolonging the oxygen deficiency in the root zone, as well as decreasing root growth and distribution (Wenkert *et al.*, 1981: Kanwar *et al.*, 1988; Hubbard and Wu, 2005).

2.3.2 Other Factors Affecting Crop Yield

Other factors affecting the quality and quantity of crop yield include soil texture and type, irrigated or rainfed water inputs, the level of fertilizer, insects, disease, weeds, levels of

evapotranspiration, radiation, frost, and the occurrence of hail. (Bushuk, 1982; Riha *et al.*, 1996).

Soil helps to determine yield quality and quantity. Fertile, well-drained soils of high available water holding capacity (AWHC) are best for crops. The AWHC, defined as the maximum amount of water held in a soil that plants can use, varies with soil type (Ash and Shaykewich, 2005). Soils with a fine texture have more total pore space, and thus can hold more available water than coarse-textured soils. Although fine-textured soils support drought-sensitive and deep-rooted crops during dry conditions, the water supply is limited for the reason that much of the water it stored is so tightly held as to be inaccessible to crops (Sullivan, 2002).

Floods also cause stress to the plant whose roots are in saturated soil for long periods, and ultimately result in reduced crop yield (Hubbard and Wu, 2005). The occurrence of wind storms, frost, hail, insects (e.g. wheat stem sawfly, cutworms and grasshoppers), and common diseases (e.g. rust, smut) also play a role in reducing crop yield. Furthermore, weeds affect yield quantity and quality by robbing moisture and nutrients.

Other factors like heat and sunlight are also necessary for plant growth, but they do not usually exhibit a great variability and thus do not normally affect crop yield (Quiring, 2001). Irrigation is also not an influential factor on determining crop yield on the prairies. For most of the Census Agricultural Regions (CARs) in the prairies, irrigated areas

account for less than 1% of the total CAR area. Only two CARs (4810 and 4820) in Alberta contained irrigated area over than 5% (9.2% and 21.6%, respectively).

2.3.3 Choosing Crop Yield as an Agricultural Drought Indicator

Agricultural drought is closely linked with a loss of agricultural production, since both are driven by a lack of precipitation. As a result, crop yield can be used as a drought indicator: by predicting reduced crop yield, one can predict droughts (Morgan, 1985, Sinha *et al.*, 1992; Kumar and Panu, 1997).

Numerous studies have used crop yield to estimate agricultural drought in agricultural regions. Kumar (1999) attempted to predict agricultural drought on the prairies using spring wheat yield. The long-term prediction was achieved by predicting wheat yield prior to planting using time series analysis. He concluded that drought can be predicted where the estimated yields are found to be significantly lower than the long-term averages of yields. Quiring and Papakryiakou (2003) conducted a performance evaluation on four drought indices to choose the most appropriate measure of agricultural drought in the prairies by predicting spring wheat yield. The study indicated that the Palmer's Z-index was the most appropriate index for measuring agricultural drought in the prairies. Rahmani *et al.* (2008) analyzed the drought effects on barley yield in east Azerbaijan. These authors used multiple regression analysis to examine the correlation between ten growing season meteorological parameters and twelve drought

indices to barley yield. Four indices were found to be more effective for predicting barley yield and thus, agricultural drought.

Based on the review of relevant research, this study will use crop yield as an agricultural drought indicator, because drought on the prairies is the single most limiting factor to crop yield (Akinremi and McGinn, 1996). This approach, in its simplest form, relies on the underlying assumption that moisture supply is the single factor in determining yield and that other factors (e.g. insects, disease and weather related damage) remain stable throughout the study period. The reliance on this assumption introduces an unknown amount of uncertainty in the analysis.

2.4 Drought Indices

Drought indices are the integration of one or more climate or hydrological variables (e.g. precipitation, soil moisture, stream flow, snowpack, groundwater levels, and reservoir storage) on a quantitative scale (Steinemann *et al.*, 2005; Hayes, 2006). Drought indices are important not only for quantifying the severity of drought in a particular region, or detecting drought onset and termination, but also for determining the spatial extent of drought and comparing drought conditions between regions (Alley, 1984; Quiring and Papakryiskou, 2003).

More than twenty drought indices have been developed and presented in the literature. These include the Percent of Normal, Deciles, Palmer Drought Severity Index (PDSI), Palmer Hydrologic Drought Index (PHDI), Palmer Moisture Anomaly Index (Z-index),

Standardized Precipitation index (SPI), Surface Water Supply Index (SWSI), Crop Moisture Index (CMI), and Reclamation Drought Index (RDI). These drought indices were designed with different intentions, each providing a different measure of drought. What follows is a review of the drought indices used in this study.

2.4.1 Palmer Drought Severity Index (PDSI)

The Palmer Drought Severity Index (PDSI), developed by Palmer (1965), is one of the most recognized and widely used drought indices in North America (Byun and Wilhite, 1999; Karl *et al.*, 1987). The PDSI is a soil moisture balance algorithm that requires a time series of daily maximum and minimum temperature, daily precipitation, the information on the AWHC of the soil, and the longitude and latitude of the site for which it is being calculated.

Calculating the PDSI involves a relatively complex procedure. A water balance is computed using historic records of temperature and precipitation (Alley, 1984). To estimate the soil moisture storage, Palmer (1965) used a two-layer soil model where the AWHC of the soil is distributed between the two layers. The upper (i.e. surface) layer is assumed equivalent to the plough layer, and 25mm of water can be stored here (Alley, 1984). The underlying layer stores the remainder of the water, the amount of which depends on the soil characteristics of the site being considered. Potential evapotranspiration (PET) is estimated using the temperature and heat index by Thornthwaite's model (1948), and water is extracted from the soil when PE exceeds

precipitation for the month. Evapotranspiration (ET) loss and recharge are assumed to take place first in the surface (upper) layer. Moisture loss from this layer is assumed to occur at the rate of PET, and moisture loss from the underlying layer depends on initial water content, computed PET and the combined AWHC of the two soil layers (Palmer, 1965). Moisture content in the underlying layer cannot be recharged until all of the available moisture has been replenished in the surface layer. It is further assumed that no runoff occurs until both layers reach field capacity (Palmer, 1965).

The first step to calculate the monthly PDSI is to determine the soil moisture anomaly:

$$d_i = P_i - \hat{P}_i \qquad [1]$$

where d_i is the magnitude of the moisture departure for month *i*, P_i is the total monthly precipitation, and $\hat{P}_i$ is the *climatologically appropriate* precipitation for month *i* (Palmer, 1965). $\hat{P}_i$ is derived from a water balance equation:

$$\hat{P}_i = \overline{ET} + \bar{R} + \overline{RO} - \bar{L} \qquad [2]$$

where $\overline{ET}$ is the expected or *climatologically appropriate* evapotranspiration, $\bar{R}$ is the expected soil moisture recharge, $\overline{RO}$ is the expected run off, and $\bar{L}$ is the expected water loss from the soil. The variables $\overline{ET}$, $\bar{R}$, $\overline{RO}$ and $\bar{L}$ are derived as follows:

$$\overline{ET} = \alpha PE \qquad [3]$$

$$\bar{R} = \beta PR \qquad [4]$$

$$\overline{RO} = \tau PRO \quad [5]$$

$$\bar{L} = \delta PL \quad [6]$$

where *PE* is the potential evapotranspiration , *PR* is the potential recharge, *PRO* is the potential runoff, and PL is the potential loss from soil. The constants $\alpha, \beta, \tau,$ and δ are derived for each month of the year as the ratios of historical averages of *ET/PE*, *R/PR*, *RO/PRO* and *L/PL*, respectively. A separate of coefficients is determined for each of the 12 months.

The Palmer Moisture Anomaly Index (Z-index) for a given month is obtained as

$$Z_i = d_i K_i \quad [7]$$

where K_i is a weighting factor for month i and is initially determined using an empirically derived coefficient, K', which is then adjusted using a regional climate correction factor to account for the variation between locations,

$$K_i = \left(\frac{14.2}{\sum D_i K_i'}\right) K' \quad [8]$$

Where $K'$is

$$K' = 1.5 \log\left(\frac{\frac{PE+R+RO}{P+L}+2.8}{D}\right) + 0.5 \quad [9]$$

where D is obtained during the calibration period by determining the mean of the absolute values of d for each month of the year.

Then the PDSI for month *i* is defined as

$$PDSI_i = \frac{1}{3} Z_i + 0.897\, PDSI_{i-1} \quad [10]$$

The classification of moisture conditions (Table 2-1) was determined by Palmer based on his original study areas in central Iowa and western Kansas (Palmer, 1965). Although the PDSI was designed to work on a monthly time step, is can also be reported on a weekly basis. In the United States, the weekly PDSI is provided by the United States Department of Agriculture in their weekly weather and crop Bulletin (Hayes, 2006).

Table 2-1 Palmer Drought Severity Index drought classifications (Palmer, 1965).

PDSI value	Drought Category	Cumulative Frequency (%)
-1.49 to 0.00	Near normal	28-50
-2.99 to -1.50	Mild-moderate	11-27
-3.99 to -3.00	Severe	5-10
≤ -4.00	Extreme	≤ 4

There are many benefits of using the PDSI. The PDSI is easy to interpret and can be generated quickly from an existing weather network (Strommen and Motha, 1987). The PDSI provides decision makers with a measurement of the abnormality of recent weather for a region (Steinemann *et al.*, 2005), aiding the detection of onset and assessment of the severity of drought (Quiring, 2001). Another useful aspect of the PDSI is that it

provides an opportunity to place current conditions in historical perspective, and provides spatial and temporal representations of historical droughts (Alley, 1984).

Despite its merits, there are considerable limitations associated with using the PDSI:

(1) The PDSI is designed for agriculture but does not accurately represent the hydrological impacts resulting from longer droughts (McKee *et al.* 1995). Thus, the PDSI is not suitable for droughts in heavily water-managed (irrigated) systems, because it excludes other surface water supplies (Steinemann *et al.*, 2005; Hayes, 2006).

(2) Although the PDSI is widely applied within the United States where it was developed, it has little acceptance elsewhere (Kogan, 1995; Steinemann *et al.*, 2005; Hayes, 2006). According to Smith *et al.* (1993), the PDSI does not do well in regions where there are extremes in the variability of rainfall or runoff (e.g. Australia and South Africa), because the PDSI are values based on departures from climate normals, without considering the variability of precipitation. Similarly, Wilhite and Glantz (1985) noted that the statistical measure of "normal" is less meaningful than other measures (e.g. median or mode of the precipitation distribution) for climatic regions with a large interannual variation of precipitation.

(3) The "extreme" and "severe" categories of drought occur with a greater frequency in some regions using the PDSI. "Extreme" droughts in the Great Plains occur with a frequency greater than 10% (Willeke *et al.*, 1994). This limits the accuracy of comparing

the intensity of droughts between two regions and makes planning response actions based on certain intensity more difficult.

(4) Snowpack, subsequent runoff and frozen ground are not included in the PDSI. All precipitation is treated as rain, so the PDSI may be less useful during the winter and spring months when snow occurs (Steinemann *et al.*, 2005; Hayes, 2006).

(5) The natural lag between rainfall and its resulting runoff is not considered in the PDSI. In addition, no runoff is allowed to take place in the PDSI's calculation until the water capacity of the surface and subsurface soil layers is full. This leads to an underestimation of runoff (Hayes, 2006).

2.4.2 Palmer Moisture Anomaly Index (Z-index)

The Palmer Moisture Anomaly Index (Z-index) was introduced by Palmer (1965) to accompany the PDSI, but it is less frequently used (Karl, 1986). The Z-index measures the monthly moisture anomaly, reflecting the departure of moisture conditions in a particular month from normal moisture conditions (usually calculated over a 30 year period) (Heim, 2002).

Although the Z-index and PDSI are derived using the same input data, their monthly values are quite different. The monthly Z-index values can vary dramatically from month to month in comparison to the PDSI, since the Z-index is not affected by moisture conditions in previous months (Quiring and Papakryiskou, 2003). Thus, it has been

argued that the Z-index is more appropriate than the PDSI for measuring meteorological and agricultural droughts, because it is more responsive to short-term soil moisture anomalies (Karl, 1986; Quiring and Papakryiskou, 2003).

2.4.3 Standardized Precipitation Index (SPI)

The Standardized Precipitation Index (SPI) is a commonly-used drought index. The SPI was introduced by McKee *et al.* (1993) to quantify the precipitation anomalies calculated over different time scales. The SPI is a standardized precipitation anomaly, and is based on the probability distribution of the long-term precipitation record (at least 30 years) for a specified time period (such as 1, 3, 6, 9, 12, 24, 48 or 60 months). The SPI represents the precipitation deficit for that time scale (McKee *et al.*, 1993).

The SPI is calculated by fitting the long-term record of precipitation over a specific time step to a probability distribution. This probability density function is then transformed into a normal distribution using an inverse normal (Gaussian) function (Edwards and McKee, 1997), and the result is a standardized index whose values classify the category of drought. For time steps longer than a month, a moving average process is used to construct a new time series for the SPI calculation. For example, if the observed data consist of a time series of monthly precipitation, and the analyst is interested in 3-month events, then a new time series is constructed by summing the first 3 months' amounts, then summing the amounts in month 2, 3, and 4, then summing the amounts in month 3, 4 and 5, and so on. The 3-month SPI is calculated from this new time series.

The classifications of the SPI (Table 2-2) not only define drought intensities, but also set the criteria for a drought event for any time scale (McKee *et al.*, 1993; Steinemann *et al.*, 2005). A drought event occurs any time the SPI is continuously negative and reaches an intensity of -1.0 or less. The event ends when the SPI becomes positive. Therefore, each drought event has a duration defined by its beginning and end, and has its intensity for each month that the event continues. The positive sum of the SPI for all the months within a drought event can be termed the drought's "magnitude" (Hayes, 2006).

Table 2-2 Standardized Precipitation Index drought classifications (McKee et *al.*, 1993)

SPI value	Drought Category	Cumulative Frequency (%)
-0.99 to 0.00	Mild	16-50
-1.49 to -1.00	Moderate	6.8-15.9
-1.99 to -1.50	Severe	2.3-6.7
-2.00 or less	Extreme	<2.3

A number of advantages arise from the use of the SPI. First, its evaluation is relatively simple because it is based only on precipitation amount. Second, it provides the temporal flexibility to assess drought conditions over multiple time scales. The SPI for shorter durations can be used for agricultural interests, while the SPI for longer durations can be used for water supply and water management interests (Guttman, 1999; Hayes, 2006). The third advantage comes from its standardization. The SPI is standardized so its values are spatially and temporally comparable (Cacciamani *et al.*, 2007). Fourth, the SPI

provides the criteria for drought initiation and termination, which are two highly desirable factors among many drought planners.

The SPI can be computed only when a sufficiently long and possibly continuous time series of monthly precipitation data are available (at least 30 years) (Hayes, 2006). Its accuracy is highly dependent on the sample size (Guttman, 1999). Since the SPI is a moving average process for periods longer than one month, the longer the time scale considered (i.e. the number of months over which the precipitation is accumulated) that is considered, the smaller the sample size will be, and thus, the less accurate the index (Quiring, 2001). For this reason, one disadvantage of this method is that it is not always possible to have access to a sufficiently long and reliable time series to produce a robust estimate of the distribution parameters (Steinemann *et al.*, 2005). Because of the data limitations, Guttman (1999) emphasized that SPI values computed with time scales longer than 24 months might not be reliable.

2.5 Blended Drought Indices

Although there have been many studies focused on drought index development and evaluation, little prior work exists on methods for blending multiple drought indices into drought monitoring and forecasting. According to Steinemann *et al.* (2006), the process of combining drought indices can be considered in two ways. One way is to synthesize several indices into one overall index. However, its scientific justifications are tenuous, because there is no objective criteria for determining appropriate weights assigned to

each individual index in the overall index. Another way is to use several indices for operational drought management, but there has been a lack of systematic methods for their combination, use, and evaluation in a drought plan (Steinemann *et al.*, 2006).

In recent years, there have been some attempts to fill this gap. The U.S. Drought Monitor (USDM) is a state-of-art drought monitoring tool used in the United States (Svoboda *et al.*, 2002). It was developed using a hybrid approach that incorporates various drought indices, models and the input from regional and local experts around the country. One analysis tool developed specifically for the Drought Monitor is the Objective Blend of Drought Indicator (OBDI). It combines drought indices such as the SPI, PDSI and Z-index, as well as the CPC soil moisture model. The weights of the indicators are considered differently in terms of short-term and long-term drought monitoring, which focus on 1-3 months and 6-60 months respectively (Drought Monitor, 2008). A percentile approach was used to transform all input data into a standardized scale to which drought category thresholds could be assigned. The short-term and long-term OBDIs are computed weekly on a climate division level and present drought conditions in a Drought Monitor map. The OBDI is beneficial in determining a single "average" drought designation for the current week's map, providing a comprehensive assessment of drought conditions across the country (Svoboda *et al.*, 2002). The Drought Monitor, however, is not meant to capture local drought conditions, and this is a major limitation. It should not be used for making decisions at relatively local resolutions, such as individual counties (Steinemann *et al.*, 2005).

Wu *et al.* (2004) developed an agricultural drought risk-assessment model for Nebraska, USA, as related to soybean and corn yield. The model was designed to assess real-time agricultural drought risk before and during the growing season integrating the SPI at multiple time steps and a crop-specific drought index (CSDI). The historical SPI and CSDI variables were assigned to two groups, low-risk and high-risk, relative to yield residuals. Canonical and classificatory discriminate analyses were performed on two groups for each selected critical crop phenological stages to assess drought risk at that stage. The results of this study showed that the risk-assessment accuracy improves with the growth stages of the crop. For corn, the average correct assessment possibility reached 85% in late July. For soybeans a reliable assessment with 80% possibility began at mid-August. The model was demonstrated providing early assessment of drought risk on crop yield, as the final crop yields in that region for the current year are published officially in January or later in the next year.

Brown *et al.* (2008a) developed a hybrid geospatial drought monitoring tool, the VegDRI (Vegetation Drought Response Index) model, to produce a 1km resolution indicator of the geographic extent and intensity of drought stress on vegetation in seven states of north-central United States. The models integrate climate-based drought indices (PDSI and SPI) and satellite-derived vegetation condition information (the Percent Average Seasonal Greenness (PASG) and Start of Season Anomaly (SOSA)) with other biophysical information (soils, land use, land cover, and the ecological setting). The model was empirically derived for three seasonal phases (spring, summer and fall) by

applying a supervised classification and regression tree analysis technique for each phase. The seasonal models were then applied to the geospatial data to produce a map at a two-week time step for each phase. The results demonstrated that more spatially detailed drought patterns can be characterized and monitored in the 1 km VegDRI maps, compared to the commonly used USDM map. Brown *et al.* (2008b) then further examined the effectiveness of the VegDRI for agricultural drought monitoring by evaluating the relationship between VegDRI and soybean and corn yields during critical periods affecting crop yield for the year of 2006 and 2007. The VegDRI correlated best with the detrended yield for corn ($R^2 = 0.48$) in the second half of August. The VegDRI had a much less significant relationship with soybean yields over these two years. This indicates that soybeans are less vulnerable to drought than corn.

The review of these relevant research findings highlights the efforts that have been made to improve drought monitoring and forecasting capabilities. There is a recent tendency to consider more than one drought index to assess drought conditions. It would also be useful to examine the sensitivity and accuracy of drought indices, and explore how well they complement each other in the context of a specific research objective. Although drought has been extensively studied on the prairies, no study has explored blending multiple drought indices to predict agricultural drought in a timely manner. Thus, this study attempts to fill this gap in the scientific literature.

Chapter 3: Methodology

This chapter is presented in three sections. The first section introduces the study area. The second section outlines the data sources and processing procedures for the meteorological, crop yield, soil and Census Agricultural Regions data. The third section discusses the methods and techniques that were used to 1) select and calculate drought indices, 2) select crop and detrend crop yield data, 3) define drought categories, 4) create agricultural drought regions, and 5) develop an agricultural drought risk assessment model.

3.1. Study area

The study area is the agricultural region of the Canadian prairies. The prairie region is located close to the centre of the North American continent (Figure 3-1), crossing southern Alberta, Saskatchewan and Manitoba (approximately 49 - 54°N latitude and 96 - 114°W longitude) (Raddatz, 1998). The total area of the prairies is about 47 million hectares. Of this area, 70% is classified as cropland, 27% is classified as rangeland and pasture, and the remaining 3% is classified as deciduous forest (Environment Canada, 2008a). The landscape of the prairies is dominated by plains and gently rolling terrain underlain by deep glacial deposits (Environment Canada, 2008a). The generally flat landscape can be further divided into three ascending levels of plains: the Manitoba lowlands, the Saskatchewan plains and the high plains of Alberta (Cohen *et al.*, 1992). The absence of any significant topographic barrier in the vast north-south corridor

between the Arctic Ocean and the Gulf of Mexico is responsible for the great variety of weather (Hare and Thomas, 1919).

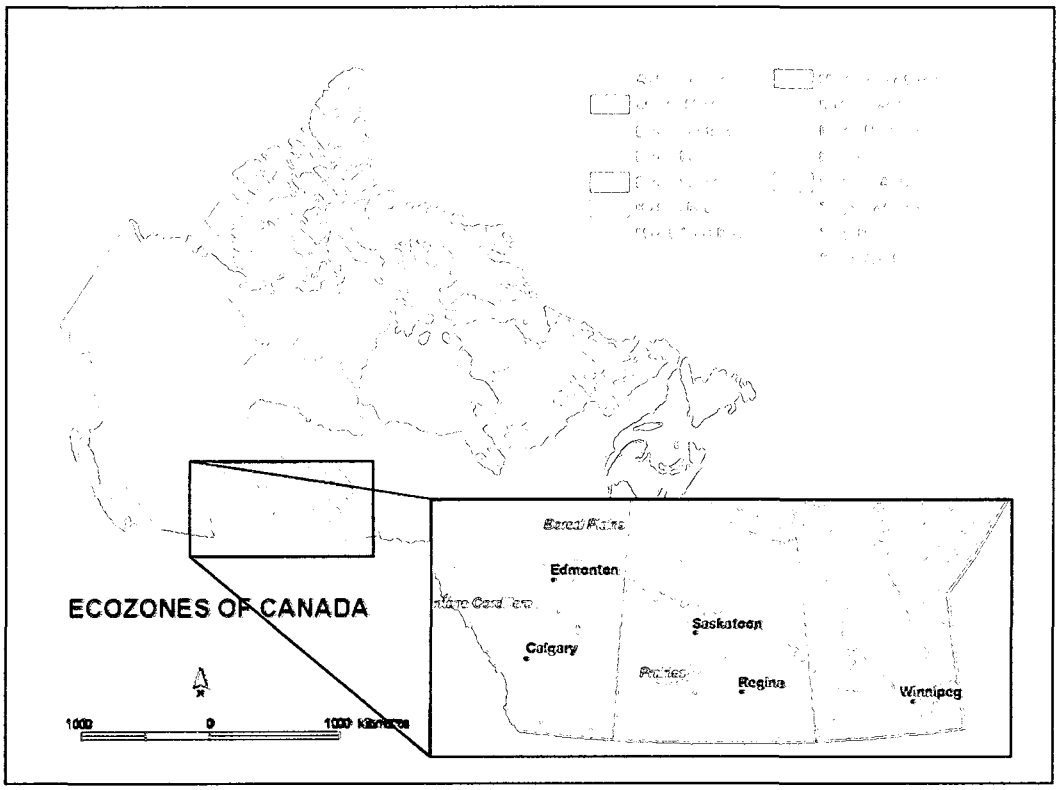

Figure 3-1 Location of the Canadian prairies

The prairies are dominated by a semi-arid climate, and precipitation is highly variable and unevenly distributed. The driest areas are found in the south and southwest of the prairies. Because the precipitation generally increases towards the east, the wettest parts are generally found in the north and northeastern prairies (Herrington *et al.*, 1997). The annual precipitation in this region ranges from 300 to 550 mm (Cohen *et al.*, 1992). Growing season precipitation averages about 200 mm, and this is lower than crop water

demand (approximately 300 mm) (Ash *et al.*, 1992). Winter precipitation in the form of snowfall is important, accounting for approximately one third of annual precipitation and producing 80 percent or more of annual local surface runoff (Gray *et al.*, 1986; Pomeroy and Goodison, 1997; Fang, 2007).

Termed "Canada's breadbasket", the prairie region is one of the world's major agricultural areas, producing over 40 million tons of grain including wheat, oats, barley, and canola (Statistics Canada, 2008). The high natural fertility and good moisture holding capacity of many of the soils of this region, coupled with the largely level topography makes the area ideal for mechanized farming (Acton and Gregorich, 1995). Droughts are frequent on the prairies, and a moderate or severe drought can cause severe economic impact. The vulnerability of the region to agricultural droughts was discussed in detail in section 2.2.

3.2. Data Sources and Data Process

3.2.1 Census Agricultural Region Data

To avoid the problems associated with using regions that are too large to be climatologically homogeneous, a finer scale, defined by the Census Agricultural Region (CAR), was selected. An appropriate scale of analysis for drought risk assessment on the prairies will be defined from these CARs. Also, using CARs to create agricultural drought regions aids data management, as the yield data are collected on a CAR level.

The 2006 CAR boundary file in ESRI Shapefile format was obtained from Statistics Canada (Statistics Canada, 2007). This file contained the boundaries of all 82 CARs of Canada, with each CAR identified by a unique code. A total of 34 CARs were selected for this study (Figure 3-2). 26 of these CARs are entirely contained within the prairies, while the remaining 8 CARs have 40 percent or more of their area within the prairies. This yields 6 CARs in Alberta, 19 in Saskatchewan, and 9 in Manitoba.

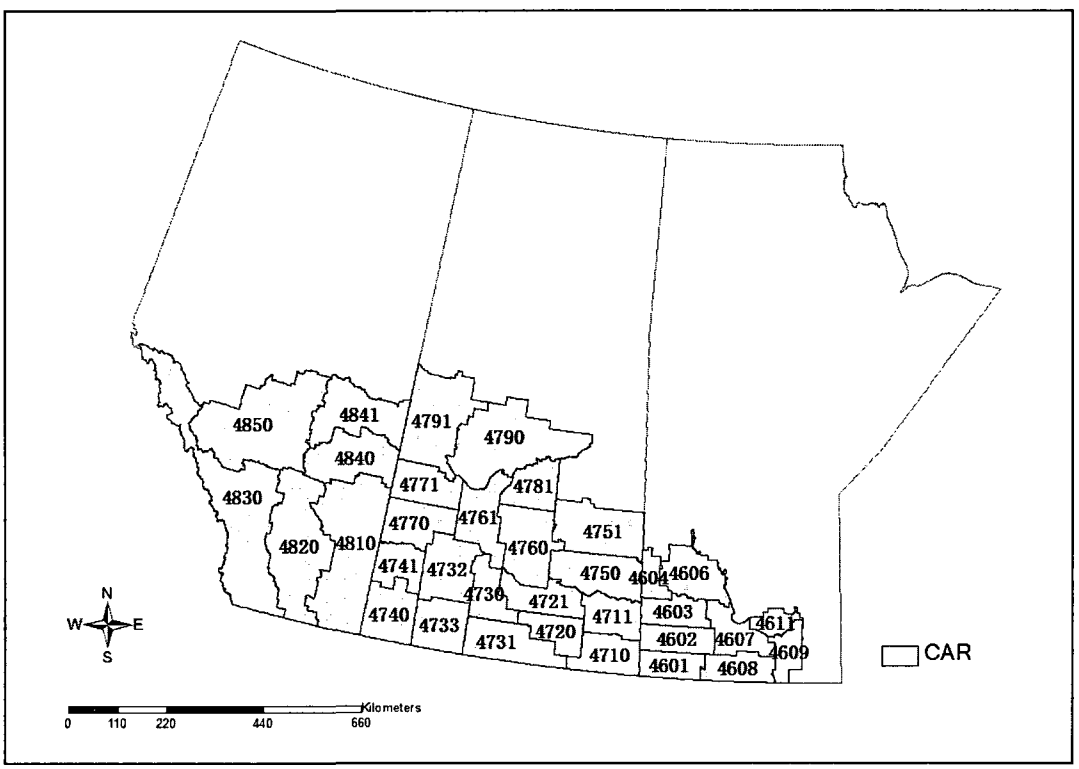

Figure 3-2 Distribution of the 34 Census Agricultural Regions selected for the study.

3.2.2 Meteorological Data

Daily maximum/minimum temperature and precipitation data for the 34 CARs were obtained from the daily 10km gridded climate dataset for Canada (1961-2003) (AAFC, 2007a). The dataset contains gridded point locations of daily maximum temperature (°C), minimum temperature (°C), and precipitation (mm) for the Canadian landmass south of 60° N. Grids were interpolated from daily Environment Canada climate station observations (Figure 3-3), using a thin plate smoothing spline surface fitting method (AAFC, 2007a).

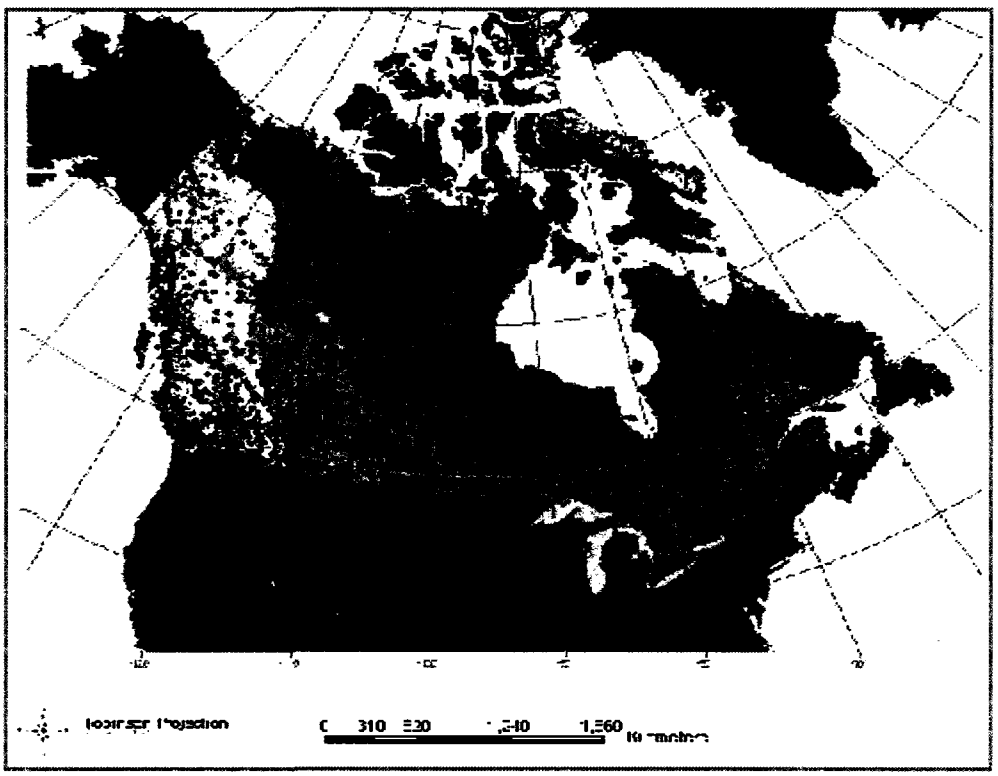

Figure 3-3 Distribution of Environment Canada climate stations (7514 stations) (AAFC, 2007a).

5712 grid cells within the 34 CARs were extracted from the gridded climate dataset using ArcGIS 9.2 (Environmental System Research Institute, 2006). The cells that fall into areas unsuitable for farming (e.g. water, ice and rocky area) were excluded from the analysis. A total of 5516 grid cells remained and were used to calculate drought indices.

3.2.3 Soil Data

Available water holding capacity (AWHC) of the soils is one of the required datasets for the PDSI and Z-index calculation. The AWHC values are defined via the Soil Landscapes of Canada (SLC) Version 3.1.1. AWHC were calculated for each SLC polygon in the study area based on the component soils' AWHC and their percent distribution within the SLC polygon.

The SLC data for the three prairies provinces (Alberta, Saskatchewan and Manitoba) were obtained from Agriculture and Agri-Food Canada, in the ESRI Shapefile format (AAFC, 2007c). In total, 1325 SLC polygons for the 34 CARs were extracted using ArcGIS 9.2. Each SLC polygon comprised one or more distinct soil landscape components, some of which are unsuitable for agricultural usage (e.g. water body, rock). To assess the proportion of these components in each SLC polygon, the percent of area for these components were aggregated for each polygon, ranging from 0 to 100 percent cover. Most of these polygons are distributed in Saskatchewan and Manitoba, accounting for as much as 30 percent of the polygons in Saskatchewan and almost 20 percent in Manitoba.

A maximum of 20 percent area of the unsuitable components was set to ensure the accuracy of the polygon's AWHC value and to keep as many polygons in the analysis as possible (Warren, R. pers. comm.). 122 SLC polygons were discarded and a total of 1203 SLC polygons remained. The SLC polygons' aggregate AWHC code was then calculated by taking the summation of each components' areally-weighted AWHC code:

$$SLC\ polygon's\ AWHC\ code = \sum_{i=1}^{n} AWHC\ code_i * \left(\frac{percent_i}{percent_{total}}\right) \quad [11]$$

where i is the component, n is the number of components in a SLC polygon, and the $percent_{total}$ is in the range of 80 to 100, depending on the amount of unsuitable components excluded from the calculation.

Finally, the AWHC code was converted to a specific AWHC value based on the range of water equivalent values associated with each AWHC code in Table 3-1.

The SLC polygon's AWHC value was calculated as:

$$AWHC\ value = i + (AWHC\ code - n_{ij}) * (j - i) \quad [12]$$

where n_{ij} is the integer part of polygon's AWHC code, with its water equivalent value ranges between i and j. (e.g. if polygon's AWHC code is 4.3, n is 4, i is 150mm, and j is 199mm).

Table 3-1 Water equivalent value associate with AWHC code (AAFC, 2005)

AWHC Code	Water Equivalent
1	<50mm
2	50 - 99 mm
3	100 - 149 mm
4	150 - 199 mm
5	200 - 250 mm
6	Solonetzic or saline soils
7	High water table
8	Perennially frozen subsoils
-	Water, ice or rock

3.2.4 Crop Yield Data

Spring wheat yield data (t/ha) from the period 1976 to 2003 were obtained from Statistics Canada. The yields were collected for each CAR in the prairies, through the Agricultural Census. A summary of the yields for each CAR is presented in Table 3-2. The coefficient of variation (CV) of the yields is defined as the ratio of the standard deviation to the mean yield. It is useful for comparing the degree of yield variation with different means.

Table 3-2 Summary of spring wheat yield data for each CAR

CAR	Min. (t/ha)	Max. (t/ha)	Mean (t/ha)	Stdev. (t/ha)	CV (%)	Years
4601	1.05	2.67	1.95	0.42	21.60	28
4602	1.02	2.67	2.06	0.41	20.03	28
4603	1.38	2.70	2.16	0.33	15.09	28
4604	1.30	2.71	2.15	0.35	16.04	27
4606	1.45	2.72	2.14	0.34	15.89	28
4607	1.11	3.39	2.33	0.53	22.75	28
4608	0.96	3.31	2.33	0.53	22.61	28
4609	1.19	3.36	2.18	0.52	24.00	28
4611	1.42	3.12	2.18	0.45	20.42	28
4710	0.94	2.33	1.70	0.33	19.19	28
4711	1.08	2.51	1.87	0.37	19.73	28
4720	0.73	2.38	1.59	0.42	26.54	28
4721	0.97	2.53	1.91	0.34	17.87	28
4730	0.60	3.18	1.71	0.50	29.22	28
4731	0.53	2.25	1.67	0.42	24.99	28
4732	0.39	2.40	1.69	0.46	26.91	27
4733	0.50	2.91	1.79	0.45	24.83	27
4740	0.41	2.22	1.62	0.41	25.43	28
4741	0.44	2.41	1.67	0.55	33.05	28
4750	0.95	2.40	1.93	0.33	17.28	28
4751	1.18	2.63	2.04	0.34	16.46	28
4760	0.61	2.36	1.81	0.38	21.07	28
4761	0.48	2.48	1.83	0.46	25.19	28
4770	0.50	2.62	1.85	0.51	27.59	28
4771	0.70	2.58	1.94	0.43	22.00	28
4781	0.74	2.80	2.07	0.49	23.78	28
4790	0.65	2.58	1.99	0.39	19.39	28
4791	0.40	2.58	1.92	0.42	21.69	27
4810	0.72	2.47	1.71	0.45	26.20	28
4820	1.57	3.23	2.40	0.44	18.33	28
4830	1.09	3.16	2.29	0.53	23.14	28
4840	0.62	2.82	2.06	0.44	21.21	28
4841	0.78	2.82	2.26	0.42	18.69	28
4850	1.90	4.03	3.12	0.58	18.74	28

3.3 Methodology

This section discusses the methodologies to develop an agricultural drought risk assessment model. It involves some preparative work before model construction. These are: 1) drought indices selection and calculation, 2) crop selection, 3) drought intensity classification, and 4) the creation of agricultural drought regions. What follows is a detailed discussion of model definition, construction and validation.

3.3.1 Drought Index Selection

This study included two Palmer drought indices (PDSI and Z-index), and the SPI over three time steps (SPI_1, SPI_3 and SPI_6), which were calculated based on 1, 3, and 6-month precipitation anomalies. The selection of the drought indices was mainly based on the considerations outlined below:

Preferences for the SPI are based on its temporal flexibility to assess drought conditions over multiple time scales. The SPI for 1 month responds quickly to short term precipitation anomalies. The SPI for 3 and 6 months, with greater stability and persistence, reflect longer term dryness, minimizing possible false alarms of drought progression and recession.

The PDSI is most effective measuring soil moisture conditions, and is essential for agricultural drought monitoring. In addition to precipitation, the PDSI takes into account

the temperature, potential evapotranspiraton, potential recharge, and potential runoff at a given location, and thus provides a more comprehensive view of moisture conditions.

Despite the similarities in derivation with the PDSI, the Z-index is more sensitive to short-term soil moisture anomalies, because it is not affected by moisture conditions of antecedent months which are considered in the PDSI's calculation. The measurements from the Z-index would be valuable for short-term sensitivity, as crop growth is highly dependent on short-term soil moisture conditions during the growing season.

Lastly, all of these indices are widely used and well-developed. Their individual effectiveness measuring agricultural drought on the prairies has been widely studied (Quiring and Papakryiakou, 2003; Richards and Burridge, 2006; Wheaton *et al.*, 2008).

3.3.2 Drought Index Calculation

The SPI was calculated using FORTRAN 90/95 code provided by the National Agroclimate Information Service (NAIS) of Agriculture and Agri-Food Canada. This program requires a continuous time series of monthly precipitation data (ideally at least 30 years). Although it is possible to aggregate daily precipitation data to a monthly timestep, the error-related effects of temporal aggregation are unknown. It has been hypothesized that the generation of monthly climate grids from the interpolation of monthly-aggregated station observations may be more appropriate, because this approach will only produce one interpolation-related error, compared to the aggregation of 28, 29, 30 or 31 daily interpolation errors (depending on the month in question).

Although for the SPI calculation, the interpolation error-related effects of monthly aggregation of the precipitation grids on the prairies is the main concern, a broader investigation on the influence of temporal aggregation of the daily gridded data set was undertaken. In Chapter 4, the performance of two schemes (temporally-aggregated daily interpolations vs. interpolations of aggregated station data) for three climate variables (total precipitation, maximum and minimum temperature) at three time scales (monthly, biweekly and weekly), and across three regions (Canada south of 60°N, Canada's agricultural extent and Canada's prairie extent) was evaluated.

Although as discussed in Chapter 4, the use of monthly-aggregated daily interpolations will introduce extra interpolation-related error, this data set was still used to calculate the SPI because the error is acceptable comparing the monthly total precipitation. Also, the daily form of the gridded data is more generally available. Therefore, daily precipitation data were aggregated to monthly data for the period of 1961 to 2003. The SPI monthly values were then calculated for each grid cell over three time scales.

The PDSI and Z-index were calculated using the National Drought Model employed by the NAIS Drought Watch program. The National Drought Model is an improvement over the original Palmer Drought model (Palmer, 1968). By coupling the Versatile Soil Moisture Budget (VSMB) to the original Palmer Drought Model (Baier *et al.*, 2000), the National Drought Model improved the simulation of soil moisture in Canada, where sub-zero temperatures and snow are accounted for by using a new regional climate correction

factor of 14.2 along with snow accumulation and melt relationships (Akinremi *et al.*, 1996; AAFC, 2007b). Moreover, the National Drought Model is based on a six-layer structure which is more accurate to track the movement of soil moisture than the original two-layer model (AAFC, 2007b). Another improvement is in the calculation of potential evapotranspiration, which is now calculated using the Priestley and Taylor equation (Priestley and Taylor, 1972), which has better physical appeal than the Thornthwaite's method (AAFC, 2007b). Some of the limitations in the Palmer drought indices have been overcome by these improvements, and thus would provide a more accurate measurement of moisture conditions.

The National Drought Model requires a time series of daily minimum/maximum temperature, daily precipitation, soil AWHC values, and the longitude/latitude of the site for which it is being calculated. Daily meteorological data and the geographic coordinates for each grid cell in the study site were extracted from daily 10km gridded climate dataset for Canada (1961-2003). The AWHC values, which were calculated for each SLC polygon, were assigned to grid cells based on the location of the cells (i.e. the cells in the same polygon were assigned the same AWHC value).

Three drought indices were calculated for the entire period from 1961 to 2003, but due to the availability of crop yield data, only the data from 1976 to 2003 were used in the subsequent analysis. Gridded drought indices were then aggregated to CAR averages, by taking the average value of all grid cells within each CAR.

3.3.3 Crop Selection

On the prairies, the major crops grown are spring wheat, canola and barley. Spring wheat deserves special attention because its acreage is the highest compared with other crops in the prairies and it is growing extensively in all CARs. Also, spring wheat is widely used in the literature to represent agricultural drought on the prairies (e.g. Kumar and Panu 1997; Kumar, 1999; Quiring and Papakryiakou, 2003).

On the prairies, the growing season of spring wheat varies between 100 to 120 days, with planting dates usually range from April 30th to May 20th and maturity taking place between August 11th and 22nd (Ash and Shaykewich, 2005). Precipitation during the growing season is vital to maintain an appropriate moisture level for crop growth. A wheat crop requires an average of 275 mm to 325 mm of water from planting to maturity on the prairies, with the lowest demand in the interlake region of Manitoba and the highest demand in south central Saskatchewan (Ash and Shaykewich, 2005). Growing season precipitation, coupled with crop available soil moisture at seeding makes up the total amount of water available for spring wheat in a year.

3.3.4 Yield Data Detrending and Standardization

Before doing further analyses, spring wheat yield data were detrended and standardized. Visual inspection of Figure 3-4, 3-5 and 3-6 revealed that an underlying upward trend in yields with time exists in all CARs in Alberta and Manitoba, and some of the CARs in Saskatchewan.

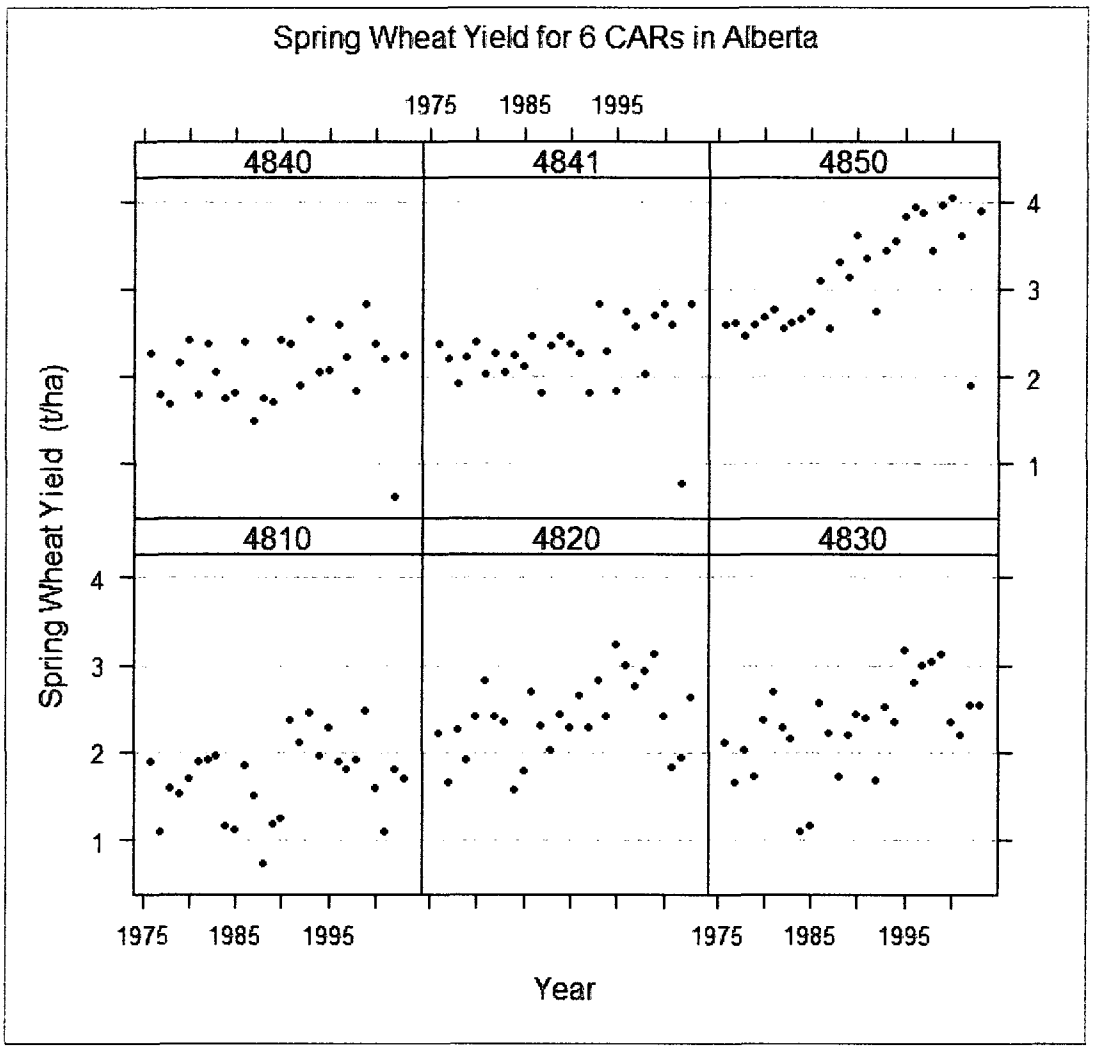

Figure 3-4 Scatter plots of spring wheat yield versus year (1976-2003) for the 6 CARs in Alberta.

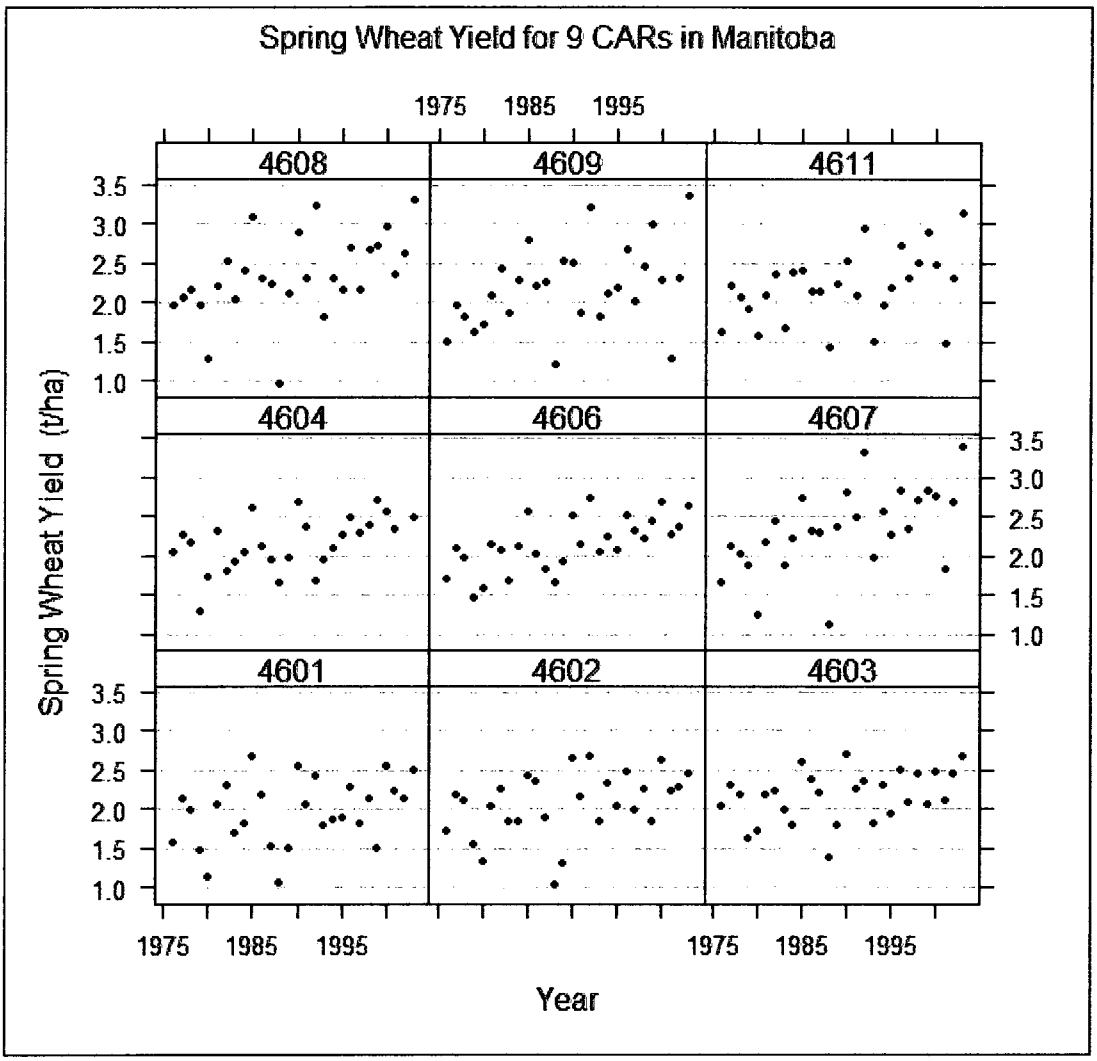

Figure 3-5 Scatter plots of spring wheat yield versus year (1976-2003) for the 9 CARs in Manitoba.

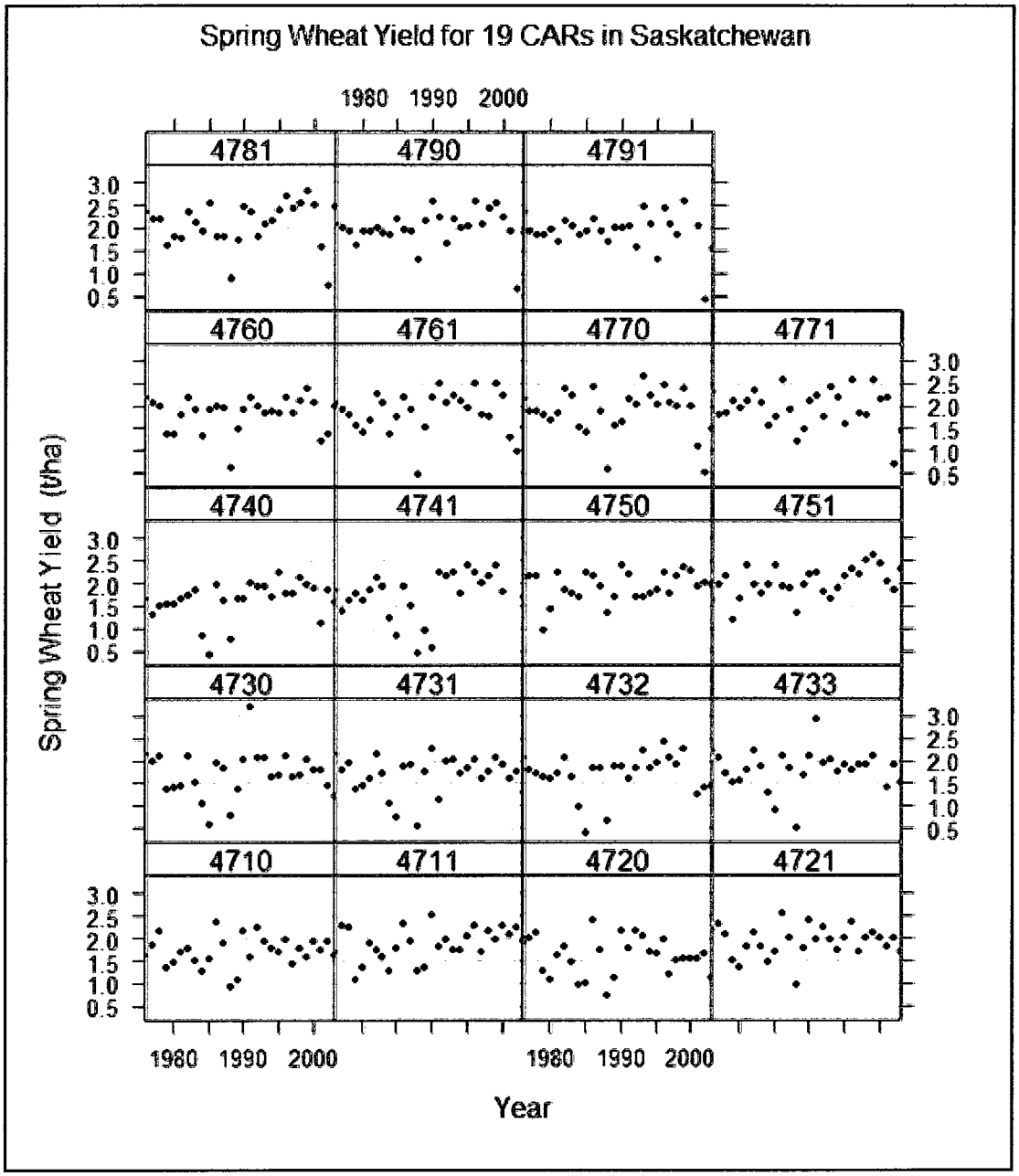

Figure 3-6 Scatter plots of spring wheat yield versus year (1976-2003) for the 19 CARs in Saskatchewan.

This trend has been noted in the literature and has been attributed to advances in agricultural technology, such as greater rates and frequency of fertilizer application, the use of new crop varieties, improved weed control and better tillage practices (Babb *et al.*, 1997; Starr and Kostrow, 1978; Quiring and Papakryiskou, 2003; Wu *et al.*, 2004; Mavromatis, 2007; Qian *et al.*, 2009). However, spring wheat yields in most of the CARs in Saskatchewan did not show an increasing trend. This may be attributed to the expansion of oilseed and pulse crops that have been increasingly planted to replace conventional summer fallow (Qian *et al.*, 2009). Although there has been a decrease in the summer fallow areas in the prairies, the rate of decline in summer fallow was greater in Saskatchewan than Alberta and Manitoba (Campbell *et al.*, 2002). This indicates that the increased fertilizer use in Saskatchewan was used for the expansion of oilseed and pulse crops instead of increased fertilization rates for the spring wheat (Qian *et al.*, 2009). Therefore, the average spring wheat yield in Saskatchewan did not show a significant increase as compared to the other two provinces.

The observed trend needs to be removed to eliminate bias due to non-climatic factors. Linear regression has been used to remove the trend in yield (c.f. Hill *et al.*, 1980; Hubbard and Wu, 2005). Because linear least squares are sensitive to outliers, outlying points (high leverage points) in Figure 3-4, 3-5 and 3-6 were excluded from the regression. These points are associated with the years when severe drought occurred (e.g. 1988, 2001 and 2002).

The residual variation from the regression reflects the effects of weather on yield (Dennett *et al.*, 1998; Mota, 1983) and amplifies yield departures from normal, making the variability of yield more obvious (Wu *et al.*, 2004). The residuals were standardized for each CAR by using z-scores, expressed as the number of standard deviations from the mean:

$$z = \frac{x - \mu}{\sigma} \qquad [13]$$

where x is the yield residual; μ is the mean of the yield residuals; σ is the standard deviation of the yield residuals.

The z-score transformation is useful when comparing the yields from distributions with different means or different standard deviations. For the yields without obvious trend in the most of the CARs in Saskatchewan, they were also standardized using the z-score transformation. The standardized yield residuals and standardized yield (if no obvious trend) were used in the subsequent analysis.

3.3.5 Agricultural Drought Intensity Classification

One of the objectives of this study is to develop a standard criterion to define the intensity of agricultural drought on the prairies. Drought intensity classification, often called drought categorization, defines the severity levels of drought, with nomenclatures such as "mild, moderate, severe, extreme drought" or "level 1, level 2, level 3 drought" (Hayes, 2006; Steinemann *et al.*, 2005; Steinemann and Luiz, 2006). Drought categories often associate with the percent chance of occurrence for each level of drought, such as

the percentile categories employed by the U.S. Drought Monitor (Svoboda *et al.*, 2002), the SPI drought classification (McKee, 1993) and the PDSI drought classification (Palmer, 1965).

Following these well known classification principles, drought intensity on the prairies is classified into five categories: non-drought, mild, moderate, severe and extreme. The categories of drought were defined on the basis of percentiles representing cumulative frequency of a particular yield (i.e. the probability that yield takes a value less than or equal to a given amount). To determine the cumulative frequencies of yields, an empirical cumulative distribution function (ECDF) of the standardized historical yields of all CARs during the 28 years was developed by using a step function:

$$F_n(t) = \frac{1}{n} \sum_{i=1}^{n} 1_{[x_i \leq t]} \qquad [14]$$

where $F_n(t)$ is the cumulative probability for a given yield t, x_i is the yield which takes a value less than or equal to the given amount t, and n is the total number of years for which yield data is available. The threshold yields for each drought category were calculated from the ECDF according to the cumulative frequency of that drought category.

3.3.6 Agricultural Drought Regions Creation

Another objective of this study is to determine an appropriate scale of analysis for agricultural drought risk assessment on the prairies. The widely used spatial scales for

drought evaluation include climate divisions (Svoboda *et al.*, 2002; Steinemann and Luiz, 2006), crop districts (Quiring and Papakryiakou, 2003), river basins (Steinemann, 2003), and political jurisdictions (e.g. countries, provinces) (Wu *et al.*, 2004). For the prairies, evaluating droughts by province is not appropriate, because administrative boundaries do not accurately reflect the physical features and climate of the region. Another available scale on the prairies is the CAR, and it can be used to create an appropriate scale for drought evaluation on prairies.

Over the prairies, the impacts of drought on the CARs are not consistent, and depend on the topographic, climate, geology and soil of each CAR. However, adjacent CARs are often characterized by a relatively homogeneous pattern with regard to topography, climate, geology and soil, and thus the yields may suffer similar impacts from droughts. It is possible to assume that a manageable number of agricultural drought regions can be identified by grouping the neighboring CARs based on the similarity of yield variations throughout the study period.

Cluster analysis has been widely used as a method to reduce a large number of subregions by classifying them into a small number of homogeneous clusters whose characteristics are similar within cluster but different among clusters. There are two broad types of cluster analysis. These are based on hierarchical and nonhierarchical methods. Hierarchical clustering starts with n clusters (where n is the number of observations). Each observation is therefore in its own cluster. Then two clusters are

merged, so that n-1 clusters remain. This process continues until only one cluster remains and this cluster contains all n observations. Once two observations have been placed together in the same cluster, they stay together for the remainder of the grouping process. The history of a sequential grouping can be represented by a dendrogram which illustrates the fusion or divisions made at each successive stage of analysis. By looking at how similar clusters are when creating additional clusters or collapsing existing ones from the dendrogram, one can determine how many clusters are needed to represent the data. Compared to hierarchical clustering, nonhierarchical clustering requires specifying the number of clusters prior to analysis. Nonhierarchical clustering requires less computational resources, so it is preferred when the number of observation is very large (Romesburg, 1984). As I aim to explore solutions with a reasonable number of clusters for a small dataset, hierarchical clustering was employed in this study.

There are different ways of defining distance between clusters, such as the single linkage method, the complete linkage method, the average linkage method, the centroid linkage method, the median linkage method and Ward's minimum-variance method. To keep the within-group variability as small as possible, Ward's minimum-variance method was applied to evaluate the distances between clusters. This method attempts to form the clusters in a manner that minimizes the loss associated with each grouping. Information loss is defined by Ward (1963) in terms of an error Sum of Squares (*ESS*) criterion.

A hierarchical cluster analysis was performed on the standardized yields (1976-2003) from all CARs. Ward's method of cluster analysis was used to determine which CARs were most similar by maximizing the proportion of variation in standardized yields explained by a particular clustering of the CARs. These clusters, called agricultural drought regions, were used in the subsequent model development.

3.3.7 Agricultural Drought Risk Assessment Model Development

3.3.7.1 Model Definition

Before the growing season, the agricultural drought risk assessment (hereafter referred to as ADRA) model assesses drought possibilities by evaluating the drought indices of the recharge period (i.e. from the previous September to current March for a given year) at the beginning of April. During the growing season (i.e. May 1st to August 31st), the model is updated at the beginning of each month by assessing the drought indices from the recharge period to the preceding month. The last stage of the model is updated at the beginning of September, since the drought indices of August will be available after this month. The timing used in the model, as shown in Table 3-3, was defined based on the following considerations:

Table 3-3 The timing used in the model, and the drought indices used at each month of assessment.

Stage	Date of Assessment	Drought Indices for Assessment					
		Sep. to Mar.	*Apr.*	*May*	*Jun.*	*Jul.*	*Aug.*
1	Apr.	√					
2	May	√	√				
3	Jun.	√	√	√			
4	Jul.	√	√	√	√		
5	Aug.	√	√	√	√	√	
6	Sep.	√	√	√	√	√	√

As mentioned previously, precipitation before the growing season, especially winter precipitation in the form of snow, is the primary resource for recharge of the soil moisture. This therefore has a large influence on drought occurrences and persistence. It is possible to detect potential drought risk at the pre-planting stage by assessing the recharge period precipitation and soil moisture status. Although large uncertainties do exist, this initial assessment is valuable, allowing policy makers have sufficient time to implement strategies to reduce the impact of droughts and also allowing the farmers to make decisions on whether to purchase crop insurance or alter planting and cultivation strategies (Luo *et al.*,1994; Wu *et al.*, 2004) .

During the growing season, the impact of moisture stress on crop yield is determined by each phenological stage associated with specific water demand. On the prairies, the

growing season of spring wheat is defined as May 1st to August 31st with four broad growth stages: tillering, stem extension, heading and ripening. Ideally, the ADRA model can be used with drought indices updated at the end of each growth stage to assess the future drought possibilities at the beginning of the next stage. However, this approach is difficult to implement. On the one hand, the variability of the weather means that the actual dates of each growth stage changes from year to year, as well as from CAR to CAR across the prairies. On the other hand, drought indices were calculated on a monthly scale, and finer scales (e.g. weekly) indices were unavailable for the current study.

Table 3-4 shows the drought indices of consideration for the specific month of the recharge period. For the SPI_1, PDSI and Z-index, their values from September to March are used as individual variables in the ADRA model. For the 3-month SPI, only the value from November to March is used. This is because 3-month SPI for November quantifies the precipitation deficit for the period of September to November. Similarly, only the value of 6-month SPI of February and March are used in the model, as the SPI_6 for February measures the precipitation anomalies from September to February.

Table 3-4 Drought indices used in the recharge period.

Drought Index	Month of the Recharge Period						
	Sep.	*Oct.*	*Nov.*	*Dec.*	*Jan.*	*Feb.*	*Mar.*
SPI_1	√	√	√	√	√	√	√
SPI_3			√	√	√	√	√
SPI_6						√	√
PDSI	√	√	√	√	√	√	√
Z-index	√	√	√	√	√	√	√

In summary, the number of variables used in the ADRA model for each stage is: 28 for April (7 SPI_1, 5 SPI_3, 2 SPI_6, 7 PDSI and 7 Z-index), 33 for May (SPI_1, SPI_3, SPI_6 PDSI and Z-index of April are added in), 38 for June (SPI_1, SPI_3, SPI_6 PDSI and Z-index of May are added in), 43 for July SPI_1, SPI_3, SPI_6 PDSI and Z-index of June are added in), 48 for August (SPI_1, SPI_3, SPI_6 PDSI and Z-index of July are added in) and 53 for September (SPI_1, SPI_3, SPI_6 PDSI and Z-index of August are added in).

3.3.7.2 Identification of Outliers

It is necessary to examine the data of each CAR to remove the outliers that appear to have an inconsistent influence on the model. As mentioned previously, both drought and flood can lead to crop water stress, thus reducing crop yield. In this study, the influence of flood on yield reduction needs to be distinguished from the impacts of drought,

because drought indices do not reflect flood-related yield reduction. The criteria for identifying the outliers relate to the consistency between the standardized yields and the drought indices values before and during the growing season. In cases where the values of drought indices before and during the growing season were high and the final yields were much lower than the historical normal, it is necessary to find more information on historical flood records to determine if the data of those years can be treated as outliers.

For example, 1997 was a severe flood year in Manitoba. The Red River flooding severely damaged farm buildings, equipment and delayed spring planting in rural areas (Environment Canada, 2008b), and as a result the yield was very poor in this year (e.g. the standardized yield for CAR 4609 was -1.04). However, the yield predicted by the drought indices were higher than normal in affected CARs. Therefore, the data of 1997 were identified as outliers for most of the CARs in Manitoba and were excluded from the analysis.

3.3.7.3 Model Development

Principal component analysis (PCA) and multiple regression analysis were used to establish a predictable relationship between drought indices and yields using R 2.8.0 (R Development Core Team, 2008). The R code for the model is presented in Appendix A.

Before regression, PCA was performed on the explanatory variables to reduce the number of variables and to reduce the effects of multicollinearity. Multicollinearity refers

to a situation in which two or more explanatory variables in a multiple regression model are highly correlated, with a larger portion of shared variance and lower levels of unique variance (Coolidge, 2000). For each stage of assessment, the explanatory variables are likely to be correlated. For example, for a given month, the SPI_1, SPI_3 and SPI_6 are correlated to some extent because they all include the current month's precipitation into the calculation. The PDSI and Z-index also contain overlapping information because the PDSI considers Z-index's value into its calculation. PCA can be carried out both on the correlation and covariance matrices. Covariance matrix was used to perform PCA in this study, because this method obtained better predicted results than using the correlation matrix.

PCA extracts the smallest number of uncorrelated components (i.e. principal components) that account for most of the variation in the original multivariate data and summarizes the data with little loss of information (King and Donald, 1999; Rogerson, 2001). The first component accounts for the largest amount of variance in the data. The second component explains the second greatest amount of variability, and is uncorrelated with the first component. Each succeeding component accounts for as much of the remaining variability as possible. Therefore, most of the variance in the correlated variables can be summarized into a small number of uncorrelated variables, called principal components (PCs). The first several PCs that account for 90% of the total variance of the explanatory variables were retained in this study. This led to a reduction in the number of variables

used from between 28 and 53 (28 for April, 33 for May, 38 for June, 43 for July, 48 for August and 53 for September) to no more than 10.

By using PCA, drought indices were linearly combined into a small number of new variables (i.e. PCs), hereafter called blended drought indices. These independent blended drought indices, which weights are statistically determined by the PCA, summarize 90% of the variance in the original drought indices and were used as predictor variables in multiple regression analysis.

3.3.7.4 Model Validation

A leave-one-out cross-validation (by year) approach was used to evaluate assessment accuracy. The cross-validation involves an iterative process. For a total of 28 years, in each iteration, 27 years of data were used to develop the model, which will subsequently be tested on data for a single withheld year to evaluate its predictive accuracy. A different withheld year was selected as the validation data set in each iteration until every year in the 28 year dataset was withheld for testing. Thus, a leave-one-out cross-validation was performed for each ADRA model by replacing the test year at each iteration.

The performance of the model was evaluated using three goodness-of-fit measures: the coefficient of determination (R^2), the root mean square error (RMSE) and the mean bias error (MBE). Coefficient of determination represents the proportion of the variation in

the dependent variable that has been explained by the multiple regression model. It is calculated as:

$$R^2 = 1 - \frac{SSE}{SST} \quad [15]$$

where *SSE* is the sum of the squared estimated residuals, and *SST* is the sum of squared deviations from the mean of the dependent variable:

$$SSE = \sum_i (y_i - \bar{y})^2 \quad [16]$$

$$SST = \sum_i (y_i - f_i)^2 \quad [17]$$

where y_i are the observed values, and f_i are the predicted values.

The MBE and RMSE are directly interpretable in terms of measurement units. They are defined as:

$$MBE = \frac{1}{n} \sum_{i=1}^{n} (P_i - Q_i) \quad [18]$$

$$RMSE = \sqrt{\frac{1}{n} \sum_{i=1}^{n} (P_i - Q_i)^2} \quad [19]$$

The MBE and RMSE are both error measures used to represent the average differences between models predicted (P_i) and observed (O_i) values. The MBE values represent the degree of bias between measured and estimated values. Positive values indicate overestimation while negative values indicate underestimation. The RMSE measures the magnitude of the error and is sensitive to large errors, since the errors are squared before they are averaged. Low values of MBE and RMSE are desired, but it is possible to have

a large RMSE values and at the same time a small MBE, or relatively a small RMSE and a large MBE (Almorox *et al.*, 2004).

Chapter 4: Temporal Aggregation of Interpolated Daily Climate Grids: An Error Assessment

4.1 Introduction

Reliable and spatially explicit high-resolution climate data are becoming increasingly important for ecological, hydrological and agricultural applications, such as environmental modelling, climate monitoring and forecasting, and potential impacts of climate change assessment (Jeffrey *et al.*, 2001; Jolly *et al.*, 2005; DeGaetano and Belcher, 2006; Newlands *et al.*, 2008). Despite the data need, climate observations are often still only available at single (station) locations that are distributed unevenly and (often) sparsely through space and time (Stahl *et al.*, 2006). Interpolation techniques have been widely used to estimate climate variables at unsampled locations, providing spatially continuous information over extensive areas.

Although there is a rich literature describing and comparing interpolation techniques, few research efforts have assessed the uncertainties associated with applying interpolation products generated at a fine temporal resolution (e.g. hourly, daily) to applications requiring data at a coarser temporal resolution (e.g. weekly, monthly). The application of AAFC's *Daily 10km Gridded Climate Dataset for Canada (1961- 2003)* (AAFC, 2007a), which has been used to map and understand historical drought conditions in Canada, is one such example. Drought conditions can be represented by drought indices whose calculations involve temperature and precipitation; however,

many of these indices (e.g. Standardized Precipitation Index) require climate data at coarser temporal resolutions than the typical reporting frequency for these data. Although it is possible to aggregate daily interpolations to match this desired timescale, the error-related effects of temporal aggregation are unknown. In such cases, it has thus been hypothesized that the generation of monthly climate grids from the interpolation of monthly-aggregated station observations may be more appropriate, because the latter approach will only produce one interpolation-related error (compared to the aggregation of 28, 29, 30 or 31 daily interpolation errors using the former method).

In this chapter, the accuracy of two proposed schemes for generating weekly, bi-weekly and monthly climate grids was evaluated. These schemes are (1) the temporal aggregation of daily interpolated climate grids to create grids of coarser temporal resolution (hereafter referred to as scheme A), and (2) the temporal aggregation of daily station data to create grids at the same temporal resolution (hereafter referred to as scheme B). Because geographic location (Hutchinson, 1995; Kurtzman and Kadmon, 1999; Price *et al.*, 2000; Jarvis and Stuart, 2001; McKenney *et al.*, 2006; Newlands *et al.*, 2008) and season (McKenney *et al.*, 2006; DeGaetano and Belcher, 2006; Newlands *et al.*, 2008) have been shown to affect interpolation error, the temporal (seasonal) and spatial variation in the error of two schemes was also assessed.

4.2 Methods

4.2.1 Comparison of Two Approaches

The interpolation errors associated with three climate variables – total precipitation (TotPrec) and maximum temperature (Tmax) and minimum temperature (Tmin) – were assessed at three time scales (week, bi-week, month). The performances of each scheme were evaluated for four seasons (Spring=April, Summer=July, Fall=October, Winter=January) and across three regions: a "national" extent (i.e. Canada south of 60°N), Canada's agricultural extent (consisted of the ecozones of the Prairies, the Atlantic Maritime and the eastern part of the Boreal Shield) and Canada's prairie extent (as defined by the Canadian Prairie Ecozone). Evaluations used the mean bias error (MBE) and root mean square error (RMSE) statistics to assess the influence of temporal and spatial scales on the performance of two schemes and to determine if scheme B is significantly better than the scheme A under specific conditions. The workflow of this study is illustrated in Figure 4-1.

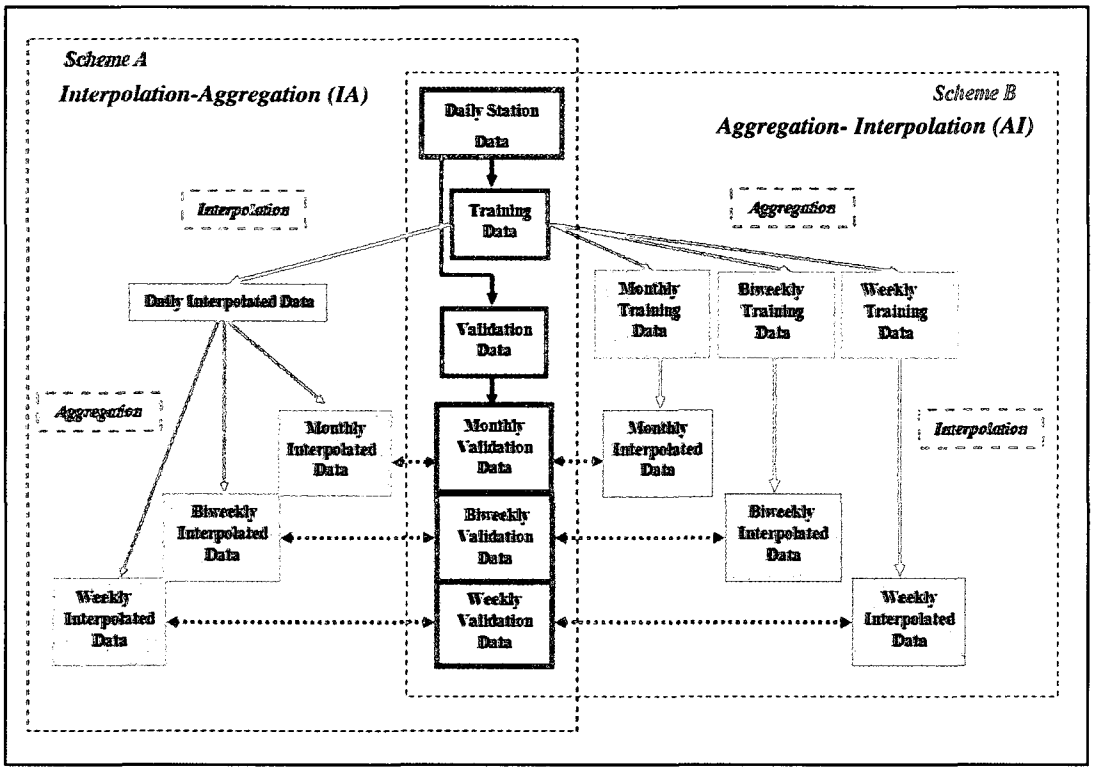

Figure 4-1 Scheme A (Interpolation-Aggregation, IA): Aggregating daily interpolations to monthly, biweekly and weekly data. Scheme B (Aggregation-Interpolation, AI): Interpolating monthly-, biweekly- and weekly-aggregated station data. Fifty withheld stations were used to generate monthly, biweekly and weekly validation data for cross validation of each approach. The errors produced by two schemes are assessed using MBE and RMSE statistics as described in the text.

4.2.1 Climate Data

Daily precipitation (mm), daily minimum temperature (°C), daily maximum temperature (°C) station data and station elevation (m) were obtained from Environment Canada's Meteorological Service of Canada (MSC) for the full historical record (1891-2004). Based on a consideration of adequate number and coverage of stations and data quality, a

reference period for comparing the two approaches was identified as 1961-1990. A more detailed description of the reference period can be found in Newlands *et al.* (2008). The reference dataset consists of 6616 climate stations.

To keep consistent with the development of, and previous research (Newlands *et al.*, 2008) on, AAFC's Daily 10km Gridded Climate Dataset for Canada (1961- 2003) (AAFC, 2007a), the same fifty climate stations from the reference dataset were withheld for cross-validation purposes. Validation stations were selected as follows: A list of 368 'high-quality' Reference Climate Stations (RCS) were provided by MSC. From this RCS set, 150 stations were selected having: 1) at least 27 years of data, 2) at least 90% temporal coverage, and 3) a location south of the boundary line determined by: latitude = -0.15 * longitude + 42.0 (Newlands *et al.*, 2008). Of these 150 stations with long-term, high-quality daily precipitation data, 53 stations were selected using a procedure (SELNOT program) by covering the full range of latitude, longitude and elevation under study. 3 stations with few neighbouring stations were removed, and the remaining 50 stations (50 in the national extent, 13 in the agricultural extent and 7 in the prairies extent) were withheld for cross-validation. Figure 4-2 shows the spatial distribution of these 50 withheld stations.

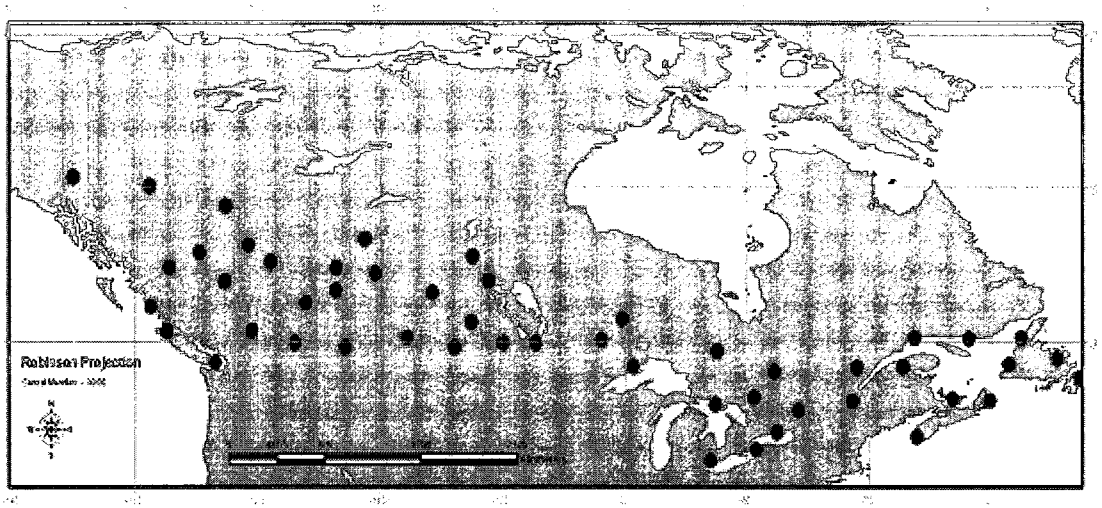

Figure 4-2 The spatial distribution of the 50 cross-validation (withheld) stations (Newlands *et al.*, 2008).

4.2.3 The ANUSPLIN Model and its Parameterization

Thin plate smoothing splines have been commonly used to smooth multivariate interpolation of irregularly scattered noisy data (Hutchinson, 1998a). Early applications to meteorological data were presented by Wahba and Wendelberger (1980), and Hutchinson and Bischof (1983). A more detailed description of the methodology can be found in Wahba (1990) and Hutchinson (1991). Further applications to climate data interpolation have been described by Hutchinson (1995, 1998a and 1998b) and McKenney *et al* (2001, 2006). Recent comparisons with methods of weighted truncated Gaussian filter and a hybrid nearest-neighbour have been presented by Newlands *et al* (2008), indicating that the thin plate smoothing spline method is preferable for interpolating daily temperature and precipitation across Canada.

Thin plate smoothing spline method works by fitting a smoothed surface to climate station data as a function of one or more independent variables. Details of the mathematical theory behind thin plate smoothing splines can be found in Wahba (1990). A general representation for a thin plate smoothing spline fitted to n data values y_i at positions x_i is (Hutchinson, 1995; 2006):

$$y_i = f(x_i) + \varepsilon_i, \; i = 1, 2, \ldots, n \qquad [20]$$

where f is an unknown smooth function to be estimated; the ε_i are assumed to be uncorrelated, normally distributed error with mean of zero and variance of σ^2. The errors account for measurement error as well as deficiencies in the spline model. The smoothing parameters of the model are determined by minimizing the generalized cross validation (GCV), a measure of the predictive error of the surface. The GCV is calculated for each value of the smoothing parameter by removing each data point in turn and summing the square of the difference of each omitted data value from the spline fitted to all other data points (Hutchinson and Gessler, 1994). Theoretical justification of the GCV and demonstration of its performance on simulated data have been given by Craven and Wahba (1979).

In this study, a trivariate spline model was used. This method has been shown to perform well when interpolating noisy climate data across complex terrain in comparisons to other interpolation techniques (Hutchinson and Gessler, 1994; Price *et al.*, 2000; Jarvis and Stuart, 2001; McKenney *et al.*, 2006; Newlands *et al.*, 2008). The trivariate spline

model incorporates the effects of latitude, longitude and elevation. Thereby, in the present application, the x_i in the above model represents longitude, latitude, and elevation. For daily precipitation interpolation, a square-root transformation was applied. This transformation is a commonly used procedure to reduce the effect of skewness in the rainfall data (Hutchinson, 1998b). There are two versions of spline model provided by the ANUSPLIN software package: SPLINA (designed for datasets with less than 2000 data points) and SPLINB (designed for datasets with less than 10,000 data points and for datasets with missing data values). As recommended by Hutchinson (2006), SPLINB can be also applied to data sets with fewer than 2000 points to save computer time and storage space and to perform more robust analyses of poor data. Considering the number of data points (i.e. stations) and missing values existing in the dataset, SPLINB was used in this study. To run SPLINB, another program, SELNOT, was required to choose an initial set of knots from the dataset. Knots are points that overlap with station locations and the number of knots specified was determined by equi-sampling independently the space of each spline variable (Hutchinson, 2006; Newlands *et al.*, 2008). In general the greater the number of knots, the more heterogeneous space is.

4.2.4 Interpolations

4.2.4.1 Aggregation of Daily Interpolated Values

Daily observed and interpolated values of TotPrec, Tmax and Tmin were provided by the Canadian Forest Service for the 50 withheld stations for the 1961-1990 period. Daily

observed and interpolated values were aggregated to weekly, bi-weekly and monthly time periods for the months of January, April, July and October of the study period. These months were chosen as they were considered the most representative months for four seasons of interest (winter, spring, summer and fall, respectively). TotPrec was calculated as the sum of daily precipitation in each period. Tmax and Tmin were calculated as the mean daily maximum and minimum temperatures, respectively, in each period.

Where daily observed values were missing, it is necessary to ensure an adequate number of days with valid observations for the above calculations. In this study, a minimum of 25 daily values were required to compute a monthly average (or sum). If the number of valid data for a given month is less than 25, that monthly mean (or sum) was excluded from analysis. Biweekly and weekly Tmax/Tmin and TotPrec were calculated in the same way: 10 daily values were required for computing biweekly data, and 5 daily values were required for calculating weekly data. The biweekly and weekly data were accounted from the first day of each month, and the first 28 daily values were used to generate two biweeks and four weeks values of the month.

4.2.4.2 Interpolation of Aggregated Daily Station Values

Daily TotPrec, Tmax and Tmin observations at each climate station were aggregated following the methods described in the previous section for missing data. Monthly, biweekly and weekly surfaces were generated using ANUSPLIN V4.3. In total, 360

monthly surfaces (30 years * 4 months * 3 climate variables), 720 biweekly surfaces (30 years * 4 months * 2 biweeks per month * 3 climate variables) and 1440 weekly surfaces (30 years * 4 months * 4 weeks per month * 3 climate variables) were generated.

Several measures of surface accuracy are provided by the ANUSPLIN package. One useful diagnostic is the signal, indicating the complexity of the surface (Hutchinson, 1998). Hutchinson (1994 and 2006) suggested that the signal should generally not exceed 80-90% of the number of knots when interpolating large datasets (over 2000 points), and signals should show regular progression in values from surface to surface. The signals from standard output with each surface were checked. The ratio of signal to the number of knots varied between about 0.4 to 0.7, indicating an appropriate degree of smoothing (c.f. McKenney *et al.*, 2006). Another robust measure of the predictive capacity of a surface provide by the ANUSPLIN package is the root generalized cross validation (RTGCV) value (Hutchinson, 2006; McKenney *et al.*, 2006). The values of RTGCV for the present study were arranged from 0.7 to 1.28°C for the temperature variables, and were arranged from 20 to 50% of the surface mean for the total precipitation, indicating a good fit between the data and the predictive surface.

In addition to check the quality of the fitted surfaces, a random subset of daily interpolations was generated to assess the interpolation of daily precipitation, Tmax and Tmin. An ad hoc comparison of these daily results to the daily interpolations provided by the CFS (used in scheme A) indicated that the evaluation of the two schemes would not

be greatly affected by any differences of interpolation (operator) skills or details of software operation.

4.3 Results and Discussion

4.3.1 Effects of Temporal Aggregation and Spatial Aggregation

4.3.1.1 Daily Maximum and Minimum Temperatures

Figure 4-3 shows the validation statistics for each of the two schemes for Tmin and Tmax. In general, scheme B performed better than scheme A. Although scheme B provided higher Tmax values for all regions (Figure 4-3 A) and lower Tmin values for the national extent in comparison to scheme A (Figure 4-3 B), the magnitude of the differences was small, less than 0.03°C. For the other two regions (agricultural and prairie extents) of Tmin, scheme B introduced less bias than scheme A. The RMSE values for both Tmax and Tmin of scheme B were consistently smaller than those for scheme A at all temporal and spatial scales (Figure 4-3 C and D). In addition, for both Tmin and Tmax, the differences in the RMSE between two schemes were similar across timescales, but vary across regions. This implies that the degree of superiority of scheme B is generally not being affected by aggregation period, but by spatial coverage.

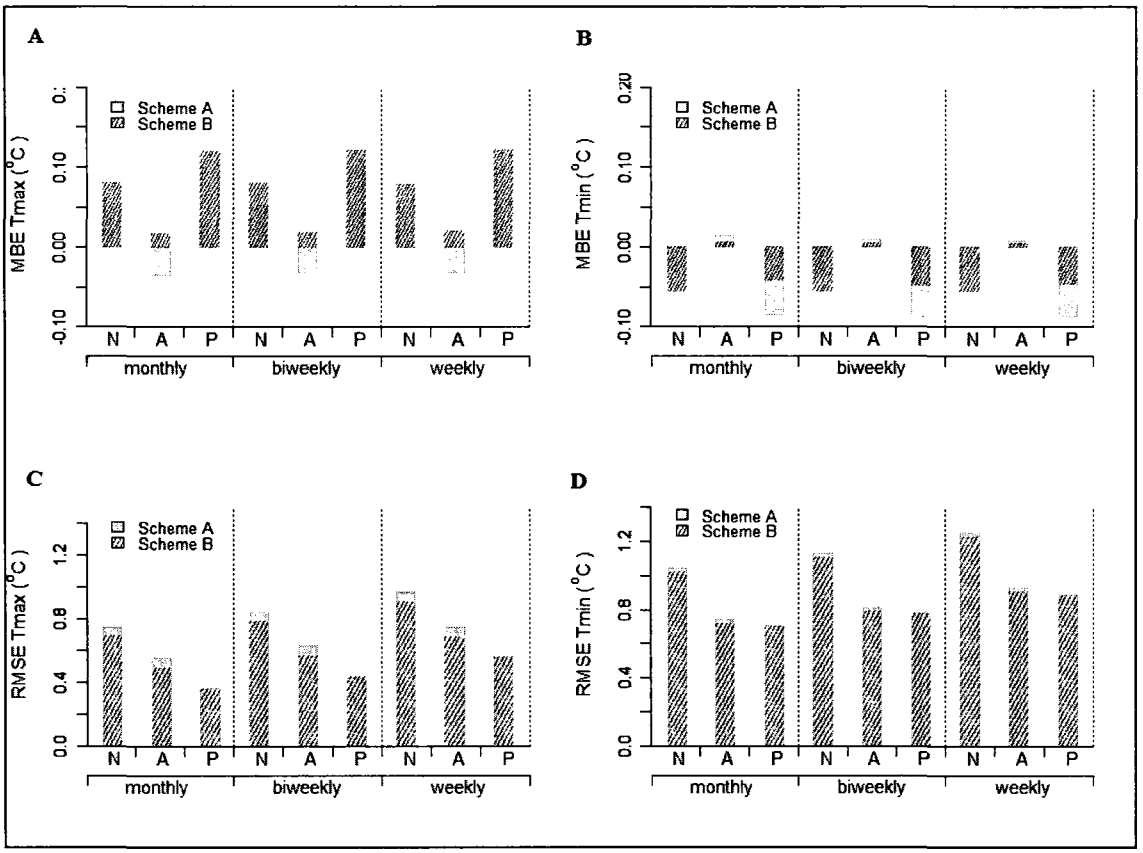

Figure 4-3 The validation statistics (MBE and RMSE) for Tmax and Tmin using scheme A (Interpolation-Aggregation) and scheme B (Aggregation-Interpolation), at three time scales (monthly, biweekly and weekly), and across three regions (national, agricultural and prairies extent), denoted by "N", "A" and "P".

Both schemes show common characteristics in Tmax and Tmin validation statistics:

1) In general, Tmax tended to be overestimated and Tmin tended to be underestimated over all temporal and spatial scales (except for the agricultural extent). This is consistent with the result of Newlands *et al.* (2008), who found an overestimation of daily Tmax and an underestimation of daily Tmin across an annual time period.

2) Quantitatively, over all temporal and spatial scales, the RMSE for Tmax was less than those for Tmin (0.3°C on average). This agrees well with the results of Jarvis and Stuart (2001), who showed that the RMSE values were in the range of 0.8°C to 0.9°C for daily Tmax, and 1.1°C to 1.2°C for daily Tmin.

3) Within each time scale, the RMSE decreased as one moves from larger to smaller geographic regions. In the case of Tmax, the decreases were somewhat linear. In the case of Tmin, the decrease was significant (0.3°C) between the national and the agricultural extents, but only slight (0.01°C) between agricultural and prairie extents.

4.3.1.2 Total Precipitation

Figure 4-4 shows the validation statistics for TotPrec using the two schemes. Both temporal and spatial scales of aggregation affected interpolation performance. Scheme B introduced less bias than scheme A on monthly and biweekly scales. In addition, at these two time scales, scheme B produced less RMSE than scheme A for the prairies extent. This suggests that scheme B performs better than scheme A when generating TotPrec over the flat terrain at coarser time scales.

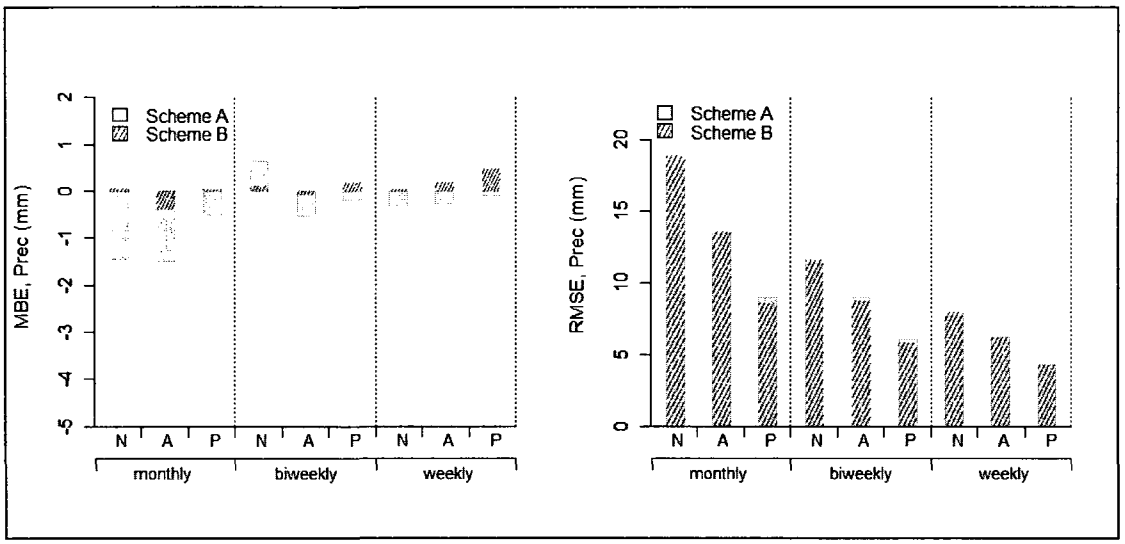

Figure 4-4 The validation statistics (MBE and RMSE) for TotPrec using scheme A (Interpolation-Aggregation) and scheme B (Aggregation-Interpolation), at three time scales (monthly, biweekly and weekly), and across three regions (national, agricultural and prairies extent), denoted by "N", "A" and "P".

4.3.2 Effects of Seasonal Variation

4.3.2.1 Daily Maximum and Minimum Temperatures

Figures 4-5 shows the seasonal MBE for Tmax using the two schemes. The most noticeable bias was occurred during the summer for the agricultural extent. Although this underestimation occurred using both schemes, scheme B reduced the bias by around 0.11°C. However, it is interesting to note that scheme B introduced more bias than scheme A for the national and prairies extents. For the other seasons, scheme B generally produced more bias than scheme A.

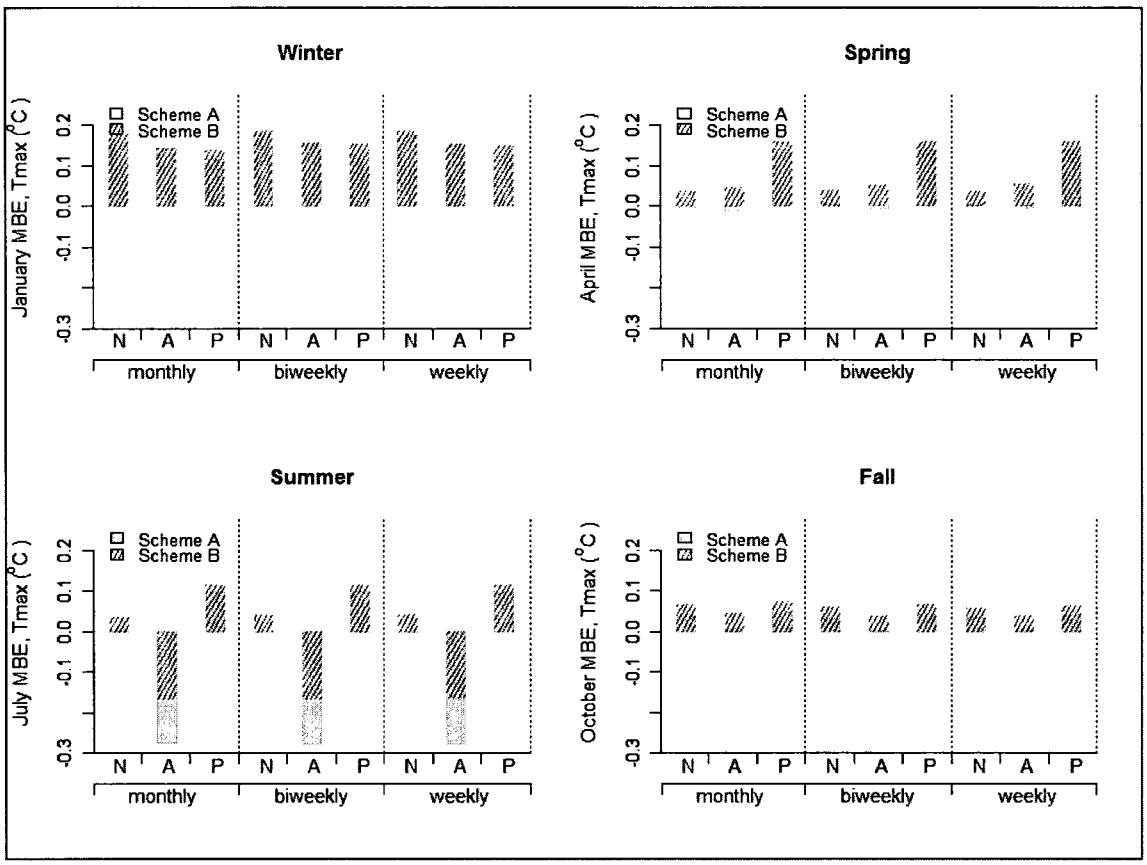

Figure 4-5 The seasonal MBE for Tmax using scheme A (Interpolation-Aggregation) and scheme B (Aggregation-Interpolation).

Figures 4-6 shows the seasonal MBE for Tmin using the two schemes. Winter and summer were the seasons that greatly influenced the annual bias. In general, Tmin was overestimated in winter and underestimated in summer over all time periods. This is consistent with Newlands *et al.* (2008), who found that Tmin tends to be overestimated for cooler climate and underestimated for warmer climate. During the winter, scheme B reduced the bias by around 0.05°C for the national and the prairie extents, and 0.04°C for the agricultural extent. In summer, scheme B reduced the bias by about 0.04°C for the

agricultural and prairie extents, but introduced slightly more bias (around 0.01˚C) for the national extent.

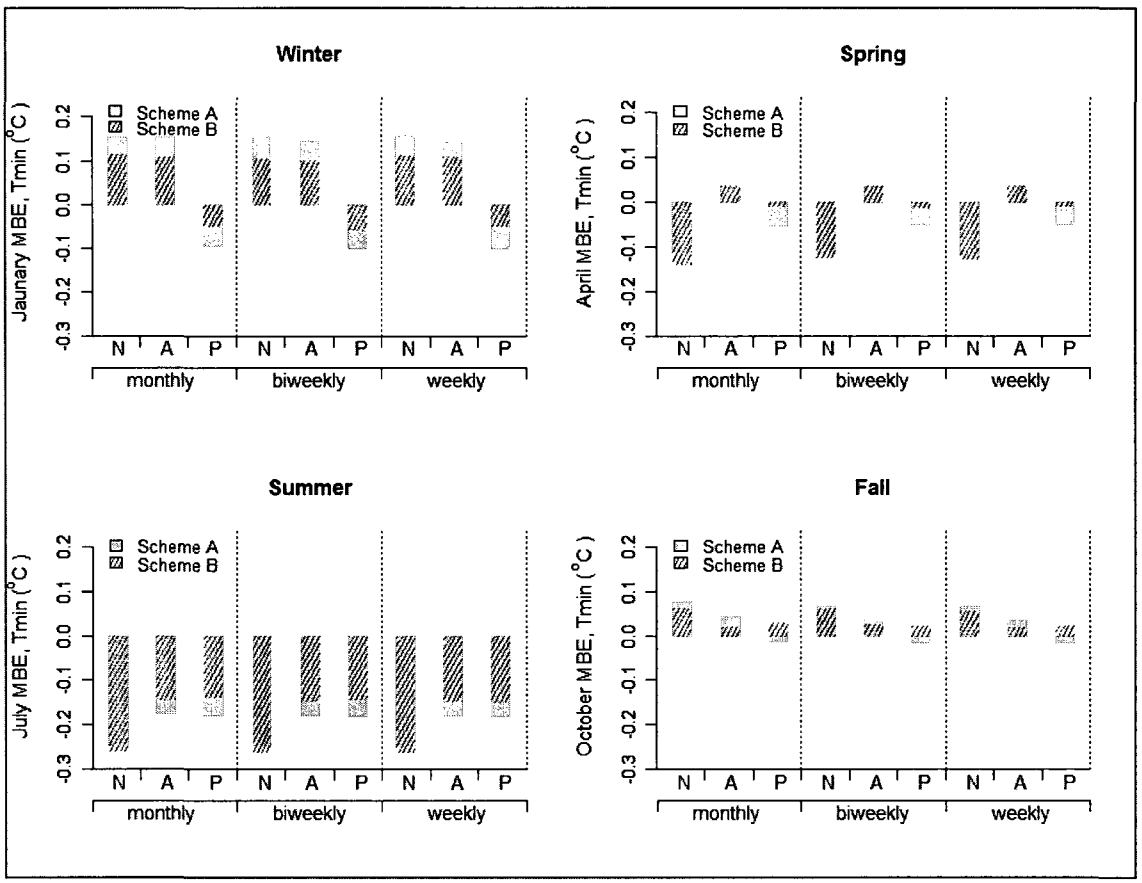

Figure 4-6 The seasonal MBE for Tmin using scheme A (Interpolation-Aggregation) and scheme B (Aggregation-Interpolation).

Figure 4-7 shows the seasonal RMSE for Tmax using the two schemes. The RMSE values of the two schemes were very similar during winter and fall. During spring and summer, scheme B introduced less RMSE than scheme A, and the degrees of superiority of scheme B over scheme A were further affected by the spatial coverage. In spring,

scheme B introduced less RMSE by about 0.11°C for the national extent, but only by about 0.04°C for the agricultural extent. During the summer, scheme B introduced less RMSE by around 0.09°C for the national extent, and by around 0.19 °C for the agricultural extent. It is also interesting to note that there were no obvious seasonal variations in the RMSE values between the two schemes for the prairie extent over all temporal and spatial scales.

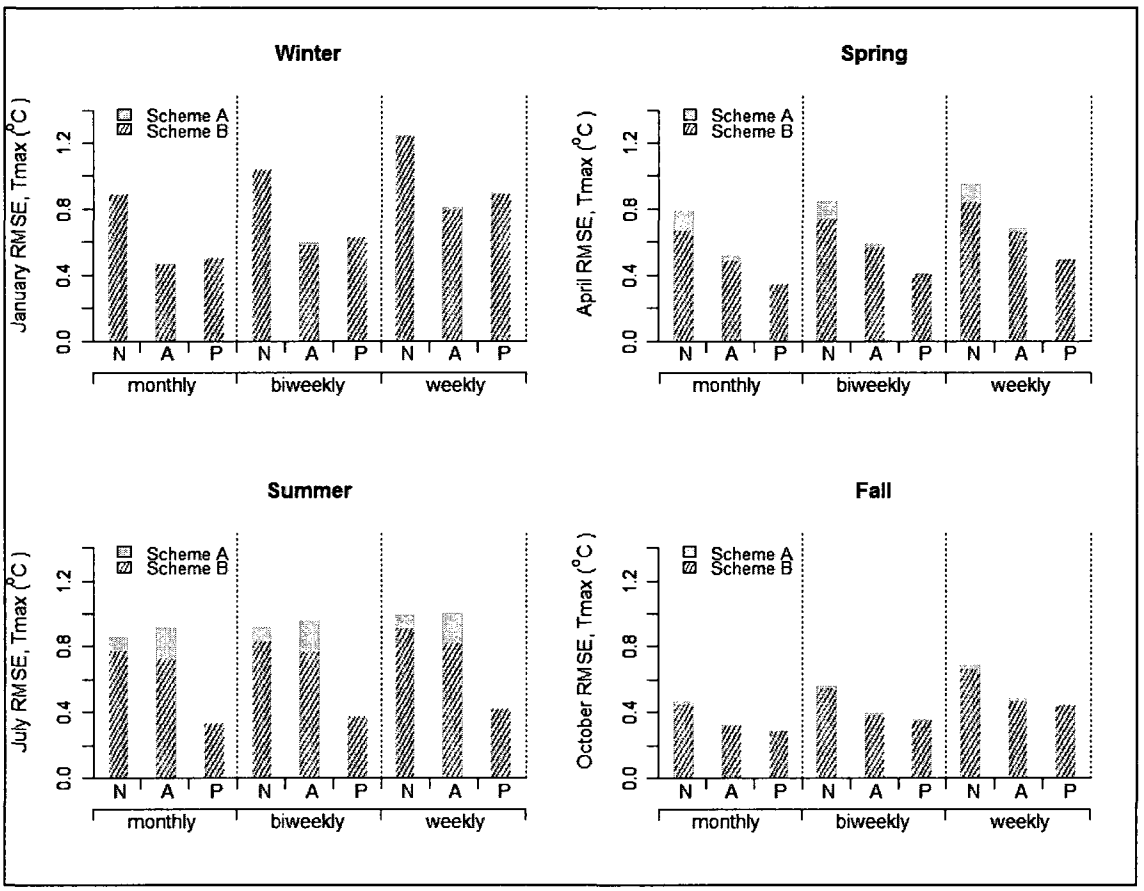

Figure 4-7 The seasonal RMSE for Tmax using scheme A (Interpolation-Aggregation) and scheme B (Aggregation-Interpolation).

Figure 4-8 shows the seasonal RMSE for Tmin using the two schemes. In general, there were no obvious seasonal variations in the RMSE values between the two schemes. Scheme B performed slightly better than scheme A for the agricultural extent in winter (with about 0.05˚C less RMSE), and for the national extent in spring (with about 0.06˚C less RMSE).

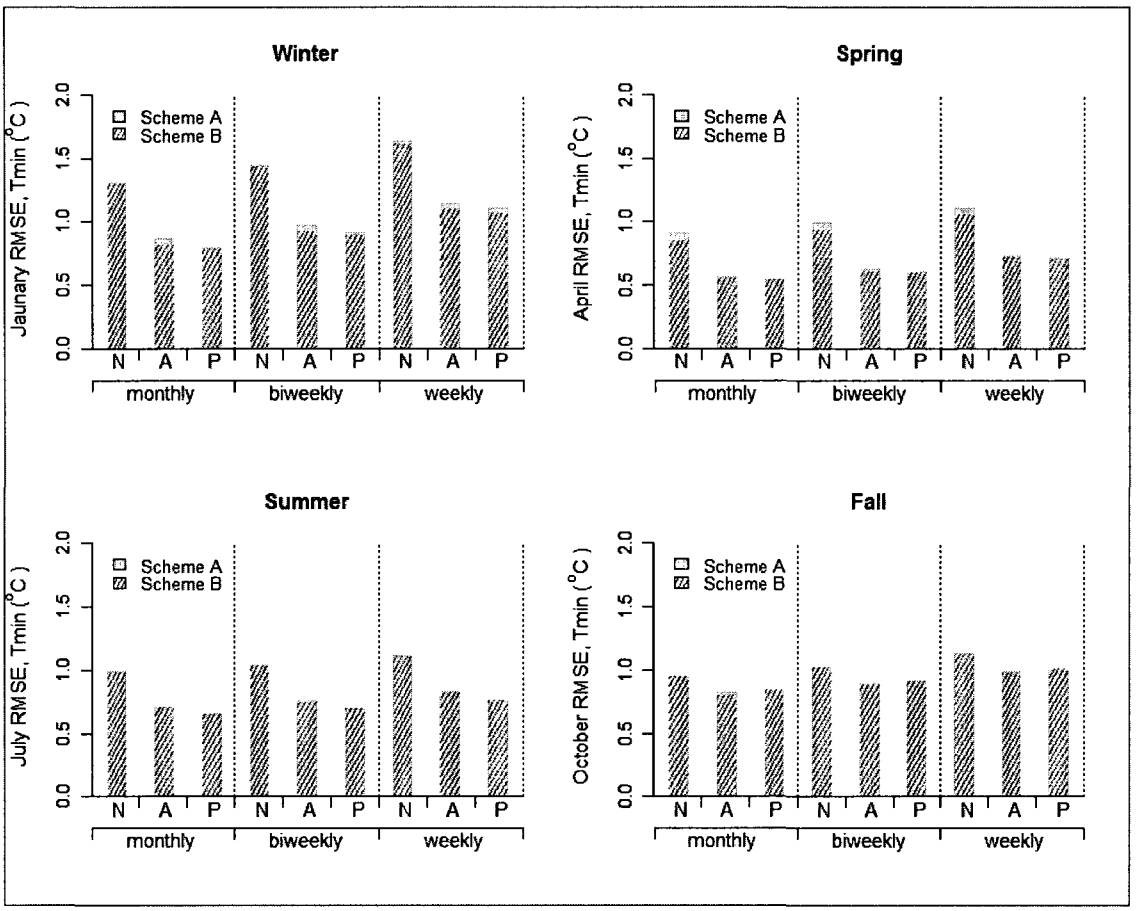

Figure 4-8 The seasonal RMSE for Tmin using scheme A (Interpolation-Aggregation) and scheme B (Aggregation-Interpolation).

4.3.2.2 Total Precipitation

Figure 4-9 shows the seasonal MBE for TotPrec using the two schemes. The large bias occurred in summer highlighted the advantages of scheme B. Compared with scheme A, scheme B reduced the precipitation bias in summer by about 3.50mm for the national extent, 3.76mm for the agricultural extent and 2.90mm for the prairies extent. Also, the fluctuation of seasonal bias values of scheme B (-2mm to 2mm) was lower than for scheme A (-5.5mm to 2.5mm) across all temporal and spatial scales.

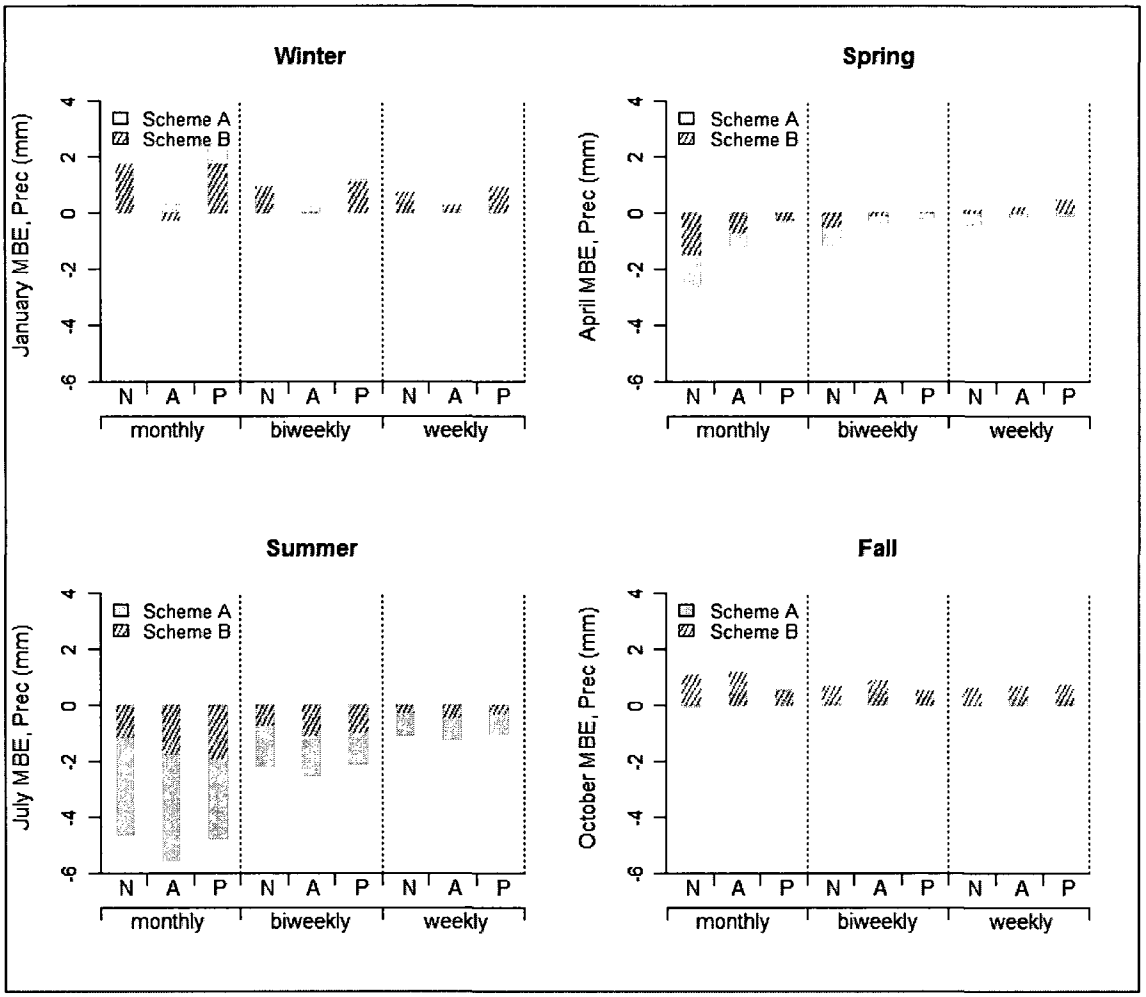

Figure 4-9 The seasonal MBE for TotPrec using scheme A (Interpolation-Aggregation) and scheme B (Aggregation-Interpolation).

The seasonal RMSE for TotPrec is shown in Figure 4-10. Higher RMSE values primarily occurred in summer and winter. This can be partially explained by the large amount of precipitation that falls in summer, and the difficulty in measuring precipitation that falls as snow in winter (McKenney, 2006). It is interesting to note that scheme B performed slightly better than scheme A in summer but did not show much advantage in winter

(except for the prairies extent). During the summer, differences in the RMSE values between the two schemes for the three regions increased from weekly to biweekly to monthly timescales.

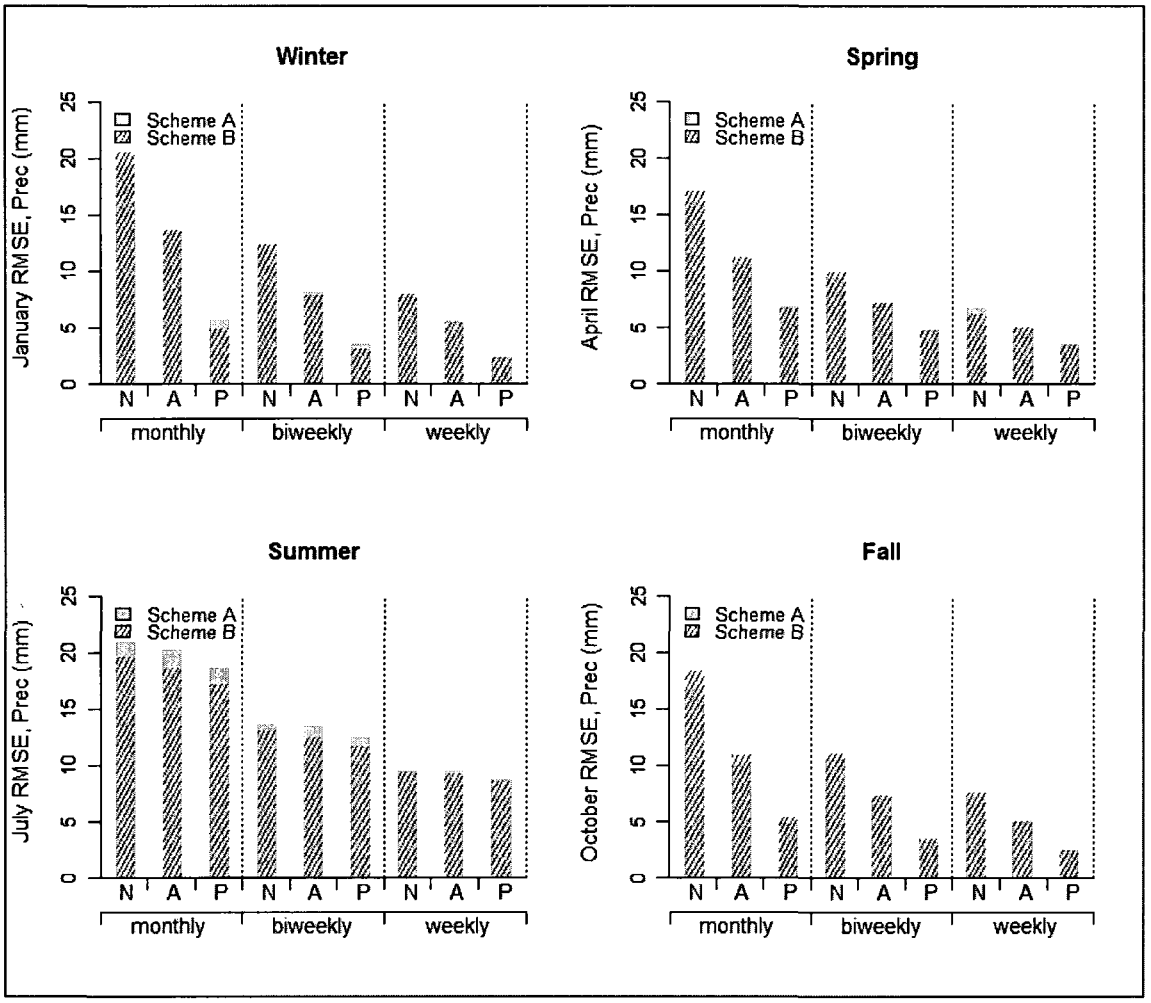

Figure 4-10 The seasonal RMSE for TotPrec using scheme A (Interpolation-Aggregation) and scheme B (Aggregation-Interpolation).

4.4 Conclusion and Recommendations

In this chapter, the performances of the two schemes (temporally-aggregated daily interpolations vs. interpolations of aggregated station data) were evaluated for three climate variables (TotPrec, Tmax and Tmin) at three time scales (monthly, biweekly and weekly), and across three regions (national, agricultural and prairies extent). The seasonal variation between the two schemes was also evaluated.

For Tmax and Tmin, the performance of scheme B, as assessed by validation statistics, proved generally superior to scheme A over all temporal and spatial scales. With lower average RMSE, scheme B proved to be more representative of the observation data than scheme A. The degree of superiority of the scheme B over scheme A depends on the variable of interest, the spatial coverage and the climate. The influences are quantified by the reduction of RMSE values in Table 4-1.

Table 4-1 A summary of the factors that affect the degree of superiority of scheme B, quantified by the reduction of RMSE (°C). The factors shaded in green have no significant influence on the difference between scheme A and B for both Tmax and Tmin. Cases where the reduction of RMSE is less than 0.01 °C are marked "×", and the differences over 0.1 °C are labelled in red. The three regions (national, agricultural and prairies extent) are denoted by "N", "A" and "P" respectively.

Factor			Reduction of RMSE (°C)	
			Tmax	Tmin
Temporal scale			×	×
Spatial Scale	N		0.05	0.02
	A		0.06	0.02
	P		×	×
Season	Winter	N	×	×
		A	×	0.05
		P	×	×
	Spring	N	0.11	0.06
		A	0.04	×
		P	×	×
	Summer	N	0.09	×
		A	0.19	×
		P	×	×
	Fall		×	×

As shown in Table 4-1, for all cases tested, the temporal scale has no significant influence on the degree of superiority of scheme B for generating temperature interpolations. In terms of the spatial coverage, scheme B is well suited for applications across large heterogeneous areas, especially for Tmax estimation. For the interpolations across flat terrain, the capabilities of the two schemes are very similar. With respect to seasonal variations, for Tmax, scheme B is desirable for applications involving spring and summer and across heterogeneous areas. For Tmin, scheme B is advantageous to applications interested in winter and spring and across heterogeneous areas.

For TotPrec, the superiority of scheme B depends on temporal and spatial scales and is further influenced by seasons. As shown in Table 4-2, scheme B is very suitable for generating precipitation interpolations on coarser time scales and under smoother spatial variation (e.g. the prairies extent). The seasonal variations are also apparent for TotPrec. Scheme B is advantageous in applications interested in summer precipitation under all terrains and in winter precipitation across homogeneous areas.

The initial evaluation of the error-related effects of temporal aggregation of daily climate variable interpolations helps decision making when using an interpolation product with a sub-optimal time scale for specific applications, saving time and resources to optimize the climate estimations. More work could be done to map the error of grid pixels. The spatially distributed error of an interpolated surface would help to more closely examine the relationship between the two schemes and the topographic structure.

Table 4-2 A summary of the factors that affect the degree of superiority of scheme B, quantified by the reduction of RMSE (mm). The factors shaded in green have no significant influence on scheme B performance. Cases where the reduction of RMSE was less than 0.3 mm are labelled "×", and the RMSE changes over 1.00 mm are labelled in red. The three regions (national, agricultural and prairies extent) are denoted by "N", "A" and "P" respectively. The three time scales (monthly, biweekly and weekly) are denoted by "M", "Bi" and "W" respectively.

Factor				Reduction of RMSE (mm)
				TotPrec
Temporal & Spatial Scale	M		N	×
			A	×
			P	0.42
	Bi			×
	W			×
Season	Winter	M	N	×
			A	×
			P	0.81
		Bi	N	×
			A	×
			P	0.40
		W		×
	Spring			×
	Summer	M	N	1.24
			A	1.64
			P	1.46
		Bi	N	0.51
			A	1.02
			P	0.81
		W		×
	Fall			×

Chapter 5: Results and Discussion

This chapter is presented in four sections. The first section presents the standardized yield data. The second section reports the five-level agricultural drought intensity classification. The third section describes the nine agricultural drought regions in the prairies. The performance of the ADRA model is evaluated in the last section. The evaluation focuses on identifying the causes of temporal and spatial variability in model performance, as well as assessing the model's prediction accuracy associated with five drought categories. The contribution of the individual drought indices to each stage of assessment is also assessed. Finally, the model is applied to three "case study" years (very dry, dry and normal) to further examine the performance of the model under different moisture conditions.

5.1 Spring Wheat Yield Data

The trend in spring wheat yield was removed for all CARs in Alberta (Figure 5-1) and Manitoba (Figure 5-2). For Saskatchewan, only the trends in CAR 4741 4751, 4781 and 4790 were removed (Figure 5-3), because there is no significant (p-value <0.05) trend in other CARs of Saskatchewan. Figure 5-4, 5-5 and 5-6 show the standardized yield of Alberta, Manitoba and Saskatchewan.

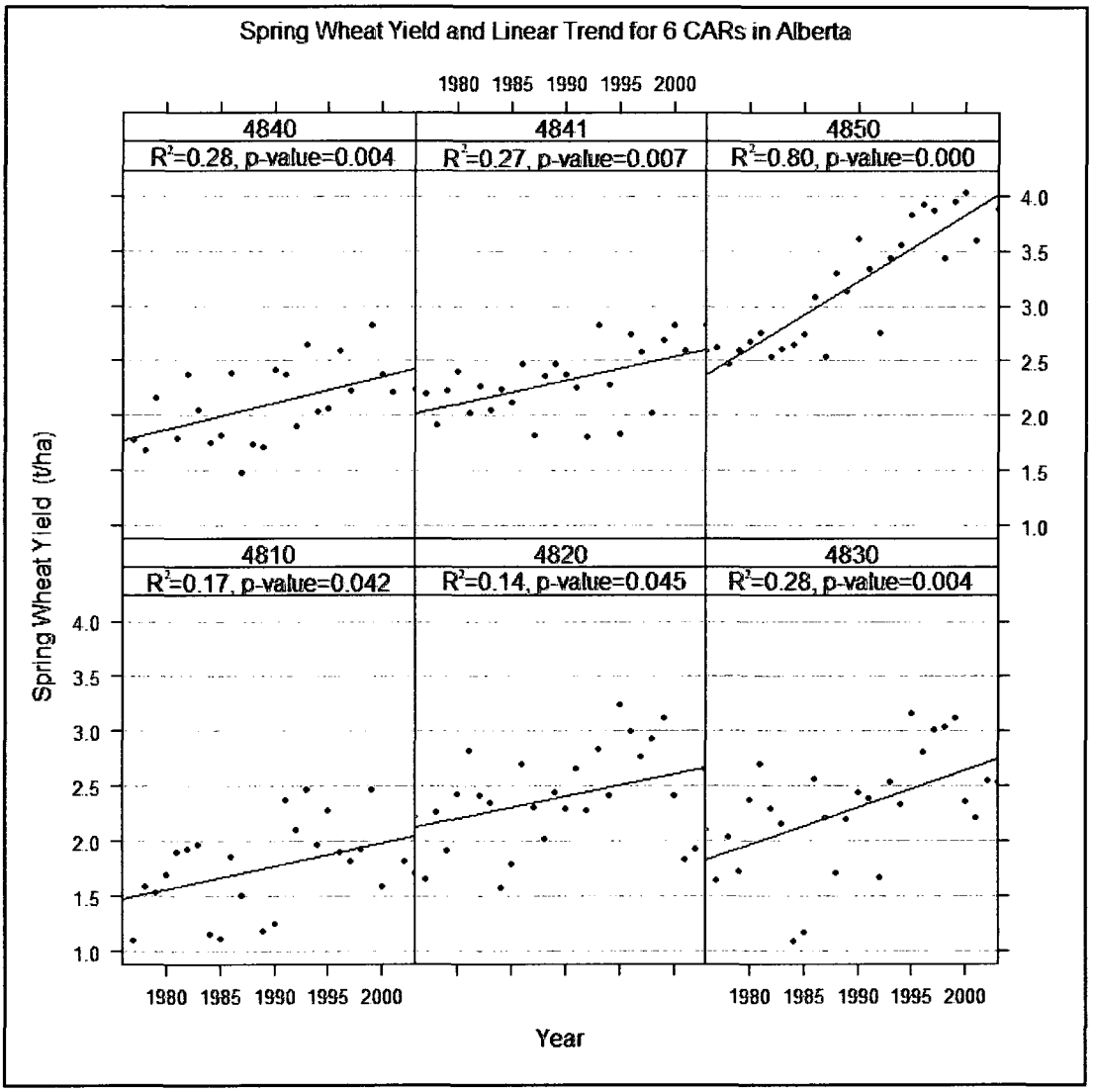

Figure 5-1 Scatter plots of regression line (with the R^2 and p-value of the regression) of spring wheat yield for the 6 CARs in Alberta.

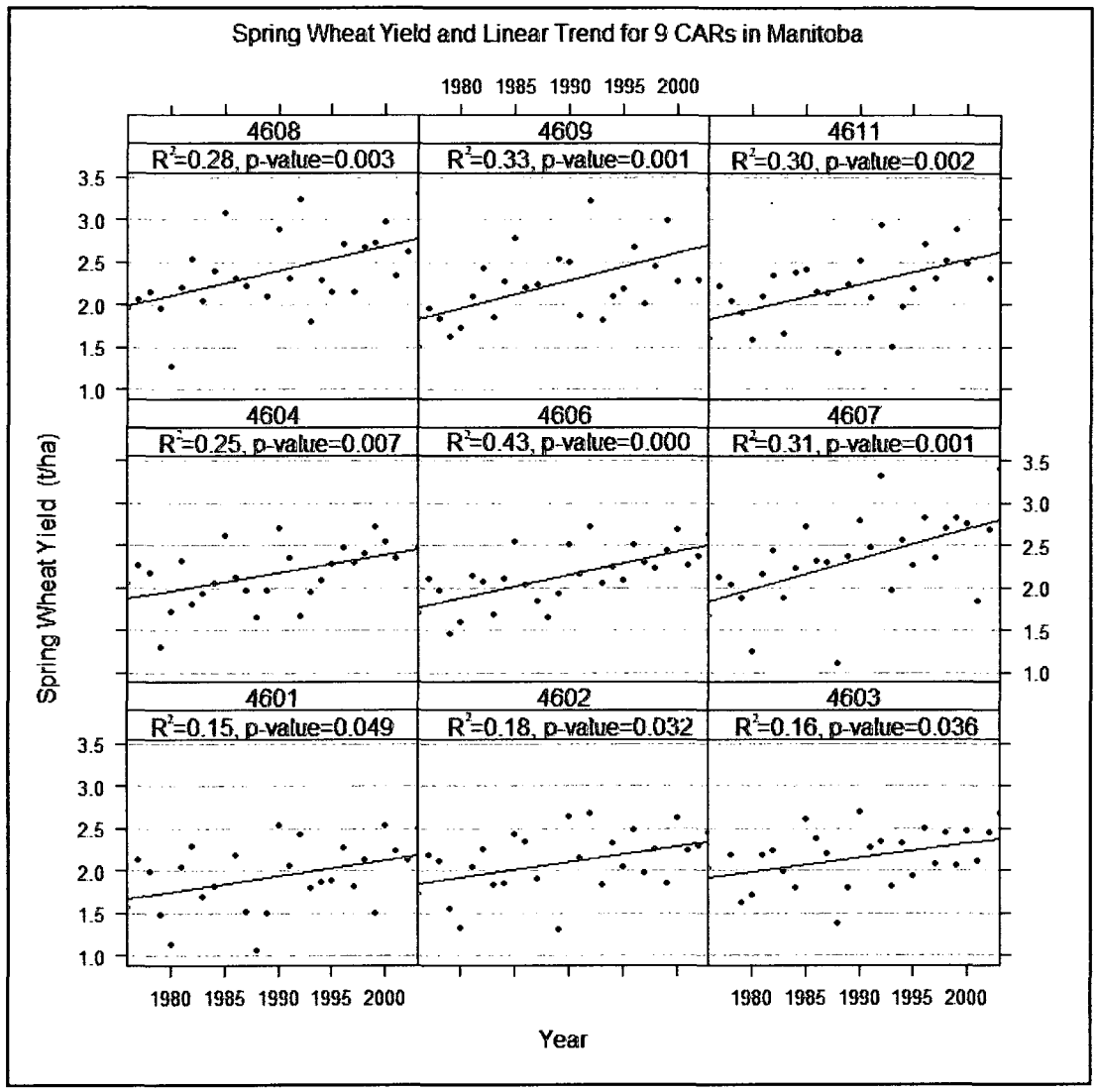

Figure 5-2 Scatter plots of regression line (with the R^2 and p-value of the regression) of spring wheat yield for the 9 CARs in Manitoba.

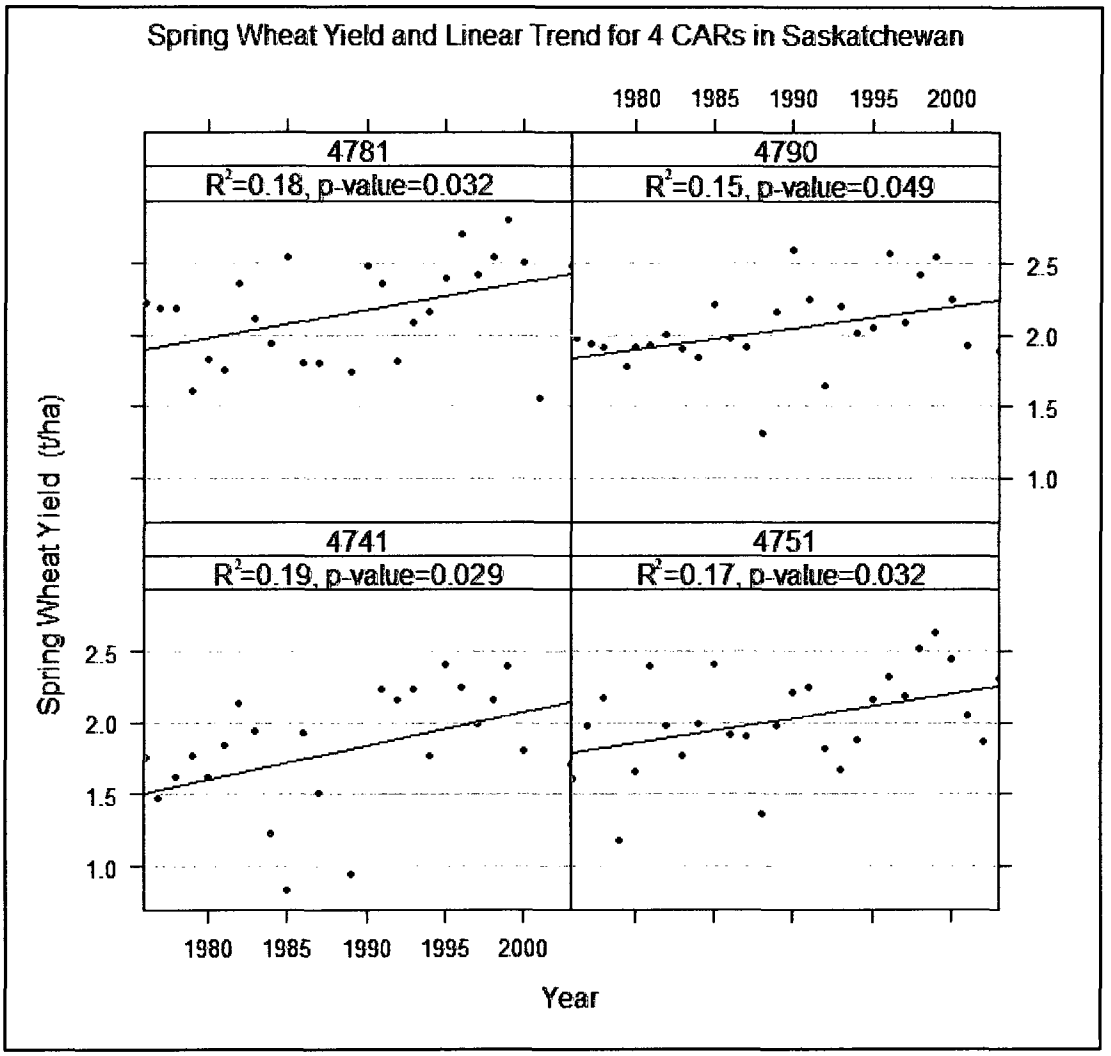

Figure 5-3 Scatter plots of regression line (with the R^2 and p-value of the regression) of spring wheat yield for the 4 CARs in Saskatchewan.

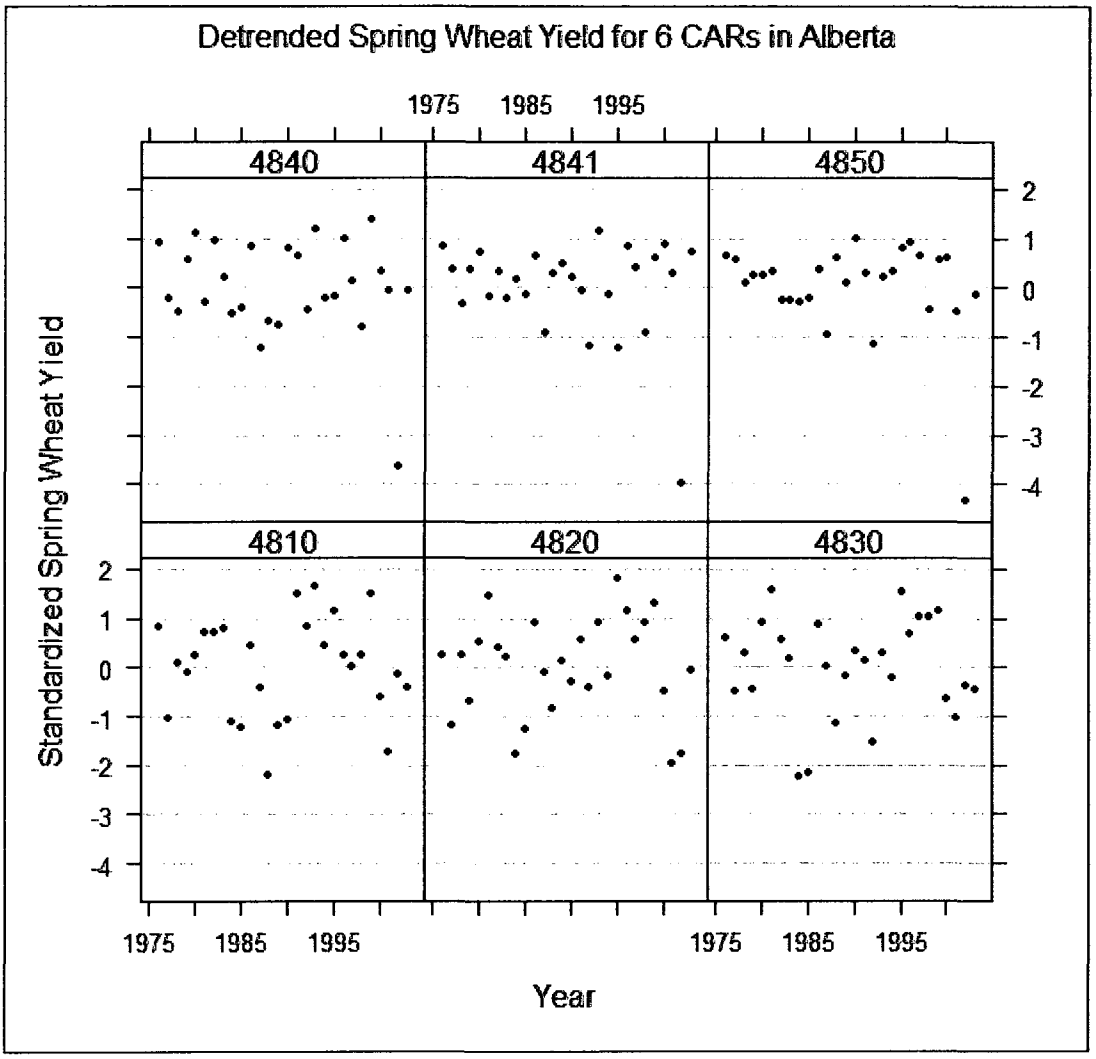

Figure 5-4 Scatter plots of the standardized yield residuals for the 6 CARs in Alberta.

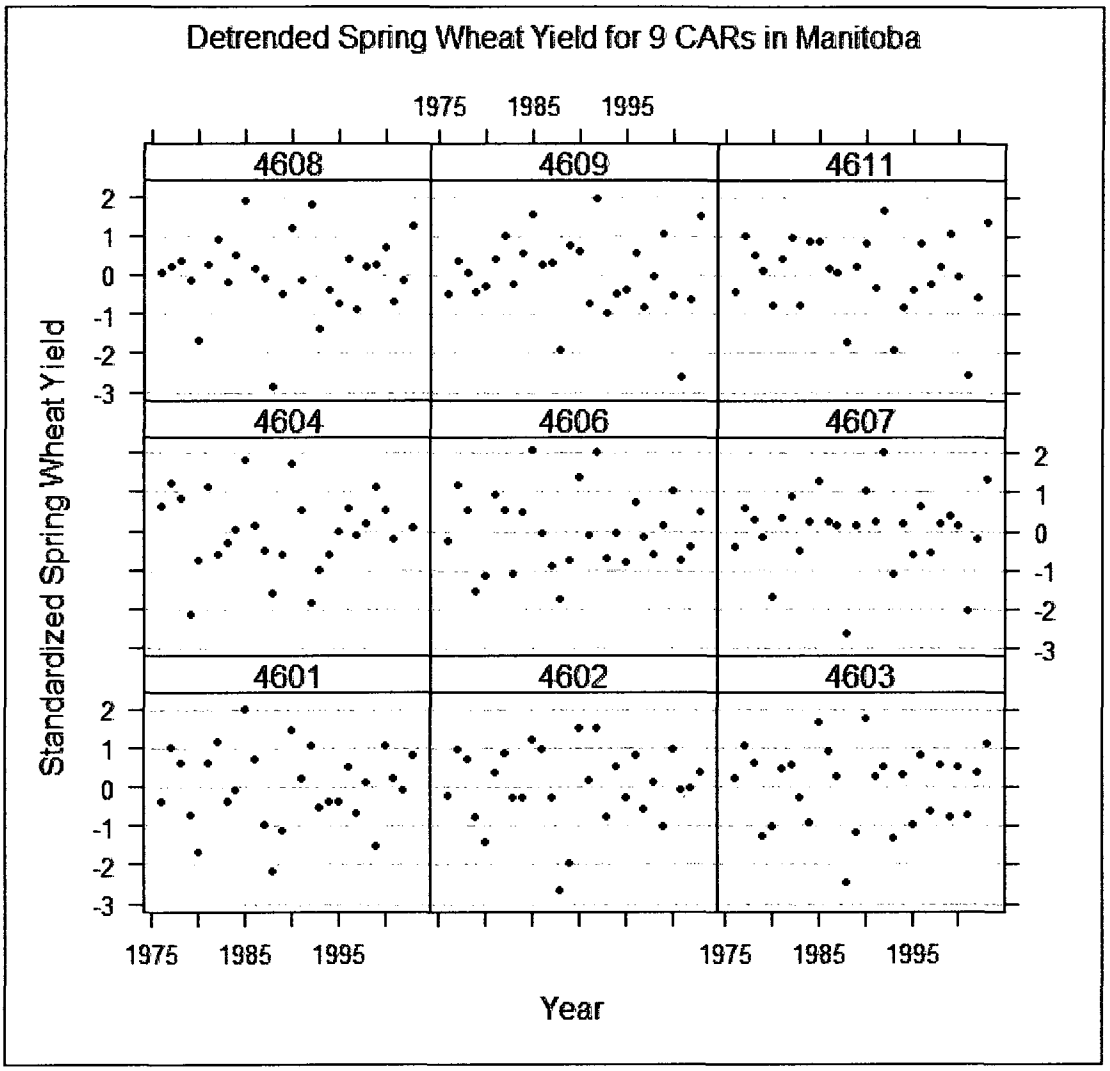

Figure 5-5 Scatter plots of the standardized yield residuals for the 9 CARs in Manitoba.

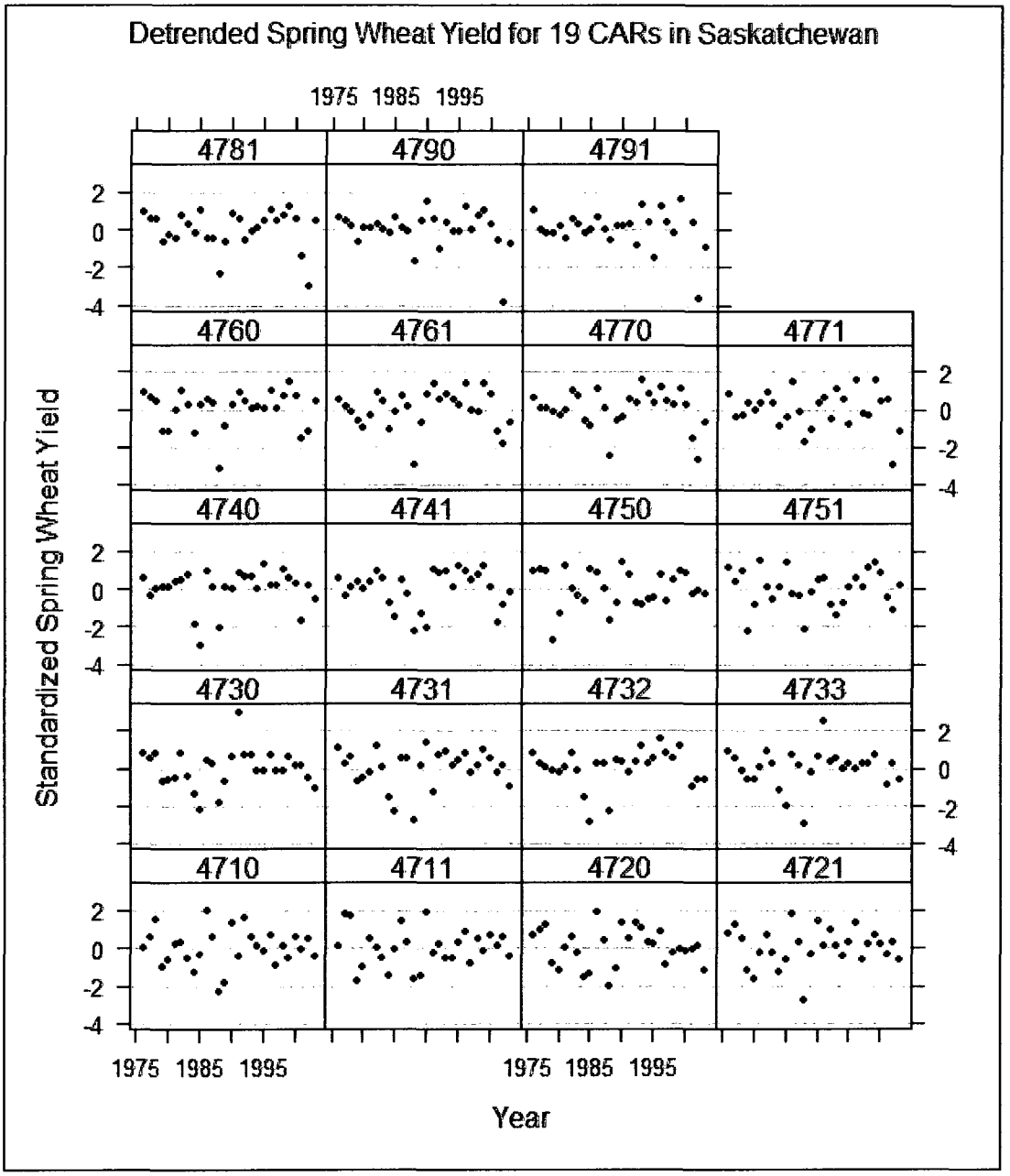

Figure 5-6 Scatter plots of the standardized yield residuals and standardized yield (if no significant trend) for the 19 CARs in Saskatchewan.

5.2 Agricultural Drought Intensity Classification

A five-level drought intensity classification – non-drought, mild, moderate, severe and extreme – was utilized for the prairies (Table 5-1). The threshold yield for each drought category was calculated from the empirical cumulative distribution function ECDF of the standardized historical yield residuals of all CARs during the 28 years (Figure 5-7). The cumulative frequencies of yields for each category generally correspond with the widely used cumulative frequency criteria on drought classification (McKee, 1993; Palmer, 1965; Svoboda *et al.*, 2002; Steinemann, 2003). According to this classification, a year can be identified as a drought year with a specific drought category when the corresponding yield is lower than the historical mean for 0.20 standard deviations.

Table 5-1 Drought intensity classification based on the cumulative frequency as related to spring wheat crop yield

Standardized Yield Residuals	Drought Category	Cumulative Frequency (%)
> -0.20	Non-drought	> 35
> -0.69 to -0.20	Mild	> 20 to 35
> -1.24 to -0.69	Moderate	> 10 to 20
> -1.84 to -1.24	Severe	> 5 to 10
≤ -1.84	Extreme	≤ 5

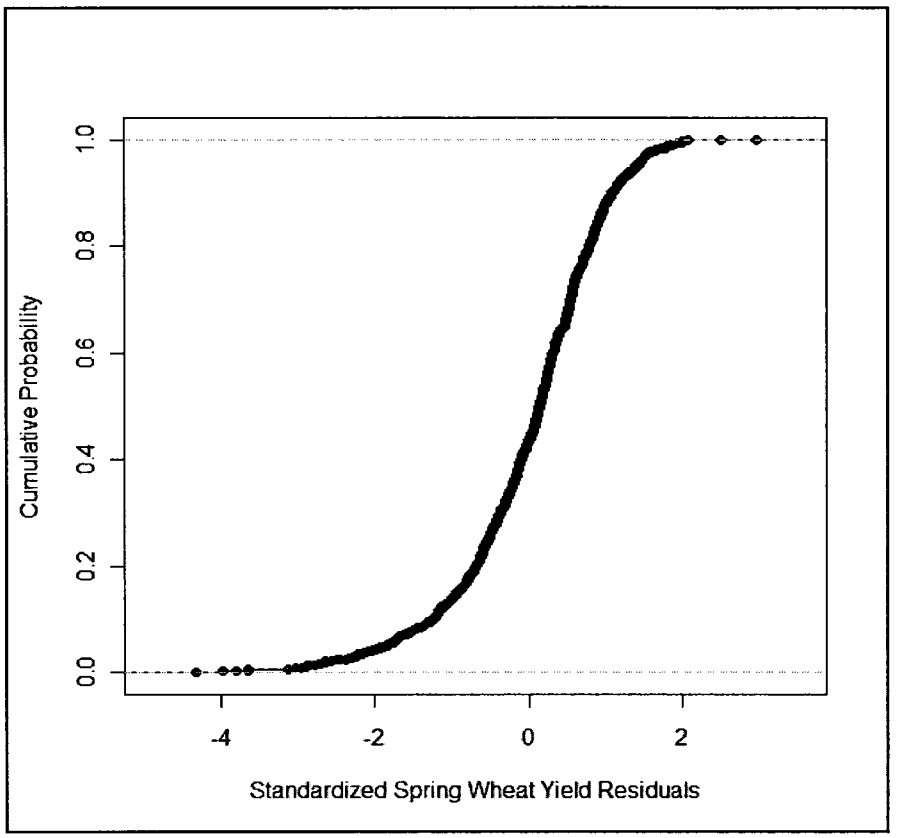

Figure 5-7 Cumulative frequency for standardized spring wheat yield residuals (1976-2003) of all CARs.

5.3 Agricultural Drought Regions

5.3.1 Agricultural Drought Regions Creation

The study area was divided into nine relatively homogeneous agricultural drought regions. A dendrogram (Figure 5-8) shows the cluster identifications. The horizontal scale of the dendrogram indicates the distance, which is determined by a sum-of-squares index (Romesburg, 1984), between the CARs that are clustered together. The larger the rescaled distances shown on the dendrogram before two clusters are joined, the larger the

variation in yield between the CARs in the cluster. Different cluster solutions were examined and a 9-cluster solution was selected, as it keeps as much similarity of the CARs within each cluster as possible, and the number of CARs is also relatively equal within each cluster.

The location of these regions is shown in Figure 5-9. Note that the clusters appeared to be primarily controlled by geographic location. This is consistent with the previous findings in the literature, where geographically close regions usually experience similar weather and crop response (Quiring, 2001; Wu *et al.*, 2004). The homogeneity of each cluster was also assessed by examining the time series of yields of the CARs in each cluster (Figure 5-10(a) and 5-10(b)). The more closely the time series of yields are plotted, the more homogeneous the cluster will be. The agricultural drought regions, referred to as C1, C2 ... C9, were then used as a spatial scale for the ADRA model development.

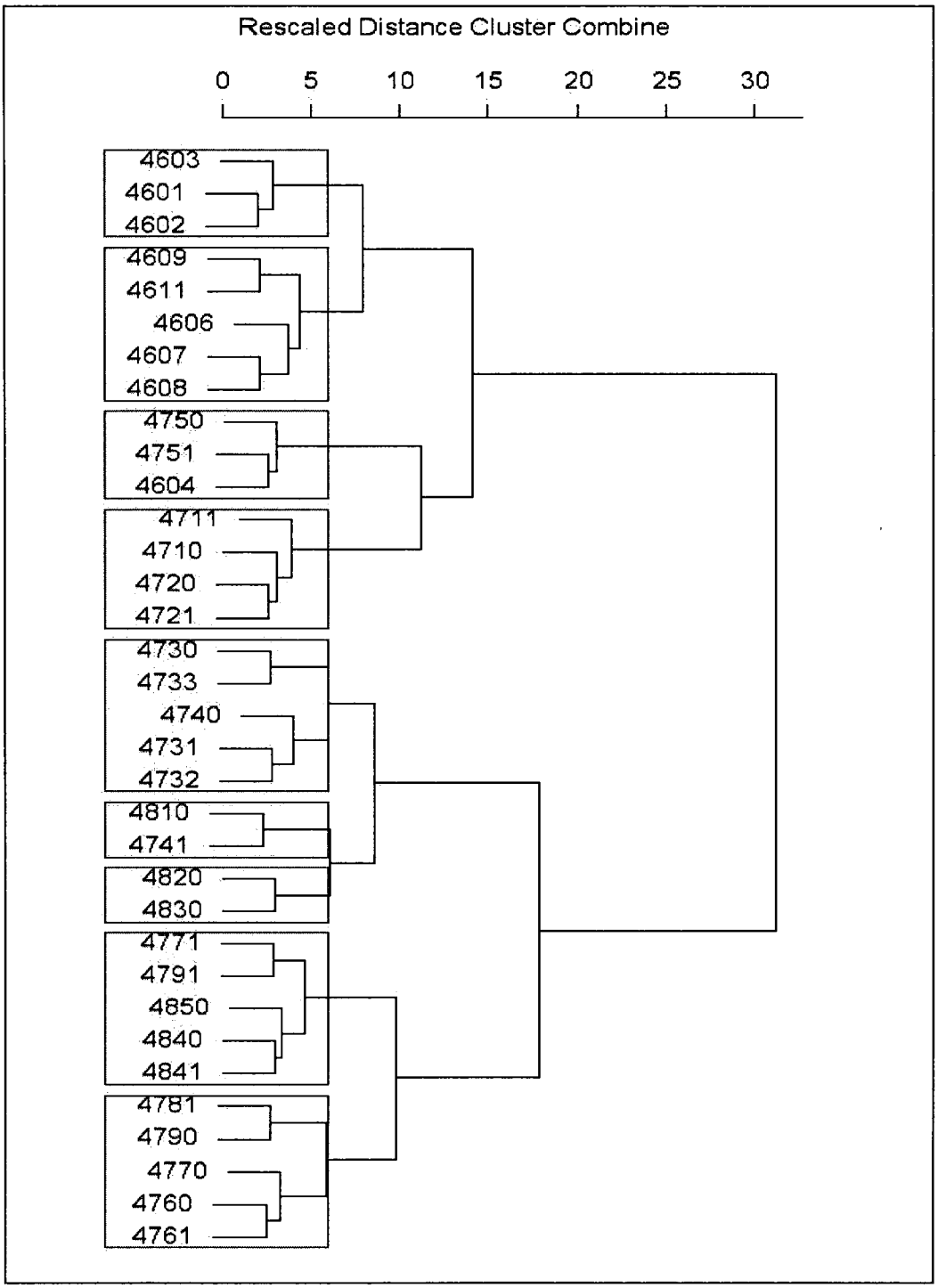

Figure 5-8 Dendrogram created by using cluster analysis on the standardized yields residuals for all CARs.

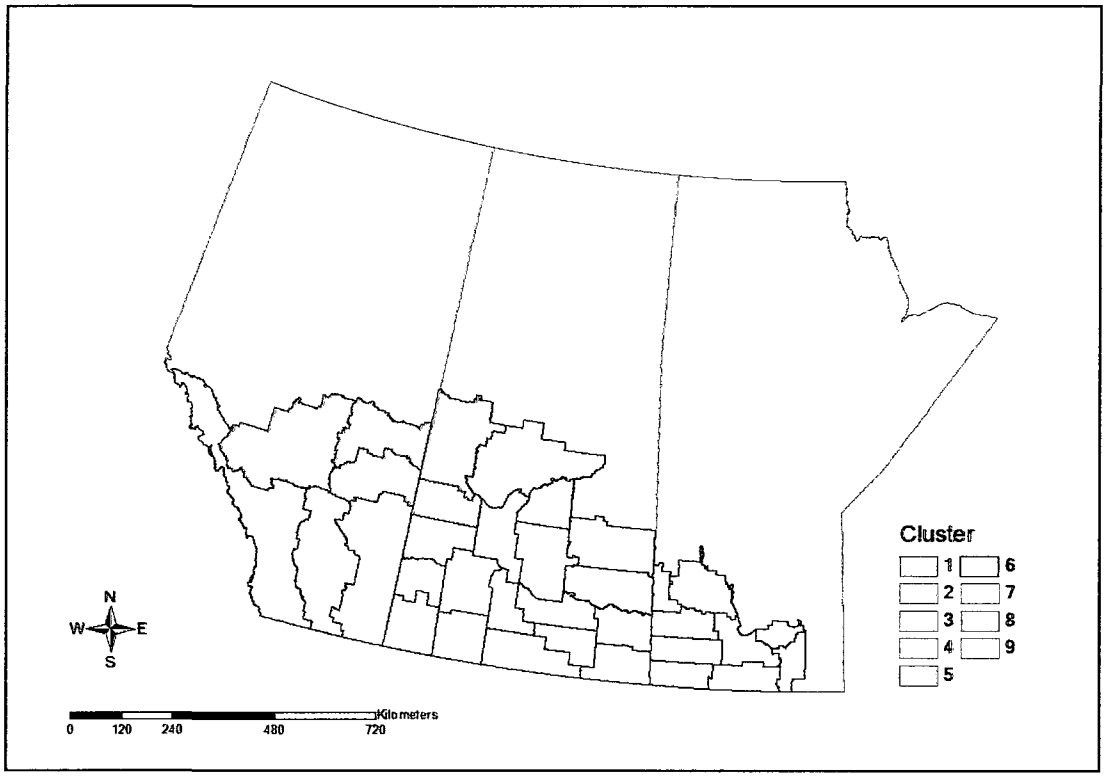

Figure 5-9 Location of the nine agricultural drought regions as determined by cluster analysis.

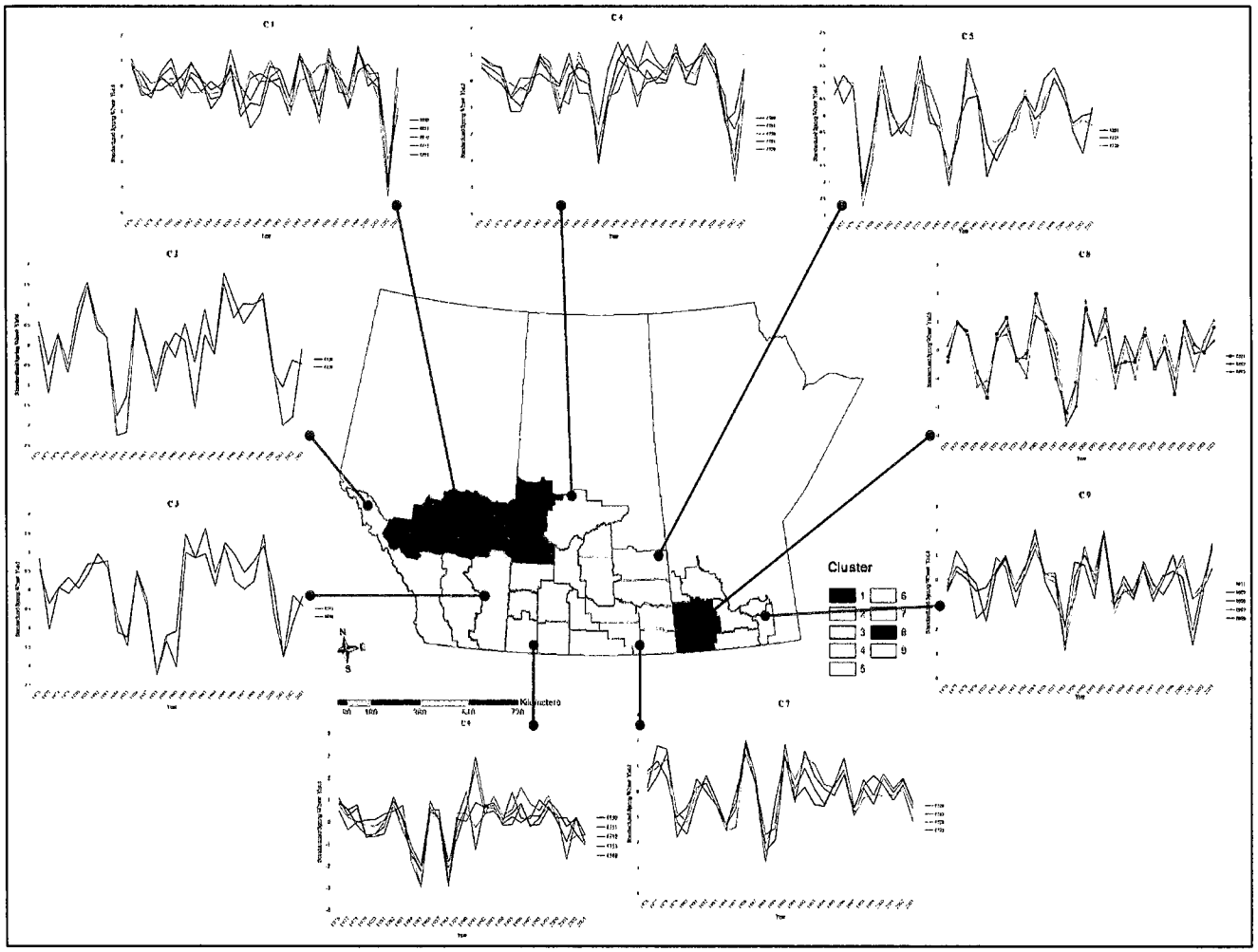

Figure 5-10(a) Time series plots of standardized spring wheat yields of the CARs within each cluster. Graphs are illustrated in more detail in Figure 5-10(b).

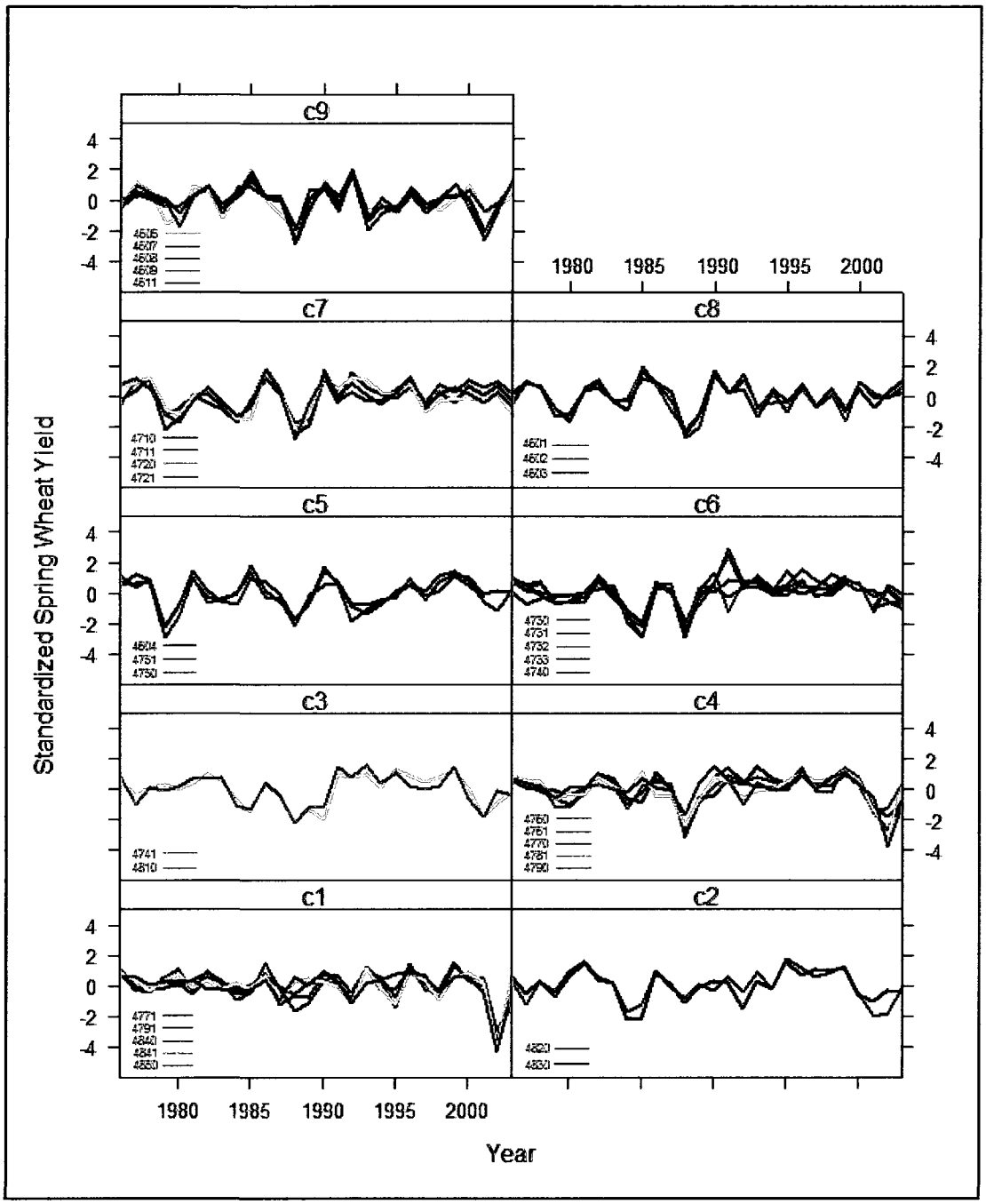

Figure 5-10(b) Time series plots of standardized spring wheat yields of the CARs by cluster.

5.3.2 Drought Frequency Analysis

Drought frequency was analyzed by cluster to examine the vulnerability of each cluster to drought. As mentioned above, flooding events also lead to poor yield, so for a given CAR, the years associated with flood-related yield reduction were excluded from analysis. Drought frequency of each cluster was calculated by summing the number of drought events of a given intensity for all the CARs within that cluster during the study period (1976-2003). Because a cluster that contains more CARs will likely have a greater number of drought events, drought frequency of each cluster was standardized by dividing the number of drought events associated with each drought category by the total number of years of calculation. Then drought frequency of a given intensity was multiplied by 100 to express it in frequency per hundred years (Table 5-2).

Table 5-2 Summary of drought frequency (per 100 years) by cluster

Cluster	Non-drought	Mild	Moderate	Severe	Extreme
C1	70.1	13.4	11.2	1.5	3.7
C2	63.5	15.4	9.6	5.8	5.8
C3	65.5	9.1	12.7	7.3	5.5
C4	71.7	9.4	9.4	3.6	5.8
C5	63.3	16.5	10.1	5.1	5.1
C6	72.6	11.9	4.4	3.7	7.4
C7	63.2	17.0	7.5	8.5	3.8
C8	71.6	14.9	7.5	3.0	3.0
C9	71.4	14.3	8.0	3.6	2.7

According to Table 5-2, C6 experienced the highest frequency (7.4/100 years) of extreme drought events during the study period. This supports the overall coefficient of variation statistics of the standardized yield from Table 3-2. All the CARs (4730, 4731, 4732, 4733, and 4740) that make up C6 had high CV values between 25 and 29%. This suggests that C6 is a region with highly variable climate (e.g. variable precipitation regime) and is vulnerable to extreme dry conditions.

C7 had the highest frequency (8.5/100 years) of severe drought events during the study period. It also experienced the highest frequency of drought events of all levels: there were 36.8 mild to extreme drought events per hundred years. The yield of this cluster was less variable than C6, with the CV values arranging from 18 to 27%.

C3 had the highest frequency (12.7/100 years) of moderate droughts during the study period. In addition, C3 is the region that experienced severe and extreme droughts most frequently, with the highest total number of severe and extreme growing season droughts which were 12.8 per hundred years. One of its CARs, 4741, had the highest CV value (33%) among all CARs, and the other CAR (4810) that composes C3 also had a relatively high CV value (26%). Similar to C6, C3 had a highly variable climate and was prone to severe and extreme drought conditions.

In general, C1, C8 and C9 were less prone to severe and extreme droughts. C9 and C1 experienced the lowest frequency of extreme (2.7/100 years) and severe (1.5/100 years) droughts during the study period, respectively. C8 ranked the second after C9 and C1, experiencing 3.0 extreme and 3.0 severe droughts per hundred years. The CV values of the CARs within C1, C8 and C9 were relatively low, with an average value of 20%, 19% and 21%, respectively.

Overall, the clusters in southeast Alberta and southern Saskatchewan appeared to be more vulnerable to agricultural drought, and especially severe and extreme droughts. Comparatively, the clusters in northern Alberta, northern Saskatchewan, and Manitoba experienced less frequency in drought occurrence during the study period. The factors that lead to spatial variations in drought frequency will be discussed further in Section 5.4.2.

5.4 Evaluation of the ADRA Model

5.4.1 Results of Cross-validation of the Model

Table 5-3 shows the number of blended drought indices used in the multiple regression analyses. The R^2, MBE and RMSE of the calibration and validation results for the 54 ADRA models (9 clusters * 6 stages) are summarized in Table 5-4. The MBE and RMSE values are expressed as the number of standard deviations away from the historical mean yield. The R^2 and RMSE are plotted by cluster (Figure 5-11 and 5-12).

Table 5-3 The number of blended drought indices used at each stage of assessment.

Cluster	Stage1	Stage2	Stage3	Stage4	Stage5	Stage6
C1	7	8	8	8	9	9
C2	6	7	7	7	8	8
C3	6	7	7	7	8	8
C4	7	7	7	8	8	9
C5	6	7	7	8	8	9
C6	6	7	7	8	8	9
C7	7	7	8	8	8	9
C8	7	7	8	8	9	9
C9	8	8	9	9	10	10

Table 5-4 Summary of leave-one-out cross-validation results for the 54 ADRA models.

			Calibration		Validation	
Cluster	Stage	R^2	MBE	RMSE	MBE	RMSE
C1	1	0.25	0.00	0.85	0.01	0.84
	2	0.26	0.00	0.85	0.01	0.84
	3	0.28	0.00	0.83	0.04	0.88
	4	0.48	0.00	0.71	0.03	0.78
	5	0.63	0.00	0.60	0.03	0.64
	6	0.63	0.00	0.60	0.02	0.63
C2	1	0.29	0.00	0.83	-0.01	0.90
	2	0.30	0.00	0.82	-0.01	0.93
	3	0.52	0.00	0.68	0.00	0.78
	4	0.57	0.00	0.64	0.03	0.73
	5	0.66	0.00	0.57	0.03	0.64
	6	0.67	0.00	0.56	0.03	0.64
C3	1	0.44	0.00	0.74	-0.01	0.73
	2	0.51	0.00	0.69	0.00	0.70
	3	0.58	0.00	0.64	0.00	0.67
	4	0.75	0.00	0.50	0.02	0.57
	5	0.85	0.00	0.38	-0.03	0.41
	6	0.85	0.00	0.38	0.00	0.41
C4	1	0.30	0.00	0.82	0.02	0.88
	2	0.37	0.00	0.78	0.02	0.85
	3	0.49	0.00	0.70	0.02	0.80
	4	0.62	0.00	0.61	0.00	0.71
	5	0.71	0.00	0.53	0.02	0.61
	6	0.72	0.00	0.52	0.01	0.62
C5	1	0.15	0.00	0.90	0.00	0.97
	2	0.14	0.00	0.90	0.02	1.00
	3	0.18	0.00	0.88	0.01	1.00
	4	0.39	0.00	0.76	0.01	0.83
	5	0.43	0.00	0.74	0.04	0.82
	6	0.44	0.00	0.73	0.03	0.80

Table 5-4 (continued)

Cluster	Stage	R^2	Calibration		Validation	
			MBE	RMSE	MBE	RMSE
C6	1	0.26	0.00	0.85	-0.05	0.86
	2	0.27	0.00	0.84	-0.05	0.87
	3	0.36	0.00	0.79	-0.04	0.81
	4	0.51	0.00	0.69	0.00	0.73
	5	0.68	0.00	0.56	0.02	0.59
	6	0.68	0.00	0.55	0.01	0.58
C7	1	0.18	0.00	0.90	0.01	0.97
	2	0.20	0.00	0.89	-0.03	0.97
	3	0.29	0.00	0.84	0.01	0.94
	4	0.43	0.00	0.75	0.03	0.82
	5	0.56	0.00	0.66	0.03	0.72
	6	0.57	0.00	0.66	0.04	0.73
C8	1	0.41	0.00	0.77	-0.05	0.85
	2	0.41	0.00	0.76	0.03	0.85
	3	0.48	0.00	0.72	-0.04	0.83
	4	0.59	0.00	0.64	0.03	0.76
	5	0.60	0.00	0.63	0.01	0.77
	6	0.61	0.00	0.62	-0.01	0.74
C9	1	0.15	0.00	0.85	0.00	0.87
	2	0.17	0.00	0.84	0.03	0.92
	3	0.21	0.00	0.83	0.04	0.90
	4	0.30	0.00	0.78	0.05	0.83
	5	0.33	0.00	0.76	0.03	0.82
	6	0.38	0.00	0.73	0.05	0.81

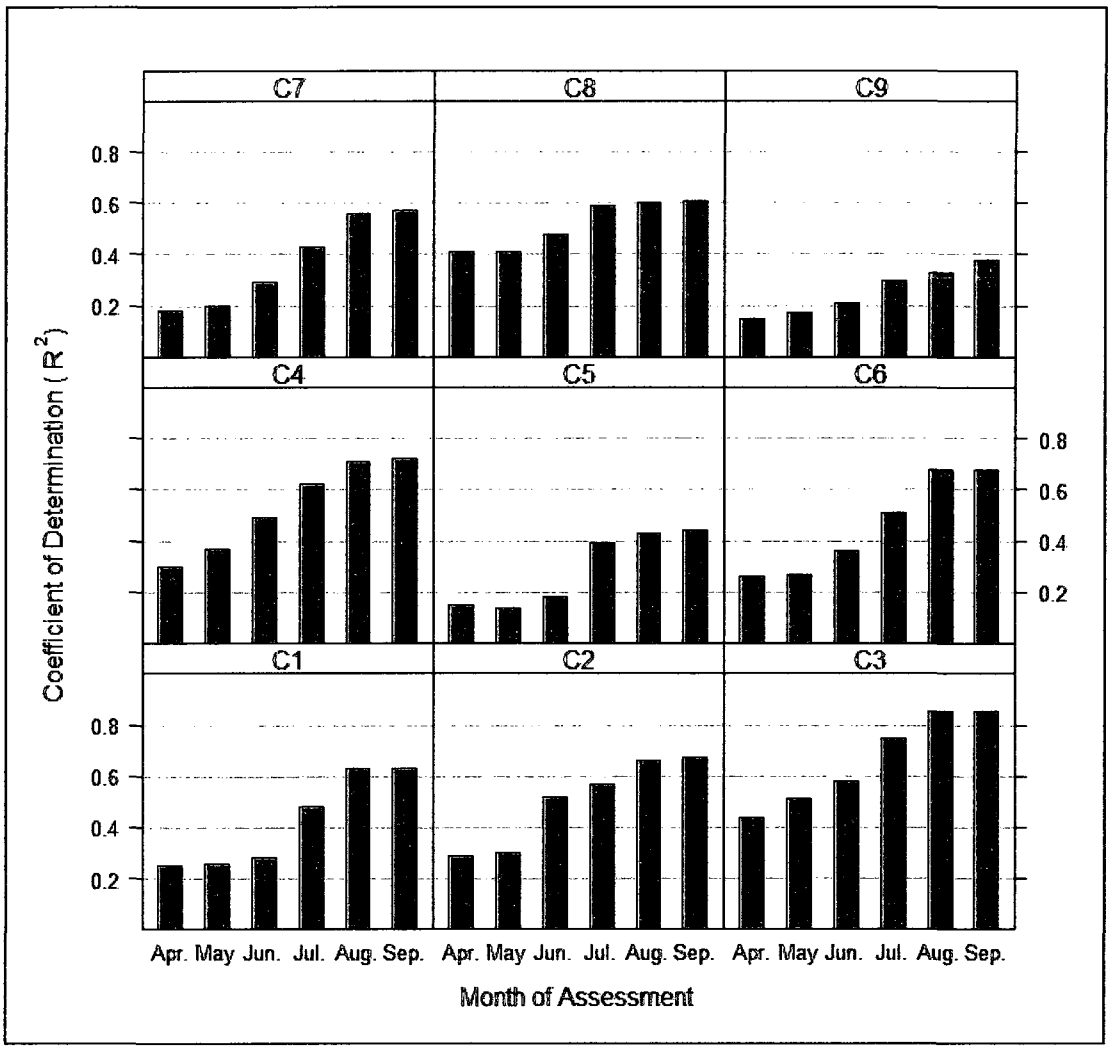

Figure 5-11 Plots of the coefficient of determination (R^2) between standardized yield residuals and the blended drought indices by cluster.

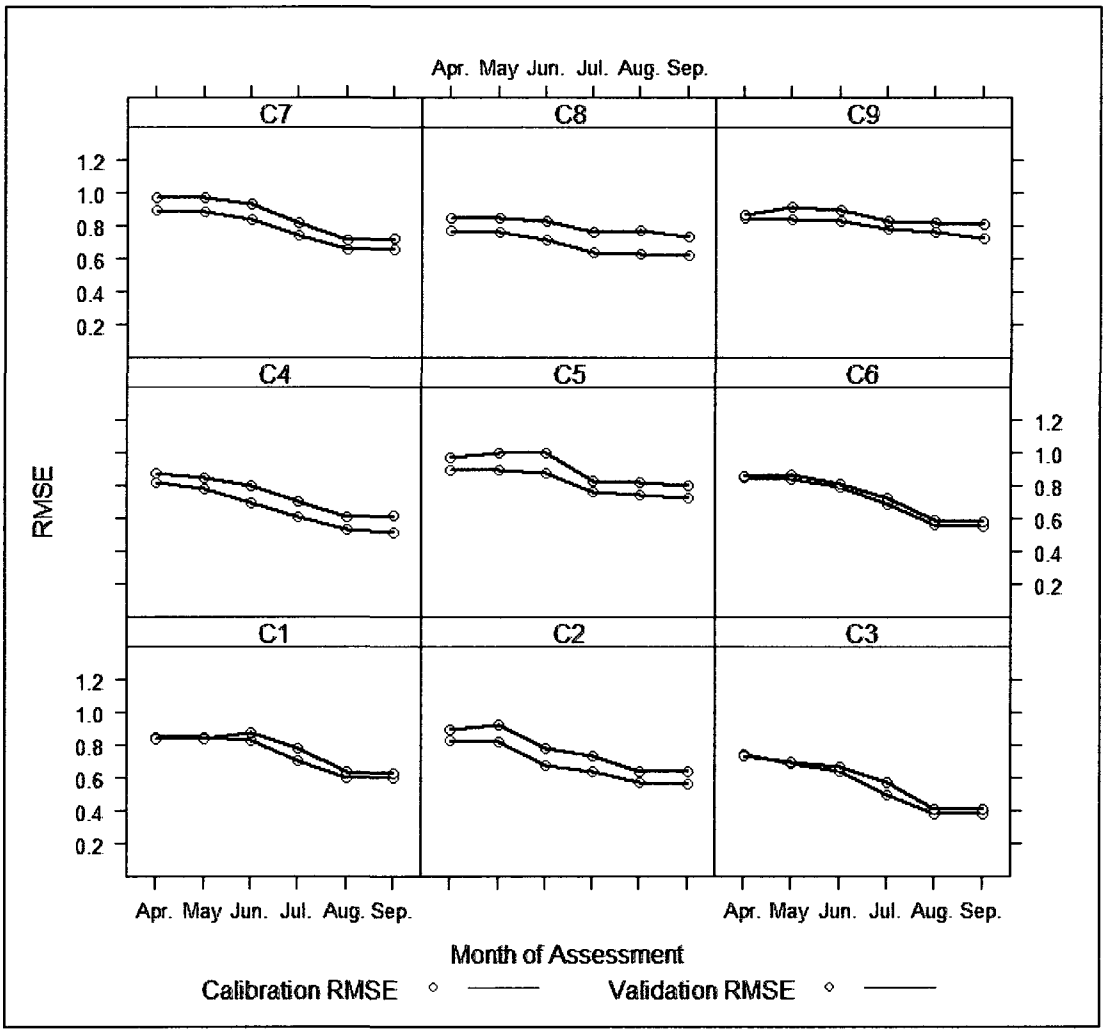

Figure 5-12 Plots of the RMSE between the observed and the predicted yields residuals by cluster.

For both calibration and validation, the degrees of bias of the observed and predicted yield residuals, as quantified by the MBE, were small (less than 0.05), indicating that in general there are no large over- or under-estimates of the yield. The calibration and validation RMSE values are similar and plotted in Figure 5-12. In general, the model accuracy improved from stage 1 to stage 6 for all clusters: as the growth period progresses, the R^2 increased and the RMSE decreased. What follows is a closer examination of the R^2 assessed at six stages from April to September.

At the pre-planting stage, R^2 values ranged from 0.15 to 0.44, with an average value of 0.27. This implies that the weather conditions of the recharge period do have an impact on the agricultural drought occurrences and persistence. Since growing season precipitation is not sufficient to meet crop demand for most of the agricultural regions on the prairies, the soil moisture status before the growing season is important. Sufficient soil moisture provides a steady supply of moisture that allows the crop to grow during the growing season. If the soil moisture levels are drier than normal, timely above normal precipitation is required during the growing season to make up the deficit (Sutton, 2003). However, the chance of this occurring in a growing season is low on the prairies. Therefore, it is possible to assess agricultural drought risk on crop yield before seeding by assessing spring soil moisture status using the weather information in the recharge period.

To further investigate the contribution of recharge period weather conditions on explaining yield variation, the model was run using only the drought indices from April to August for each stage of assessment. The comparison results of using two datasets (excluding vs. including recharge period drought indices) are plotted by cluster in Figure 5-13.

The degree of the contribution from recharge period weather conditions depended highly on the time of assessment. At earlier stages, recharge period drought indices accounted for more variance in yield residuals (i.e. variance unexplained by growing season drought indices) than at later stages. This is understandable, because spring soil moisture status would become less important to crop growth when large precipitation occurs during the growing season. However, it is interesting to note that even at the last stage of assessment, recharge period weather conditions still accounted for some of the variance that was unexplained by growing season weather conditions, although the amount of variance was very small for some clusters. This indicates that recharge period weather conditions are not only useful to detect potential drought risk at pre-planting, but also helpful to assess agricultural drought risk during the growing season.

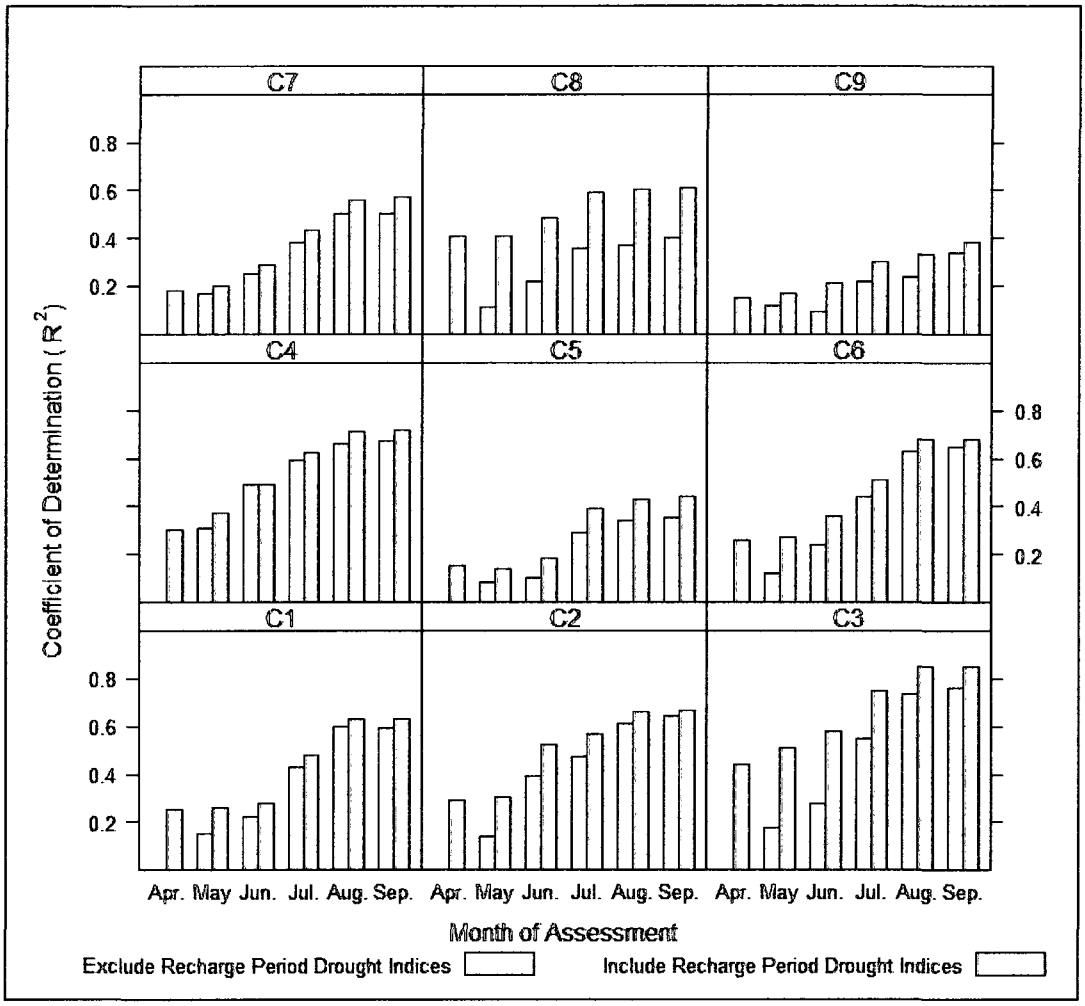

Figure 5-13 Plots of the coefficient of determination (R^2) between standardized yield residuals and the blended drought indices constructed from two datasets (excluding vs. including recharge period drought indices) by cluster.

At the second and third stages, when the assessments were updated by incorporating drought indices of April as well as both April and May, the R^2 showed a slight increase in most of the clusters (one exception was C2, with a big increase of 0.22 at the third stage). This indicates that the soil moisture conditions during the months of April and

May play a small role in determining how accurately the model can predict agricultural drought.

The assessment accuracies were further improved at the fourth stage (average $R^2 = 0.52$) and reached their highest at the fifth stage (average $R^2 = 0.61$). It is not surprising that the strongest correlation between the blended drought indices and crop yield residuals was in June and July. This agrees well with Arora *et al.* (1987) and Quiring and Papakryiskou (2003), who found that spring wheat yield is largely determined by moisture stress during the heading and soft dough stages, which usually occur during the second half of June and through July. Crops at these stages are vulnerable to drought, and even a moderate drought may reduce the yield greatly. Therefore, June and July are the most important months for determining the risk of agricultural drought.

August seemed to have little influence on the accuracy of the model, as there was no significant increase in the R^2 at the last stage, and the R^2 even decreased in C1. This suggests that weather of the last growth stage plays only a minor role in agricultural drought risk assessment, or may mislead the assessment. This is consistent with the findings of Whitmore (2000), who pointed out that drought has little further detrimental effect on the wheat from the hard dough stage up to ripening. At this point, the spring wheat that is near maturity does not respond to water stress as much as during the previous stages. A slightly drier than normal August insures that harvest could take place without difficulty or significant loss of yield (Whitmore, 2000).

In summary, the model's assessment accuracy increases as the crop develops. It is possible to assess agricultural drought risk on crop yield using weather information in the recharge period before seeding. Recharge period weather conditions also help to assess agricultural drought risk during the growing season. The moisture conditions of April and May slightly improve the accuracy of assessment. June and July are the most important months for determining the risk of agricultural drought. The most accurate assessment can be achieved at the beginning of August. The August weather plays a minor role in agricultural drought risk assessment, or may even mislead the assessment.

5.4.2 Spatial Variability in Model Performance

The performance of the model also revealed great spatial variation across the prairies in terms of the strength of the correlation between standardized spring wheat yield residuals and blended drought indices (Figure 5-14). The higher R^2 values were found in the south, southwest and central prairies and the lower R^2 values were found in the east and northeast prairies. It seems that the model performed better in high drought frequency regions, but poorly in less drought-prone areas. A further examination of the possible factors that affect the model's performance will help to better understand the causes of this spatial variability and to illuminate the strength and the weakness of the ADRA model. The factors considered here include growing season precipitation, soil AWHC and latitude.

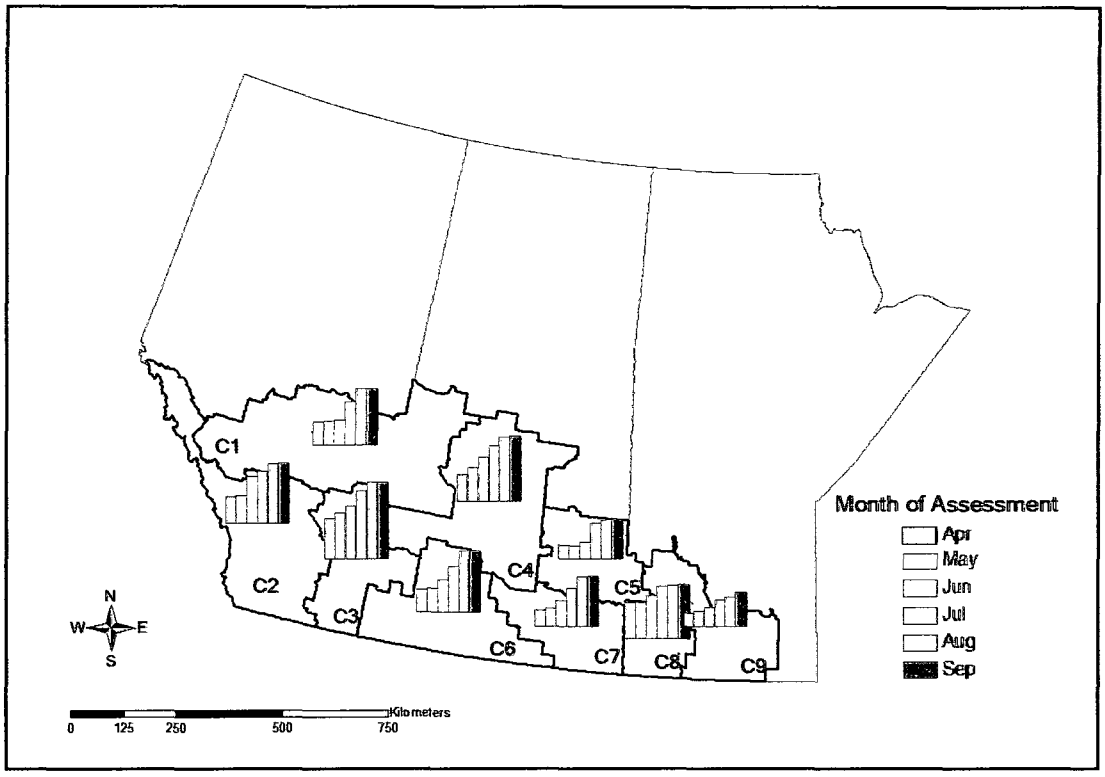

Figure 5-14 Mapping the coefficient of determination (R^2) values for the relationship between the blended drought indices and the standardized spring wheat yield residuals.

5.4.2.1 Growing Season Precipitation

Growing season precipitation is an important factor in determining yield, because soil moisture stress is the main yield-limiting factor for spring wheat grown on the prairies. The relationship between growing season precipitation and the spatial variability of model performance was examined in two ways: 1) mapping the mean growing season precipitation and 2) mapping the coefficient of variation (CV) of growing season precipitation.

- ***Mean Growing Season Precipitation***

The mean growing season (May 1st to August 31st) precipitation in the period 1976-2003 was calculated for each grid cell in the study area. Figure 5-15 shows that the prairies region received a mean growing season precipitation ranging between 160 to 360mm, in addition to 93% of its area receiving lower than 300mm precipitation, the approximate amount demanded by the crops (Ash *et al.*, 1992). The driest areas were found in the south and southwest parts of the prairies and with the precipitation generally increases towards the north and east, the wettest parts were found in the northwest and east. C3, which obtained the highest R^2 values for all stages among the clusters, is located in the centre of the driest region, receiving less than 200mm growing season precipitation. The areas of lower growing season precipitation also extended to C2, C4 and C6, where the model performed well. In comparison, C9, which obtained the lowest R^2 values for all stages among the clusters, is located in the wettest region on the eastern side of the prairies, receiving a growing season precipitation greater than 260 mm. Another region, C5, where the model performed poorly, also had a greater amount of growing season precipitation.

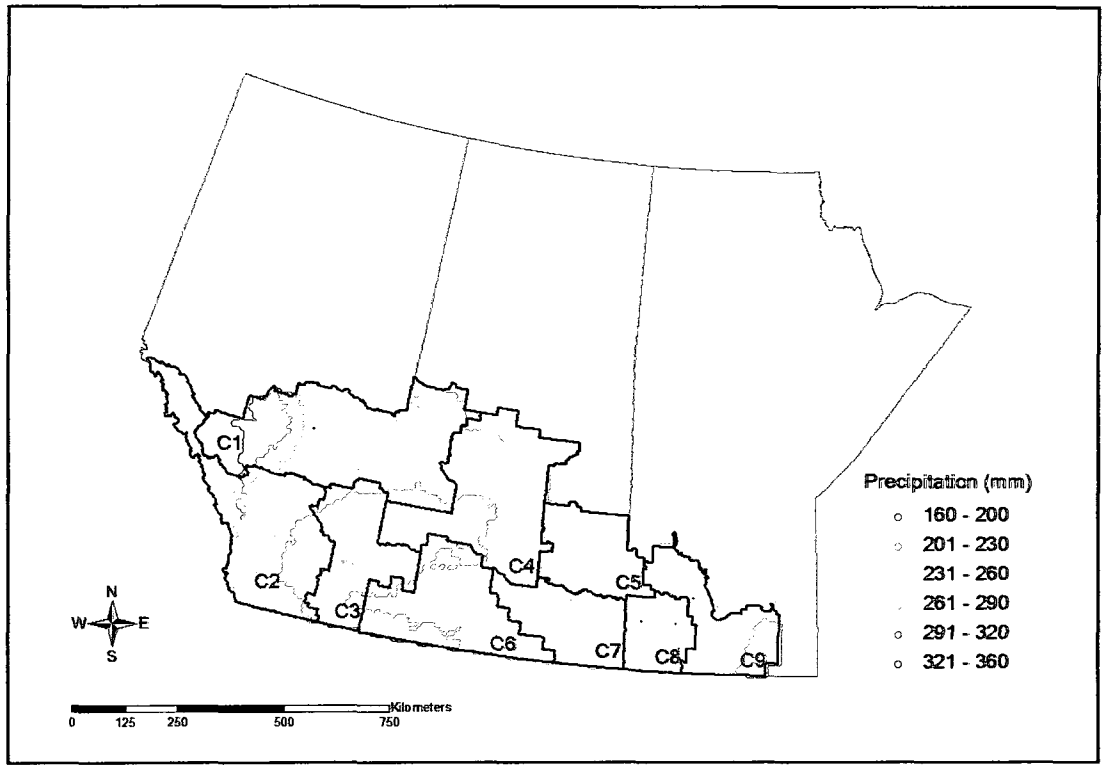

Figure 5-15 Mean growing season precipitation (1976-2003) for the prairies.

This spatial pattern indicates that as the mean growing season precipitation increases, the correlation between the blended drought indices and the spring wheat yield becomes weak. Therefore, the blended drought indices are not effective at modelling variations in yield in those areas that consistently receive relatively large amounts of precipitation during the growing season (i.e. soil moisture is no longer an important yield-limiting factor).

Growing season precipitation can explain part of the variations in model performance, but it is not the only factor. For example, it cannot explain the differences in model

performance between C8 and C5, which receive a similar amount of growing season precipitation.

- ***Coefficient of Variation of Growing Season Precipitation***

The coefficient of variation (CV) for the growing season precipitation provides a normalized measure of the relative dispersion of the growing season precipitation between 1976 and 2003. It was calculated for each grid cell by dividing the standard deviation by the mean of the growing season precipitating. The higher the CV, the greater the variability in the growing season precipitation is for a region. Figure 5-16 shows the spatial pattern of the CV for the growing season precipitation. It is obvious that the growing season precipitation was highly variable in the south and southwest of the prairies, and became less variable in the northern and eastern areas. Compared to Figure 5-15, the lower the mean precipitation, the more erratic precipitation tended to be.

The spatial pattern of the CV also resembled that of the model performance to some extent. Following the above discussion about C5 and C8, their difference can be partially explained by the CV of precipitation. Although C5 and C8 had similar amounts of mean growing season precipitation, C8 had a more variable growing season precipitation regime than C5, and thus obtained better results from the model.

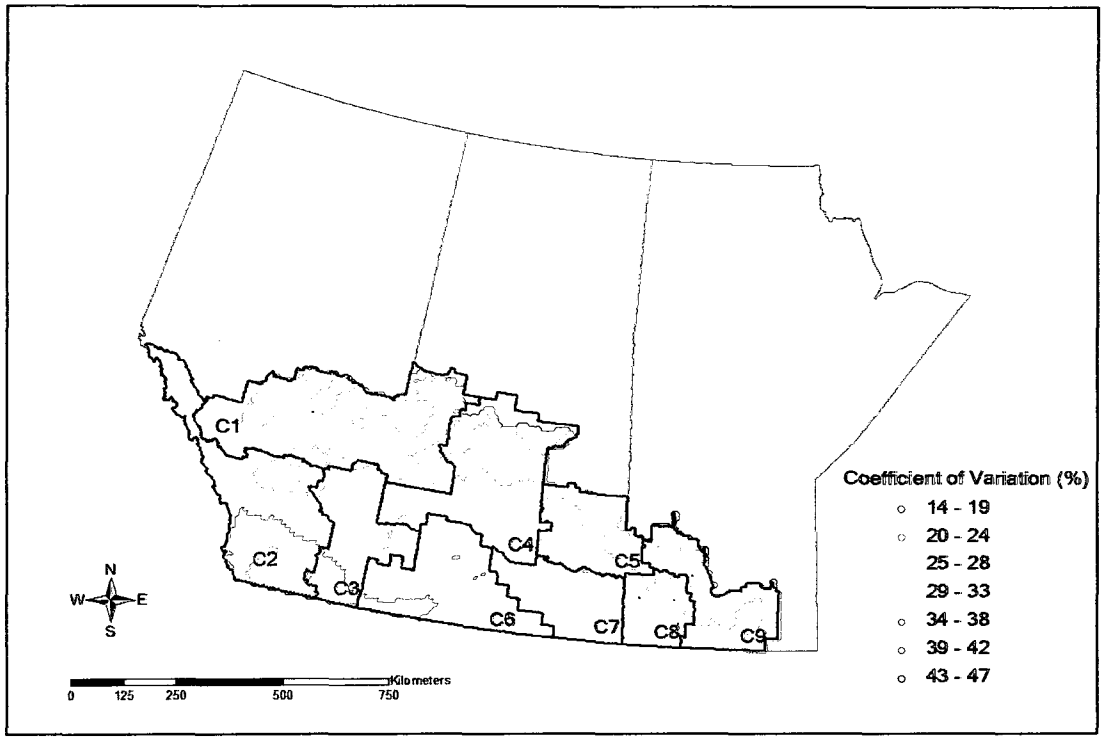

Figure 5-16 Coefficient of variation for growing season precipitation (1976-2003) for the prairies.

In general, the regions that receive lower (inadequate) amounts of growing season precipitation and have a large year to year variability in precipitation regime tend to have a stronger correlation between the blended drought indices and the spring wheat yield. The correlation becomes weak in the regions with abundant and reliable precipitation spread over the growing season. This implies that other factors that affect yield, such as soil fertility, length of the growing season, insects, disease, weeds and extreme meteorological events (e.g. hail, wind, frost), may have increased influence on the yield of these regions.

5.4.2.2 Soil Available Water Holding Capacity

Besides the growing season precipitation, the spatial patterns of the soil available water-holding capacity (AWHC) were also explored to see if they are connected to the model performance. As shown in Figure 5-17, most of the prairies had a medium level of soil water-holding capacity. Higher soil AWHC regions occurred in the west, centre and east of the prairies. A large portion of C9 was characterized by higher soil AWHC. This factor coupled with greater and less variable growing season precipitation contributed to its less drought-prone nature. Other higher soil AWHC regions were mainly distributed into C1, C2, C4, C6 and C7 and were generally located in dry regions. Although soils with higher level water-holding capacity can hold more water to sustain crop growth in short-term dry conditions, the typically lower growing season precipitation limits the influence of the soil AWHC on the correlation between the blended drought indices and the crop yield. Therefore, soil AWHC is not a dominant factor in determining model performance in the prairies.

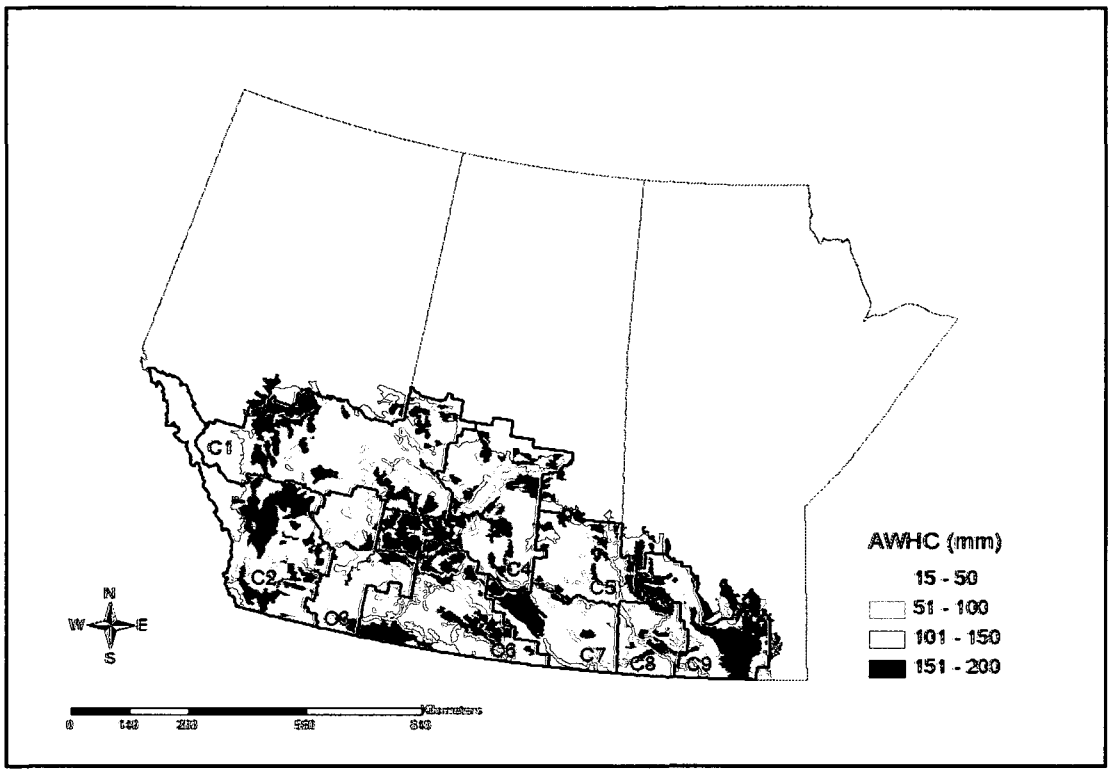

Figure 5-17 The soil available water-holding capacity (AWHC) values over the prairies.

5.4.2.3 Latitude

Latitude can explain some of spatial variation in model performance. In general, as latitude increased, model performance decreased. Latitude can be treated as a proxy variable for joint actions of multiple factors (e.g. solar radiation, temperature, soil fertility, and length of growing season), because each of these factors has a strong north-south gradient in the prairies (Acton *et al.*, 1998; Quiring, 2001; Luo and Zhou, 2006). Southern prairies tend to have more available heat, higher temperature, more fertile soils, and a longer growing season. These factors, which were not considered in the model, do

not normally limit crop growth in the south, but can be important in the more northerly prairies.

To sum up, the mean growing season precipitation and latitude are inversely related to model performance. The model performs best in the regions that have a more southerly location and a low mean growing season precipitation. As the variability of the growing season precipitation increases, the model performance increases. Latitude can be treated as a proxy variable for the north-south gradient in solar radiation, temperature, soil conditions, and growing season length. All these factors collectively influence the correlation between the blended drought indices and spring wheat yields, and should be jointly considered when interpreting their relationships to model performance.

5.4.3 Evaluation of Drought Category Prediction Accuracy

The performance of the ADRA model was also evaluated by the prediction accuracy associated with each drought category in validation period. The observed and estimated frequencies of each drought category were summarized in confusion matrices (Appendix B) to provide details on how well the observed and predicted drought categories (i.e. determined by the observed and predicted standardized crop yield residuals) were matched in different clusters. Here, a summary of the results for three representative clusters (one with the best model performance, one with the average model performance, and one with the poorest model performance), is presented.

Table 5-5 displays the confusion matrices for predictions in C3, where there was a strong relationship between actual and predicted yield. It is not surprising that the frequency of accurate predictions (diagonal elements of the confusion matrix) was generally lower at pre-planting than at later stages, as the weather conditions during the growing season are uncertain at this point. It is interesting to see that 2 of the 5 mild droughts were successfully predicted at this stage, and 2 of the 7 moderate droughts were reported as mild. Although severe and extreme droughts were not precisely predicted at this point, 3 of the 4 severe and all of the 3 extreme droughts were detected as mild or moderate by the model. This supports the previous conclusion that potential drought risk can be assessed before seeding. It should also be noted that 9 of the 36 non-drought conditions were mis-predicted as mild and 2 were mis-predicted as moderate droughts. Besides the model error, this may be due to timely above-normal growing season precipitation that makes up the deficit in soil moisture reserve in the spring. As expected, the assessment accuracy improved as the crop developed, and reached its highest point at the last stage.

Table 5-5 Confusion matrices for predictions of C3 (best model performance)

		Predicted				
Stage1		Non-drought	Mild	Moderate	Severe	Extreme
Actual	Non-drought	25	9	2	0	0
	Mild	1	2	2	0	0
	Moderate	5	2	0	0	0
	Severe	1	1	2	0	0
	Extreme	0	3	0	0	0
Stage 2		Non-drought	Mild	Moderate	Severe	Extreme
Actual	Non-drought	28	6	2	0	0
	Mild	2	1	2	0	0
	Moderate	2	3	2	0	0
	Severe	1	0	3	0	0
	Extreme	0	1	2	0	0
Stage 3		Non-drought	Mild	Moderate	Severe	Extreme
Actual	Non-drought	28	7	1	0	0
	Mild	2	1	2	0	0
	Moderate	2	3	2	0	0
	Severe	1	0	1	2	0
	Extreme	0	1	2	0	0
Stage 4		Non-drought	Mild	Moderate	Severe	Extreme
Actual	Non-drought	31	4	1	0	0
	Mild	2	0	3	0	0
	Moderate	1	4	2	0	0
	Severe	0	2	1	1	0
	Extreme	0	0	1	2	0
Stage 5		Non-drought	Mild	Moderate	Severe	Extreme
Actual	Non-drought	29	6	1	0	0
	Mild	1	1	2	1	0
	Moderate	0	3	3	1	0
	Severe	0	0	2	2	0
	Extreme	0	1	0	2	0
Stage 6		Non-drought	Mild	Moderate	Severe	Extreme
Actual	Non-drought	30	6	0	0	0
	Mild	1	3	1	0	0
	Moderate	0	3	4	0	0
	Severe	0	0	2	2	0
	Extreme	0	1	0	2	0

Table 5-6 shows confusion matrices for predictions in C7, which had an average model performance. Compared to C3, the overall prediction accuracy was lower in C7. At pre-planting, 2 of the 18 mild and 1 of the 8 moderate drought conditions were successfully predicted. 2 of the 9 severe droughts were estimated as mild, and 1 of the 4 extreme droughts was estimated as moderate drought. Similarly to C3, the prediction accuracy increased as the crop passed through its growing season.

Table 5-7 shows confusion matrices for predictions in C9, which obtained the poorest model results. Before the growing season, 4 of the 16 mild droughts were successfully predicted. None of the moderate, severe and extreme droughts was identified in the first two stages. At stage 4 (at the beginning of July), 1 of the 9 moderate droughts and 2 of the 4 severe droughts were first identified as mild droughts by the model. 2 of the 3 extreme droughts were identified as mild droughts until stage 6. It is obvious that the prediction accuracy in C9 was low and did not show significant increase at later stages, especially for mild droughts which prediction accuracy even decreased at later stages.

Table 5-6 Confusion matrices for predictions of C7 (average model performance)

		Predicted				
Stage1		Non-drought	Mild	Moderate	Severe	Extreme
Actual	Non-drought	46	17	4	0	0
	Mild	15	2	1	0	0
	Moderate	6	1	1	0	0
	Severe	7	2	0	0	0
	Extreme	3	0	1	0	0
Stage 2		Non-drought	Mild	Moderate	Severe	Extreme
Actual	Non-drought	48	13	5	1	0
	Mild	12	6	0	0	0
	Moderate	5	2	1	0	0
	Severe	6	3	0	0	0
	Extreme	3	0	1	0	0
Stage 3		Non-drought	Mild	Moderate	Severe	Extreme
Actual	Non-drought	49	11	4	3	0
	Mild	11	5	2	0	0
	Moderate	4	2	2	0	0
	Severe	6	3	0	0	0
	Extreme	3	1	0	0	0
Stage 4		Non-drought	Mild	Moderate	Severe	Extreme
Actual	Non-drought	54	6	7	0	0
	Mild	8	9	1	0	0
	Moderate	0	3	4	1	0
	Severe	5	2	2	0	0
	Extreme	1	2	1	0	0
Stage 5		Non-drought	Mild	Moderate	Severe	Extreme
Actual	Non-drought	54	10	3	0	0
	Mild	6	7	5	0	0
	Moderate	0	2	6	0	0
	Severe	1	3	4	1	0
	Extreme	1	1	2	0	0
Stage 6		Non-drought	Mild	Moderate	Severe	Extreme
Actual	Non-drought	55	9	3	0	0
	Mild	5	9	4	0	0
	Moderate	0	3	5	0	0
	Severe	1	1	6	1	0
	Extreme	1	1	2	0	0

Table 5-7 Confusion matrices for predictions of C9 (weakest model performance)

		Predicted				
Stage1		Non-drought	Mild	Moderate	Severe	Extreme
Actual	Non-drought	66	13	1	0	0
	Mild	12	4	0	0	0
	Moderate	9	0	0	0	0
	Severe	4	0	0	0	0
	Extreme	3	0	0	0	0
Stage 2		Non-drought	Mild	Moderate	Severe	Extreme
Actual	Non-drought	69	8	3	0	0
	Mild	14	2	0	0	0
	Moderate	9	0	0	0	0
	Severe	4	0	0	0	0
	Extreme	3	0	0	0	0
Stage 3		Non-drought	Mild	Moderate	Severe	Extreme
Actual	Non-drought	71	9	0	0	0
	Mild	14	2	0	0	0
	Moderate	8	1	0	0	0
	Severe	2	2	0	0	0
	Extreme	3	0	0	0	0
Stage 4		Non-drought	Mild	Moderate	Severe	Extreme
Actual	Non-drought	66	12	2	0	0
	Mild	13	2	1	0	0
	Moderate	7	1	1	0	0
	Severe	1	1	2	0	0
	Extreme	2	1	0	0	0
Stage 5		Non-drought	Mild	Moderate	Severe	Extreme
Actual	Normal	65	13	2	0	0
	Mild	15	0	1	0	0
	Moderate	6	2	0	1	0
	Severe	1	1	1	1	0
	Extreme	1	2	0	0	0
Stage 6		Non-drought	Mild	Moderate	Severe	Extreme
Actual	Non-drought	70	6	4	0	0
	Mild	14	1	1	0	0
	Moderate	7	1	0	1	0
	Severe	1	3	0	0	0
	Extreme	0	2	1	0	0

The average prediction accuracy rate of all clusters for each drought category was also calculated to help quantify the overall accuracy of the model. As shown in Table 5-8, from stage 1 to stage 6, the accuracy rate of each drought category was increased from 72 to 80% for non-drought, 23 to 33% for mild, 13 to 40% for moderate, 0 to 24% for severe, and 0 to 5% for extreme drought. The model's underprediction of severe and extreme droughts is obvious, with 69% of the severe droughts and 87% of the extreme droughts were mis-predicted as lower level droughts at the last stage.

Table 5-8 The average prediction accuracy rate of all clusters

		Predicted (%)				
Stage1		Non-drought	Mild	Moderate	Severe	Extreme
Actual (%)	Non-drought	72	21	7	1	0
	Mild	68	23	9	0	0
	Moderate	68	18	13	0	0
	Severe	66	24	11	0	0
	Extreme	68	23	9	0	0
Stage 2		Non-drought	Mild	Moderate	Severe	Extreme
Actual (%)	Non-drought	73	20	6	1	0
	Mild	72	20	8	1	0
	Moderate	61	26	11	3	0
	Severe	63	26	11	0	0
	Extreme	66	20	14	0	0
Stage 3		Non-drought	Mild	Moderate	Severe	Extreme
Actual (%)	Non-drought	75	18	6	1	0
	Mild	65	21	14	1	0
	Moderate	62	22	13	3	0
	Severe	45	29	18	5	3
	Extreme	57	25	7	11	0
Stage 4		Non-drought	Mild	Moderate	Severe	Extreme
Actual (%)	Non-drought	78	15	7	0	0
	Mild	56	28	15	1	0
	Moderate	36	30	29	5	0
	Severe	32	24	26	11	8
	Extreme	20	41	23	16	0
Stage 5		Non-drought	Mild	Moderate	Severe	Extreme
Actual (%)	Non-drought	80	15	5	0	0
	Mild	49	30	20	2	0
	Moderate	22	34	33	11	0
	Severe	11	26	32	24	8
	Extreme	9	27	34	30	0
Stage 6		Non-drought	Mild	Moderate	Severe	Extreme
Actual (%)	Non-drought	80	14	5	1	0
	Mild	44	33	21	2	0
	Moderate	26	29	39	5	0
	Severe	11	24	45	16	5
	Extreme	9	23	41	23	5

By evaluating the model's prediction accuracy associated with drought categories, two weaknesses of the models were revealed:

1) The model does not seem to be able to accurately predict large negative yield departures, as severe and extreme droughts were routinely underpredicted. One possible reason for this is the insufficient number of observations with extremely low yield. Perhaps the model would have done better at accounting for the effects of severe and extreme droughts if there was a longer period of record including more severe and extreme drought years. It is also possible that the response of yield to dry conditions may not be linear when the soil moisture drops below a certain threshold. A nonlinear model may be more appropriate to estimate yields under very dry conditions.

2) The model's prediction accuracy did not always show a stable increase from stage to stage during the growing season. A certain level of drought that has been correctly predicted at earlier stages is likely to be mis-predicted as other categories at later stages. This may due to the uneven distribution of the growing season precipitation.

Besides total precipitation amounts, the distribution of the precipitation over the growing season is also critical to crop yield. An excess of precipitation falling with bad timing can be detrimental to crop yields. Extremely large precipitation prior to planting can delay seeding. Excess May precipitation may prevent the seedlings from establishing deep root systems, and making them more susceptible to moisture stress later in the growing season (Quiring, 2001). Excess August precipitation also significantly decreases

yield by delaying the harvest and causing waterlogging (Wenkert *et al.,* 1981). Moreover, in some cases, several large precipitation events will skew the monthly precipitation totals, and the empirical nature (i.e. temporal resolution) of this model may miss cases of inadequate precipitation in certain critical, water-sensitive periods (e.g. at the end June and the beginning of July). Therefore, above average but poorly distributed growing season precipitation can also lead to poor yield. Conversely, even if the total growing season precipitation complies with a numerical definition of drought, it could possibly be so well-distributed in terms of a crop's pattern of water demands, that it provides an adequate or even superior crop yield (Whitmore, 2000). However, the timing and the distribution of the growing season precipitation are not accounted for by the drought indices, thus limiting model's predictive ability. It is likely that the amount of explained variance in spring wheat yields could be further increased if drought indices were calculated on a weekly or biweekly basis and were weighted according to the pattern of crop water demands.

In addition, some mis-predicted observations might be affected by factors other than drought, such as insects, disease, weeds and weather-related damages (e.g. hail, wind, frost). Furthermore, the model could also be affected by the quality of the climate data that is being used to calculate drought indices. As discussed in Chapter 4, the aggregation of daily precipitation interpolations involved extra error. The observed yield data also have errors, which are difficult to quantify.

5.4.4 Evaluation of Drought Indices

This section evaluates the variance contribution of individual drought index to the first three PCs, which account a considerable portion of the variability in drought indices (approximately 53 to 78% of the total variance) of all stages and all clusters.

The variance in each individual drought index accounted for by a PC was calculated by summing the variance in the variables that were associated with that drought index. For example, at stage 1, the variance of a PC contributed by the PDSI was captured by summing the variance in the PDSI of last September, the PDSI of last October, and so on, up to the PDSI of this March. The proportion of variance in the first three PCs explained by a drought index was calculated by dividing the variance in first three PCs accounted for by a drought index by the total variance of the first three PCs.

As shown in Figure 5-18, the PDSI accounted for the greatest proportion of variance (around 31 to 53%) in the first three PCs. The Z-index ranked second, accounting for almost 19 to 37% of the variance. The variances explained by the SPI_1, SPI_3 and SPI_6 were very close, approximately 6 to 14%, 9 to 15% and 5 to 13%, respectively.

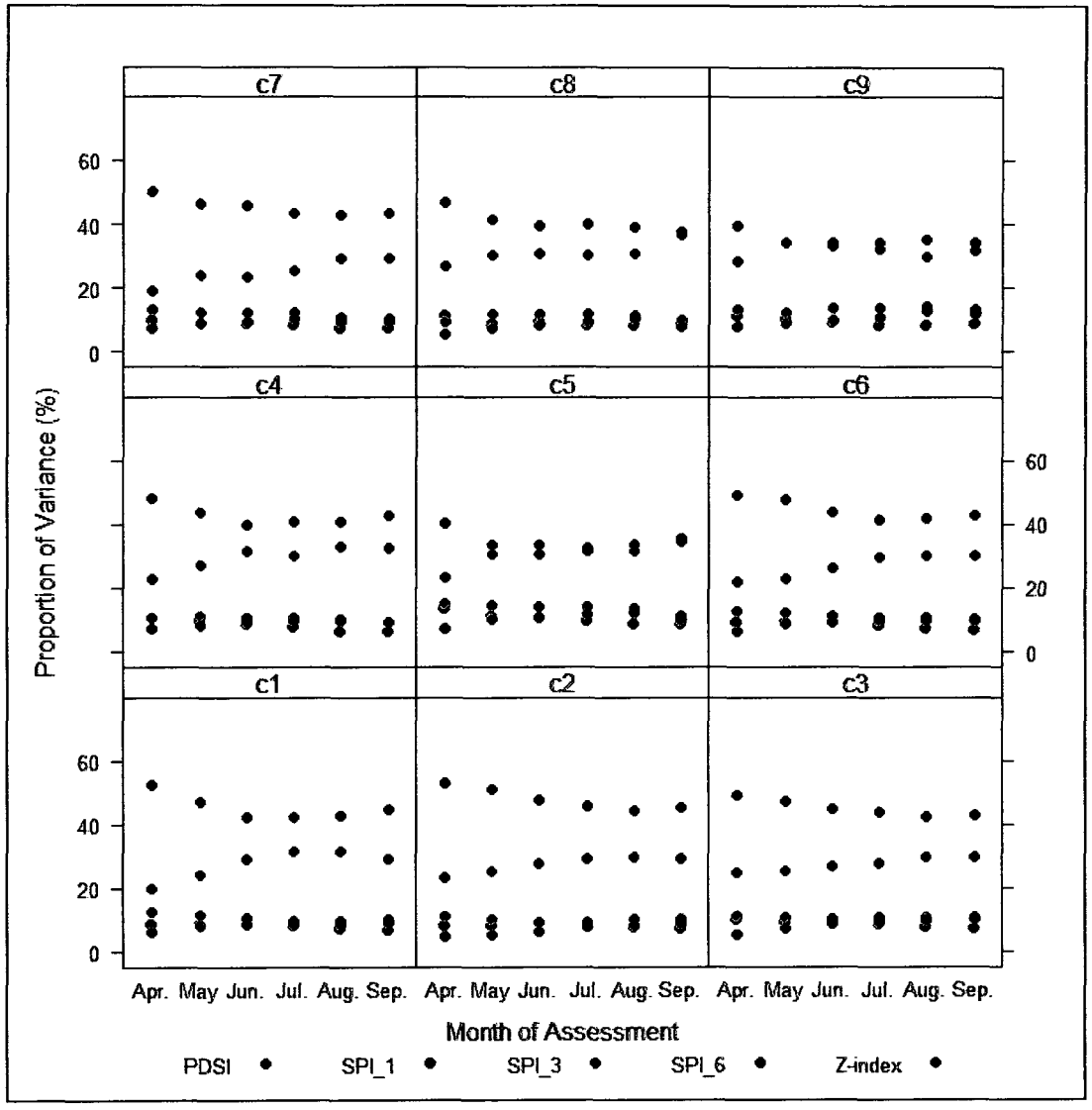

Figure 5-18 The proportion of variance in the first three PCs accounted for by individual drought index.

It is evident that, for most of the clusters, the proportions of variance in the first three PCs explained by the PDSI and Z-index were not constant from stage 1 to stage 6. The percentage variance explained by the PDSI decreased as the crop develops and remained

relatively stable at later stages. In comparison, the percentage variance explained by the Z-index increased during earlier stages, and kept relatively stable at later stages. It is not surprising that the Z-index's variance contribution increased when soil moisture stress occurs during the growing season. As mentioned previously, the Z-index is not affected by moisture conditions in previous months, so it is more sensitive to short-term soil moisture anomalies. The PDSI varies more slowly because it highly depends on antecedent conditions (i.e. it has a long memory of previous moisture conditions) (Guttman, 1998). Since crop growth is highly dependent on short-term moisture conditions, some studies suggest that the Z-index is more appropriate than the PDSI for agriculture and forestry applications because it is more responsive to those conditions (Karl, 1986; Quiring and Papakryiakou, 2003). At pre-planting and earlier growing season, however, the PDSI is more important than the Z-index for assessing cumulative moisture deficits in soils. In C5 and C9, where the model performed poorly, the proportions of variance explained by the PDSI was smaller than in other clusters. This may attribute to the higher amount and lower variability of the growing season precipitation of these regions, as discussed in section 5.3.2.

Two Palmer drought indices (PDSI and Z-index) together explained the majority (approximately 64 to 76%) of the variance in the first three PCs. The variance contributions from the 1-, 3- and 6-month SPI were relatively small. To further analyze the contribution of the SPI in explaining the variance in crop yield (i.e. to see how much variance that unexplained by the Palmer drought indices can be explained by the three

SPIs), the variances in spring wheat yield explained by the blended drought indices constructed from different drought indices combinations (PDSI & Z-index vs. PDSI, Z-index, SPI_1, SPI_3 & SPI_6) were compared.

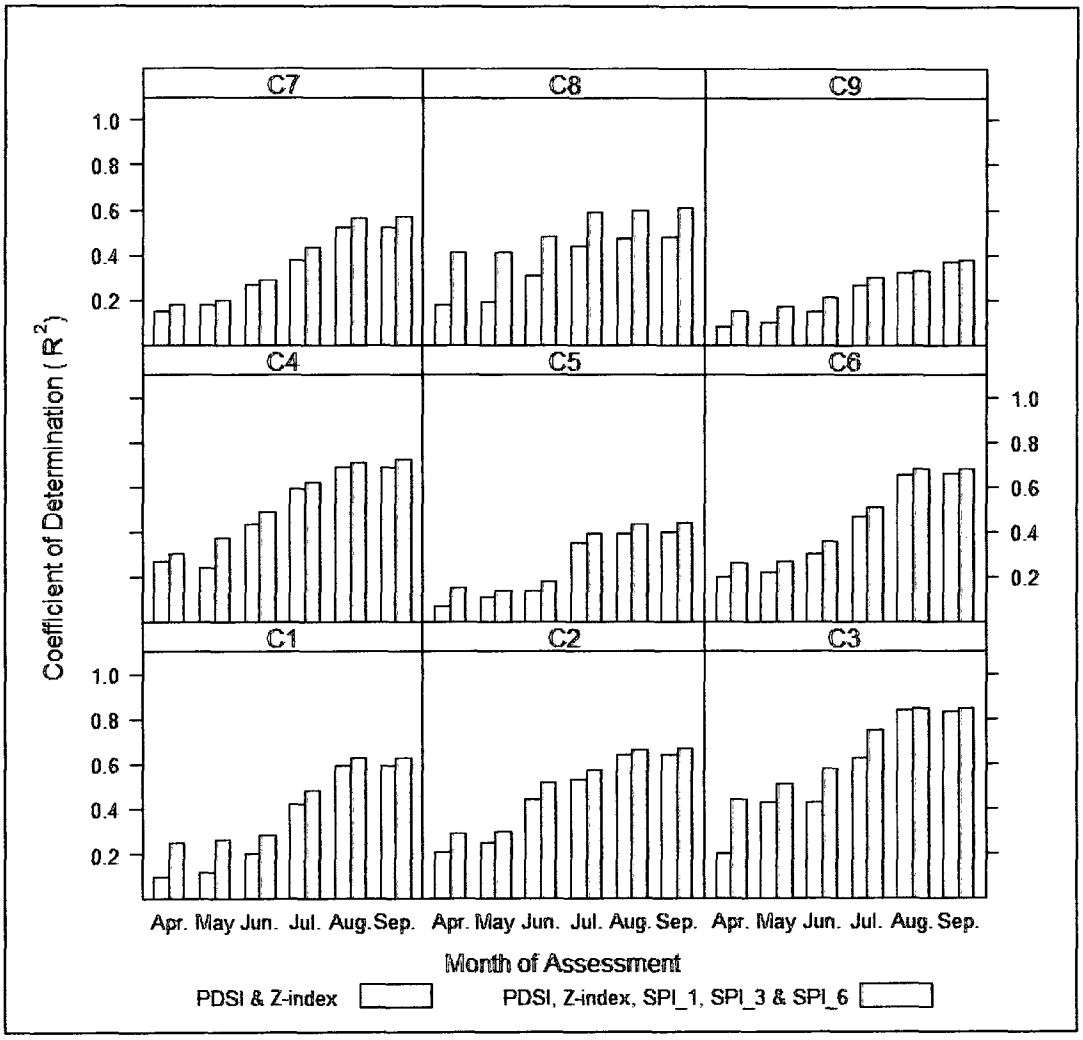

Figure 5-19 Comparison of the coefficient of determination (R^2) between standardized spring wheat yield residuals and the blended drought indices constructed from different drought indices combinations (PDSI & Z-index vs. PDSI, Z-index, SPI_1, SPI_3 & SPI_6).

The results shown in Figure 5-19 illustrate the amount of extra explained variance in yield resulting from the SPI. It is clear that the SPI accounted for some of the variance in yield that was unexplained by the Palmer drought indices, although the amount of this variance was small for some of the clusters. As noted in previous research (Karl, 1986), the Palmer drought indices are more physically-based than the SPI. Although both of the PDSI and Z-index are strongly weighted by precipitation and temperature anomalies, the SPI is calculated using only precipitation (Hu and Willson, 2000). Besides precipitation and temperature, the Palmer drought indices also consider soil AWHC, potential evapotranspiraton, potential recharge, and potential runoff, which are important variables in determining crop growth (Quiring and Papakryiakou, 2003). The National Drought Model that was used to calculate the Palmer drought indices in this study has been improved by coupling the Versatile Soil Moisture Budget (VSMB) to the original Palmer Drought Model to better estimate the soil moisture balance. This improved the ability of the PDSI and Z-index to measure soil moisture status. In addition, the extra explained variance decreases from stage 1 to stage 6 across the prairies. This further demonstrates the effectiveness of the Palmer drought indices in measuring soil moisture anomalies during the growing season. The SPI alone may not reflect the spectrum of drought-related conditions, but they can serve as a pragmatic solution in data-poor regions (Smakhtin and Hughes, 2004).

To sum up, the Palmer drought indices (PDSI and Z-index), accounting for the majority of variance in drought indices, are more effective for agricultural drought assessment

then the SPI. The PDSI is important for assessing drought risk at pre-planting and earlier growing season. The Z-index is sensitive to short-term soil moisture anomalies, and thus important for growing season drought risk assessment. The SPI, although it did not perform as well as the Palmer drought indices, is also a useful measure of agricultural drought, accounting for some of the variance in yield residuals that were unexplained by the Palmer drought indices.

5.4.5 ADRA Model Application

Two drought years (one severe and one moderate drought year) and one normal year in the study period were selected to provide a better visualization of the agricultural drought risk assessment by the model.

The most recent drought of 2001was identified as the most severe drought on record of parts of the prairies (Bonsal and Wheaton, 2005). The ADRA map for the prairies' agricultural regions from stage 1 to stage 6 for 2001 is shown in Figure 5-20. Alberta and western Saskatchewan were identified as under drought risk at pre-planting, and the risk spread to more regions in Saskatchewan at later stages. Compared to the actual drought conditions of 2001, which were determined by the observed standardized crop yield residuals (Figure 5-21), the overall assessment resembled the dry conditions in 2001 (except for northeastern Alberta and northwestern Saskatchewan, where dry conditions were over-estimated). It is noted that the low yields in Manitoba shown in the shaded

area of Figure 5-21 resulted from floods rather than drought, thus it was not counted to drought-related yield reduction.

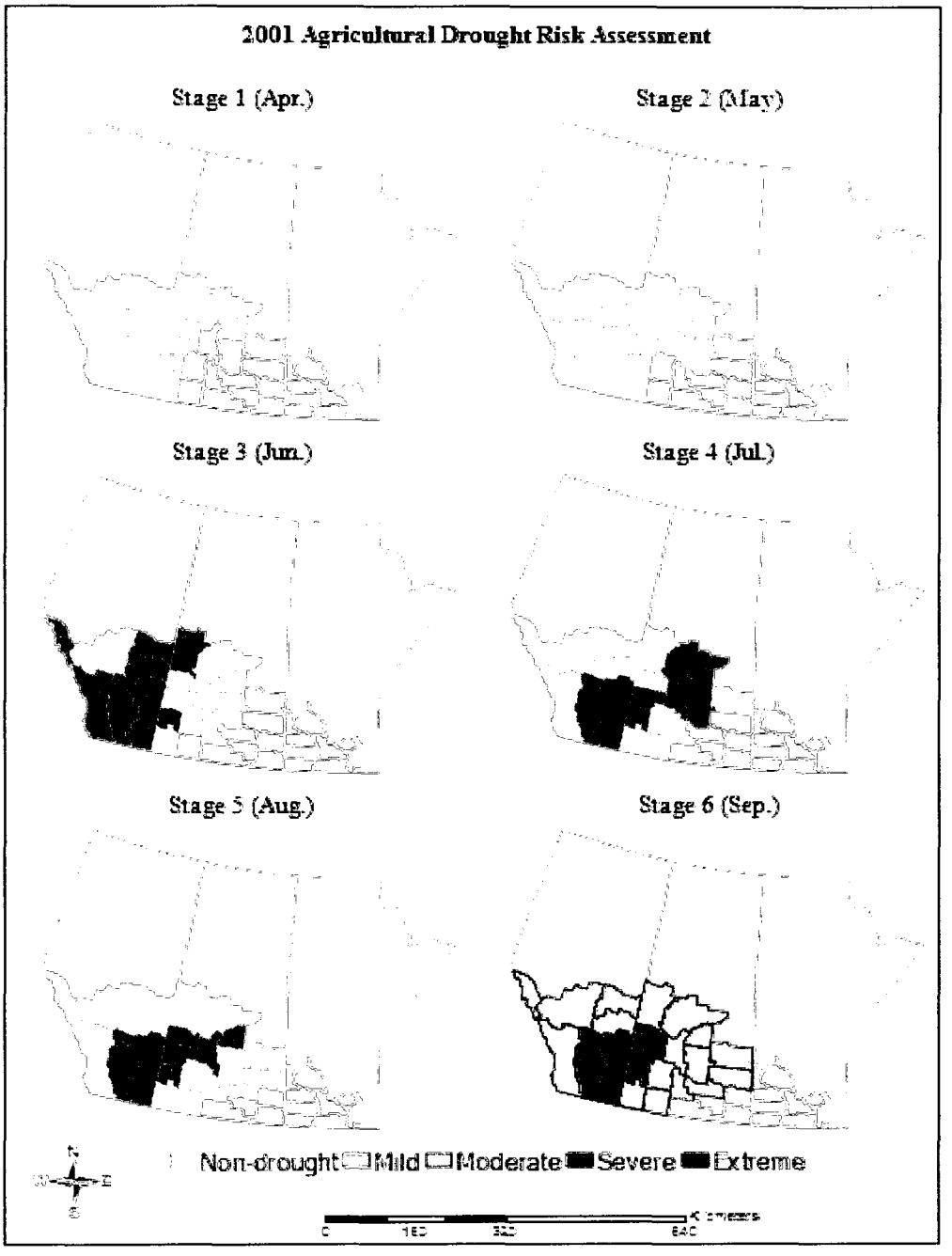

Figure 5-20 Agricultural drought risk assessment map for 2001.

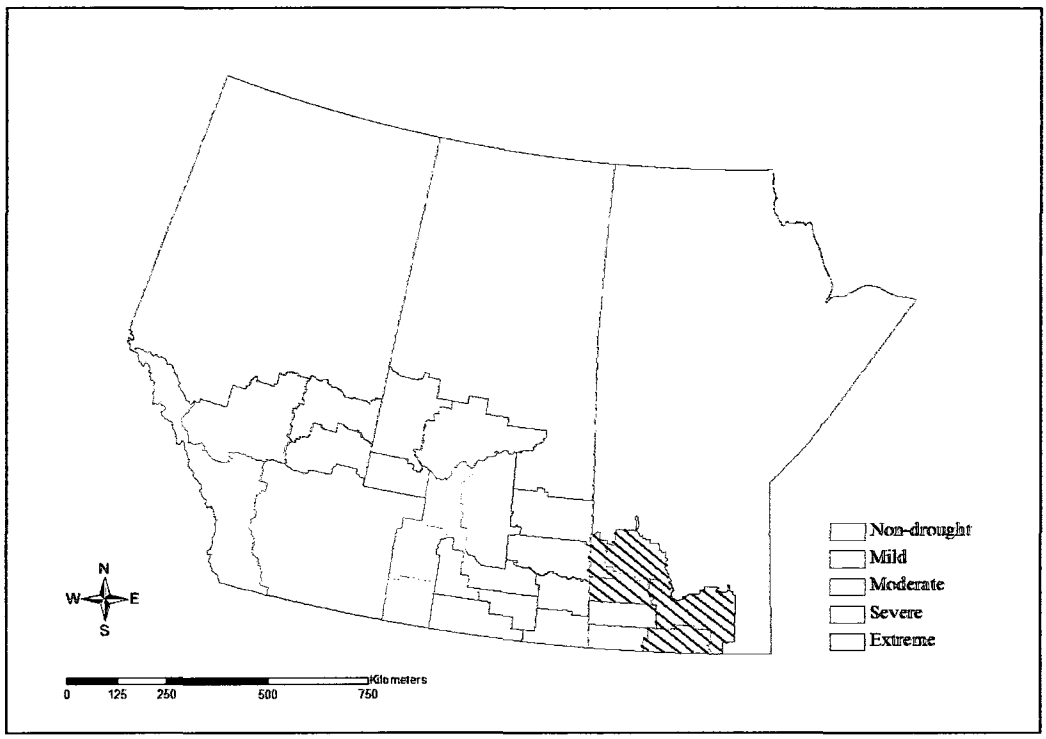

Figure 5-21 Drought conditions of 2001 as determined by the observed standardized crop yield residuals (shaded area denotes flood-related crop yield deduction).

1980 was a moderate drought year in the prairies. The ADRA map is shown in Figure 5-22. As indicated by Figure 5-22, drought first occurred in eastern Saskatchewan and southwest of Manitoba, and then spread to almost whole Saskatchewan and Manitoba. The most severe region was located in eastern Saskatchewan and western Manitoba, generally coincident with the actual drought conditions of 1980 (Figure 5-23).

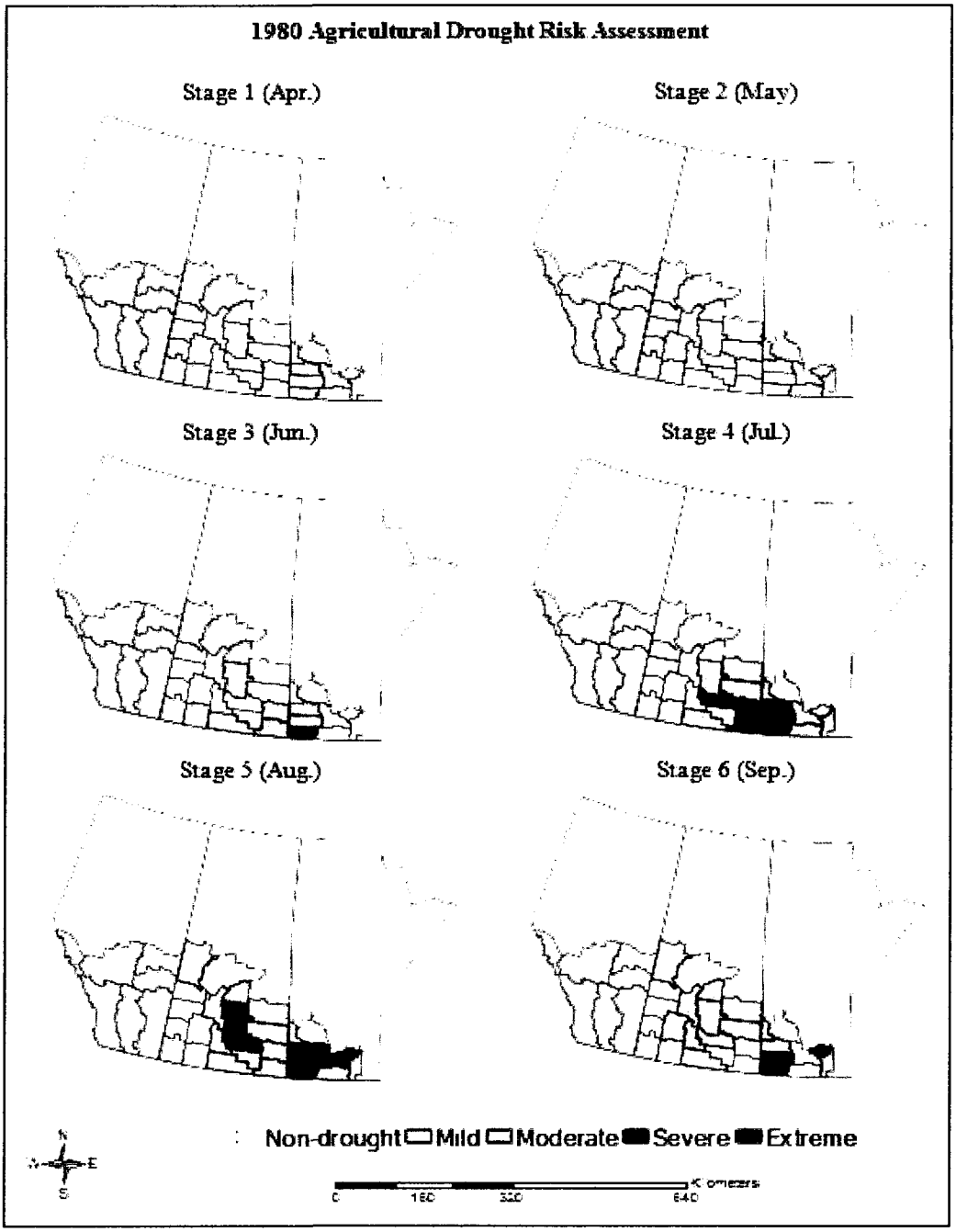

Figure 5-22 Agricultural drought risk assessment map for 1980.

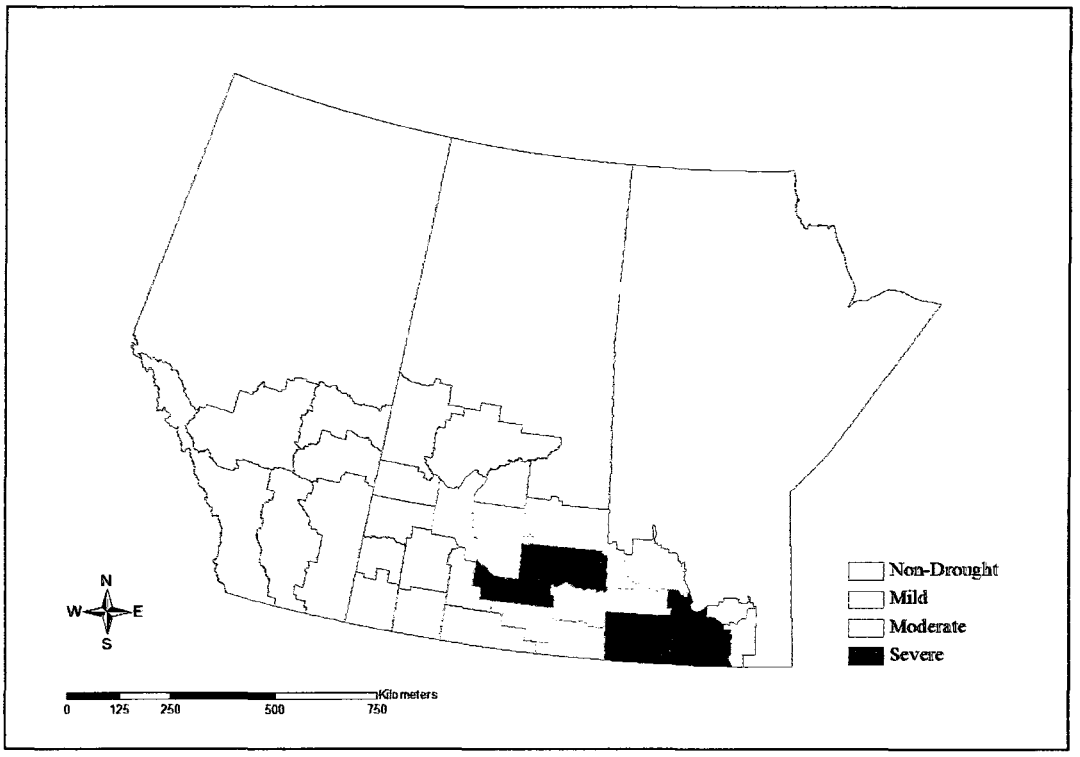

Figure 5-23 Drought conditions of 1980 as determined by the observed standardized crop yield residuals.

The ADRA model was finally applied to a normal (non-drought) year, 1996. As shown in Figure 5-24, most of the regions in the prairies were identified as no risk in 1996. Only a few CARs were estimated under the risk of mild drought. The actual conditions of 1996 are shown in Figure 5-25 and none of the CARs experienced drought in this year. In general, the model is able to assess non-drought conditions during years when moisture supplies are favourable.

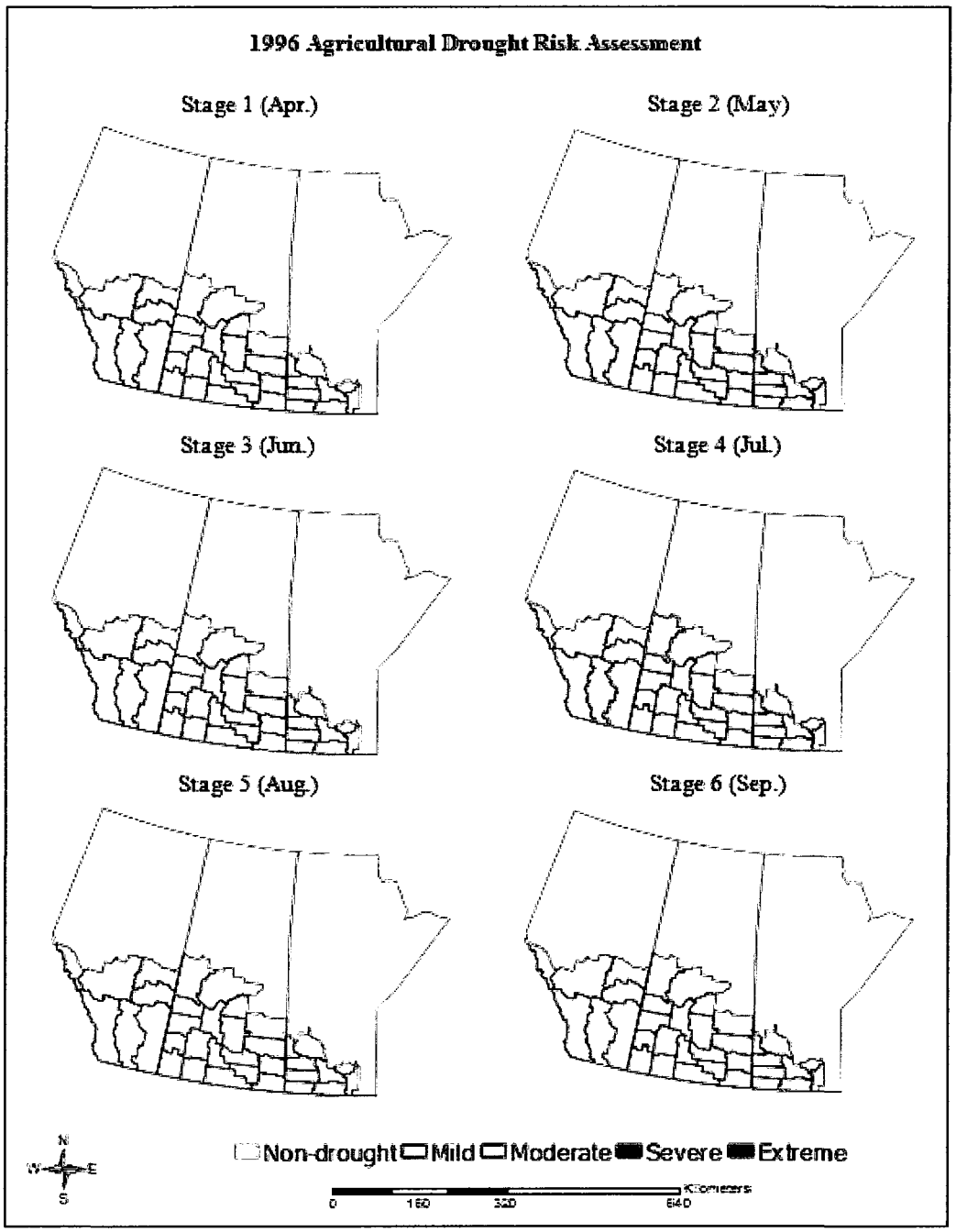

Figure 5-24 Agricultural drought risk assessment map for 1996.

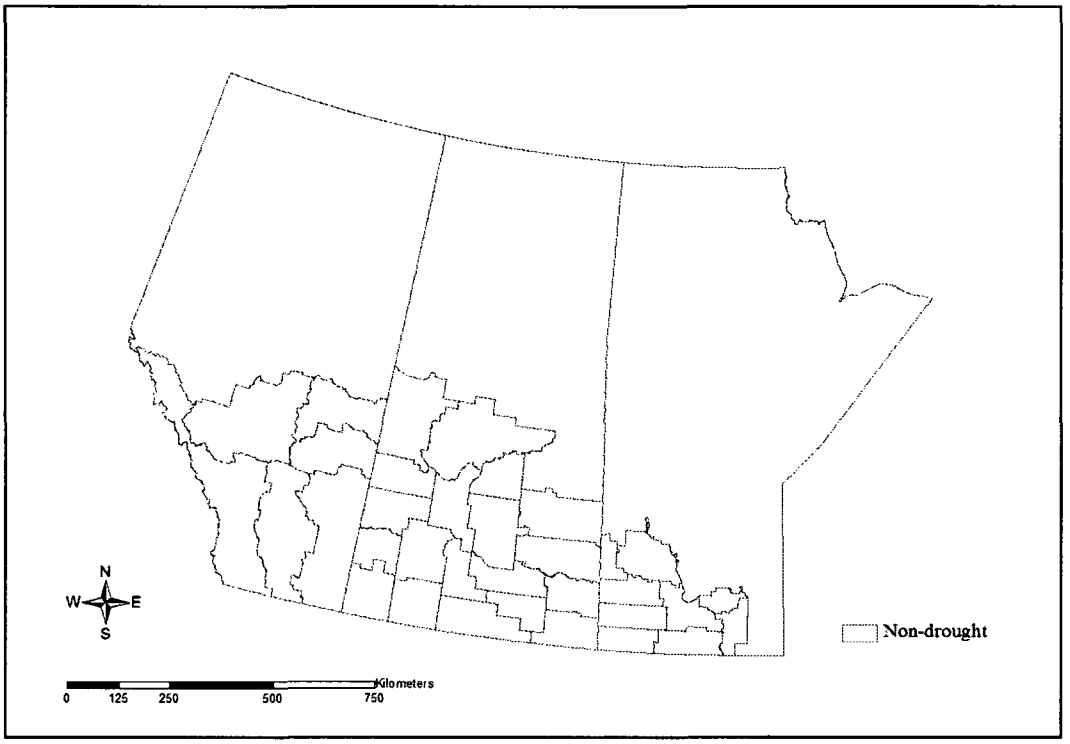

Figure 5-25 Drought conditions of 1996 as determined by the observed standardized crop yield residuals.

Based on the assessment results of the three representative years, it is concluded that the ADRA model is able to assess drought and non-drought conditions on the prairies before and during the growing season. Considering the model is designed to assess agricultural drought risk based on the historical weather information at each stage, the overall assessment ability is strong.

Chapter 6: Conclusion and Recommendations

6.1 Summary

The purpose of this study was to develop a methodology to integrate multiple drought indices to assess agricultural drought risk in a timely manner before and during the growing season for the Canadian prairies. The study was undertaken with the following objectives:

1) to establish a classification of drought intensity on the prairies based on the cumulative frequency of historical crop yield;

   To achieve this objective, an ECDF of the standardized historical yield residuals of all CARs during the study period was developed. The threshold yields for each drought category were determined from the ECDF according to the category's cumulative frequency, which generally correspond with the widely used cumulative frequency criteria on drought classification. A five-level drought intensity classification – non-drought, mild, moderate, severe and extreme – was utilized for the prairies.

2) to define an appropriate scale of analysis for drought risk assessment on the prairies;

   To achieve this objective, Ward's minimum-variance hierarchical cluster method was used to divide the study area into nine relatively homogeneous agricultural drought regions by maximizing the proportion of variation in standardized yields residuals

explained by a particular clustering of the CARs. These drought regions are composed of between 2 and 5 crop CARs. The most drought vulnerable regions were found in southeast Alberta and southern Saskatchewan, with the highest drought frequency. The regions in northern Alberta, northern Saskatchewan, and Manitoba experienced less frequency of droughts during the study period.

3) to develop an operational model framework to assess real-time agricultural drought risk by establishing a predictable relationship between blended drought indices and the standardized spring wheat yield residuals for the prairies.

To achieve this objective, the ADRA model is designed to assess the risk of agricultural drought at six stages from pre-planting to harvest. At pre-planting, the model is developed at the beginning of April to assess drought probabilities using the drought indices of the recharge period. During the growing season, the model is updated at the beginning of each month to assess potential drought risk using the drought indices from the recharge period to the preceding month. The last stage of the model is updated at the beginning of September. Blended drought indices are the weighted linear combination of drought indices, and the weights are statistically determined by the PCA at each stage of assessment. The performance of the model was evaluated by cross-validation, drought category prediction accuracy and three representative years. The model's overall assessment ability is strong.

6.2 Conclusion

The following conclusions were drawn from this study:

1) It is possible to assess potential drought risk on crop yield using weather information in the recharge period before seeding. Although uncertainties exist, the initial assessment at this point is valuable for policy makers and farmers. Recharge period weather conditions also help to improve assessment accuracy during the growing season. From stage 1 to stage 6, the model's assessment accuracy increases. April and May moisture conditions slightly improve the accuracy of assessment. June and July are the most important months for determining the risk of agricultural drought. The most accurate assessment can be achieved at the beginning of August (average $R^2 = 0.61$). The weather of August plays a minor role in agricultural drought risk assessment, or may even mislead the assessment.
2) The performance of the ADRA model was also evaluated by the prediction accuracy associated with each drought category in validation period. From stage 1 to stage 6, the assessment accuracy rate of each drought category increased from 72 to 80% for non-drought, 23 to 33% for mild, 13 to 40% for moderate, 0 to 24% for severe, and 0 to 5% for extreme drought. Although severe and extreme droughts were routinely underpredicted by the model, it still provides useful information on the spatial and temporal patterns of dry conditions.
3) The performance of the model also revealed great spatial variability across the prairies in the strength of the correlation between standardized spring wheat yield

residuals and blended drought indices. Some of the variation in model performance can be attributed to variations in mean growing season precipitation and latitude. Both factors are inversely related to model performance. The model performs best in the regions that have a more southerly location and a low mean growing season precipitation (i.e. the soil moisture stress has a strong impact on crop production). Blended drought indices are not effective at modelling variations in yield in those areas that consistently receive relatively large amounts of precipitation during the growing season (i.e. soil moisture is no longer an important yield-limiting factor). In addition, as the variability of the growing season precipitation increases, the model performance increases. All these factors collectively influence the correlation between spring wheat yield and blended drought indices, and should be jointly considered when interpreting their relationships to model performance.

4) Based on the evaluation of drought indices that were used to construct blended drought indices, the Palmer drought indices (PDSI and Z-index), accounting for the majority of variance in drought indices, are more effective for agricultural drought assessment than the SPI. The PDSI is important for assessing drought risk at pre-planting and earlier growing season. The Z-index is sensitive to short-term soil moisture anomalies, and thus important for growing season drought risk assessment. The SPI is also a useful measure of agricultural drought, accounting for some of the variance in yield residuals that was unexplained by the Palmer drought indices.

6.3 Recommendations for Future Research

A number of problems and limitations were raised in this study. The suggestions as to future research are as follow:

1) The monthly time scale of assessment limits the opportunity to assess the impact of droughts that occur for shorter intervals or to associate the water stress to critical growth stages that are less than a month. The drought indices used in the current study were calculated on a monthly scale. It would be valuable to generate drought indices on shorter time scales (e.g. weekly, biweekly) to assess short-term dry spells during important crop phenological stages, which may not be detected by longer-term predictions.
2) In addition to the total growing season precipitation, the timing of the precipitation and its distribution in the growing season are critical to crop yield. However, these two factors are not accounted by the drought indices, thus limiting the model's predictive ability. Model performance would be further increased if drought indices were calculated on a weekly or biweekly basis and were weighted according to the pattern of crop water demands.
3) The ADRA model does not perform well to accurately predict the large negative yield departures, as severe and extreme droughts were routinely underpredicted. One possible reason is the insufficient number of observations with extremely low yield. A longer period of record including more severe or extreme drought years may improve the predictive accuracy. It is also possible that the response of yield to dry

conditions may not be linear when the soil moisture is below a certain threshold. A nonlinear model may be more appropriate to estimate yields under very dry conditions.

4) The ADRA model could be improved if additional data were available that measure some of the other factors affecting crop yield, such as insects, diseases, and weather-related damages (e.g. hail, wind, frost). Furthermore, latitude can be treated as a proxy variable for the north-south gradient in solar radiation, temperature, soil conditions, and growing season length.
5) The model could also be affected by the quality of the climate data that is being used to calculate drought indices. For the SPI, using precipitation data from the interpolation of monthly-aggregated station observations will introduce less interpolation-related error. As to the study of comparison of two schemes (the temporal aggregation of daily interpolated climate grids to create grids of coarser temporal resolution vs. the temporal aggregation of daily station data to create grids at the same temporal resolution), more work could be done to map the error of grid cells. The spatially distributed error of an interpolated surface would help to more closely examine the relationship between two schemes and topographic structure.
6) Further improvements can be made by introducing remote sensing vegetation indices, such as the Normalized Difference Vegetation Index (NDVI), Enhanced Vegetation index (EVI), and Vegetation Condition Index (VCI), as extra predictors in the model to help assess drought risk during the growing season. Remote sensing indices have a

few advantages over the traditional climate data related drought indices, such as good spatial resolution (i.e. no interpolation is needed), and comprehensive coverage over large areas. Indeed, at present, Statistics Canada (AVHRR, 1km pixel resolution) and Agriculture and Agri-Food Canada (MODIS, 250m pixel resolution) have developed medium-resolution remote sensing-based products based on the NDVI, that allow current weekly crop conditions to be compared to longer-term averages. However, remote sensing techniques are of limited value to assess recharge period weather conditions, drought risk before seeding and near harvest. At pre-planting, the depth of the soil water estimated is relatively shallow compared to the rooting depth of spring wheat (Boisvert *et al.*, 1997; Qian *et al.*, 2009). Near harvest, remote sensing vegetation indices approach a saturation level during the last stage of crop development, making this method also less effective (Qian *et al.*, 2009)

7) This study chose spring wheat as an agricultural drought indicator. It would be useful to extend this study to cover other crops that are important to the prairies, such as canola and barley. The ARDA model may not be appropriate for all crops, because the influence of moisture conditions on yield tends to be different for different crops, and the crops' reaction to moisture stress are different.
8) The ADRA model cannot be applied in all situations (e.g. flood regions, well-irrigated areas). In flood-prone regions, a hybrid method that couples the ADRA model with flood forecasting models would be valuable to agriculture sectors, providing a more comprehensive assessment on crop yield.

References

AAFC (Agriculture and Agri-Food Canada). (2005). *Available Water Holding Capacity.* Retrieved September 20, 2008, from Canadian Soil Information System (CanSIS) Web site: http://sis.agr.gc.ca/cansis/nsdb/slc/v3.0/component/awhc.html.

AAFC (Agriculture and Agri-Food Canada). (2007a). *Gridded Climate Data.* Retrieved March 4, 2008, from National Land and Water Information Service Web site: http://www4.agr.gc.ca/AAFC-AAC/display-afficher.do?id=1227620138144&lang =eng.

AAFC (Agriculture and Agri-Food Canada). (2007b). *PDI Description.* Retrieved February 11, 2009, from Drought Watch Web site: http://www.agr.gc.ca/pfra/drought/nlplmrdesc_e.htm.

AAFC (Agriculture and Agri-Food Canada). (2007c). *Soil Landscapes of Canada Version 3.1.1.* Retrieved September 20, 2008, from Canadian Soil Information System (CanSIS) Web site: http://sis.agr.gc.ca/cansis/nsdb/slc/v3.1.1/intro.html.

Acton, D.F. & Gregorich, L.J. (1995). *The health of our soils: toward sustainable agriculture in Canada* (138pp). Centre for Land and Biological Resources Research, Research Branch, Agricultural and Agri-Food Canada, Ottawa.

Acton, D.F., Padbury, G.A. & Stushnoff, C.T. (1998). *Prairies.* Retrieved December 5, 2008, from the encyclopedia of Saskatchewan Web site: http://esask.uregina.ca/entry/prairies.html.

Akinremi, O.O. & McGinn, S.M. (1996). Evaluation of Palmer drought index on the Canadian prairies. *Journal of Climate, 9*, 897-905.

Alley, W.M. (1984). The Palmer drought severity index: limitations and assumptions. *Journal of Climate and Applied Meteorology, 23*, 1100-1109.

Almorox. J., Benito, M. & Hontoria, C. (2004). Estimation of monthly Angstrom-Prescott equation coefficients from measured daily data in Toledo, Spain. *Renewable Energy, 30*, 931-936.

Arora, V.K., Prihar, S.S. & Gajri, P.R. (1987). Synthesis of a simplified water use simulation model for predicting wheat yields. *Water Resources Research, 23*(5), 903-910.

Ash, G.H.B. & Shaykewich, C.F. (2005). *Agricultural climate of the eastern Canadian prairies*. Retrieved November 10, 2008, from Manitoba Agriculture, Food and Rural Initiatives Web site: http://www.gov.mb.ca/agriculture/climate/waa00s00.html

Ash, G.H.B., Shaykewish, C.F. & Raddatz, R.L. (1992). Moisture risk assessment for spring wheat on the eastern prairies: a water-use simulation model. *Climatological Bulletin, 26*(2), 65-78.

Babb, J.C., Khandekar, M.L. & Garnett, E.R. (1997). An analysis of PNA indices for forecasting summer weather over the Canadian prairies with implications for wheat yield and protein. In *Proceedings of the Long-Range Weather and Crop Forecasting Work Group Meeting III* (pp. 31–36). Canadian Meteorological Centre, Dorval, QB.

Baier, W.J., Boisvert, J.B. & Dyer, J.A. (2000). *The Versatile Soil Moisture Budget (VB) reference manual* [Computer program], ECORC Contribution No. 001553. Ottawa, ON: Agriculture and Agri-Food Canada, Eastern Cereal and Oilseed Research Centre.

Bonsal, B.R. & Wheaton, E.E. (2005). Atmospheric circulation comparison between the 2001 and 2002 and the 1961 and 1988 Canadian Prairie droughts. *Atmosphere-Ocean, 43,* 163-172.

Bonsal, B.R., Zhang, X. & Hogg, W.D. (1999). Canadian prairies growing season precipitation variability and associated atmospheric circulation. *Climate Research, 11*, 191-208.

Boisvert, J.B., Gwyn, Q.H.J., Chanzy, A., Major, D.J., Brisco, B. & Brown, R.J. (1997). Effect of surface soil moisture gradients on modelling radar backscattering from bare fields. *International Journal of Remote Sensing, 18*, 153–170.

Bordi, I. & Sutera, A. (2007). Drought monitoring and forecasting at large scale. In Rossi, G. *et al.* (Eds.), *Methods and Tools for Drought Analysis and Management* (pp. 3–27). New York: Springer.

Briffa, K.R., Jones, P.D. & Hulme, M. (1994). Summer moisture variability across Europe, 1892-1991: an analysis based on the Palmer drought severity index. *International Journal of Climatology, 14*, 475-506.

Brown, F.J., Brian, D.W., Tadesse, T., Hayes, M.J. & Bradley, C.R. (2008a). The vegetation drought response index (VegDRI): a new integrated approach for monitoring drought stress in vegetation. *GIScience & Remote Sensing, 45:*16-46.

Brown, F.J., Perves, S., Brian, D.W. (2008b). Assessment of 2006 and 2007 drought patterns in the vegetation drought response index across Nebraska. *Pecora 17-The Future of Land Imaging...Going Operational*, Denver, Colorado.

Bumsted, J.M. (1999). *Dictionary of Manitoba Biography.* Winnipeg: University of Manitoba Press.

Bushuk, W. (1982). Environment and grain quality components. In *Grains and Oilseeds: handling, marketing, processing,* 3rd Ed. (pp. 463-472). Winnipeg: Canadian International Grain Institute.

Byun, H.R. & Wilhite, D.A. (1999). Objective quantification of drought severity and duration. *Journal of Climate, 12,* 2747-2756.

Cacciamani, C., Morgillo, A., Marchesi, S. & Pavan, V. (2007). Monitoring and forecasting drought on a regional scale: Emilia-Romagna region. *Water Science and Technology Library, 62*, 29-48.

Cancelliere, A., Mauro, G.D., Bonaccorso, B. & Rossi, G. (2007). Drought forecasting using the standardized precipitation index. *Water Resource Manage, 21*, 801-819.

Campbell, C.A., Zenter, R.P., Gameda, S., Blomert, B. & Wall, D.D. (2002). Production of annual crops on the Canadian prairies: trends during 1976-1998. *Canadian Journal of Soil Science, 82*, 45-57.

Chopra, P. (2006). Drought risk assessment using remote sensing and GIS: a case study of Gujarat. *Msc Thesis*. International Institute for Geo-Information Science and Earth Observation, Enschede, the Netherlands.

Cohen, S.E., Wheaton, E. & Masterton, J. (1992). Impacts of climate change scenarios in the prairies provinces: a case study from Canada. *Saskatoon: Saskatchewan Research Council.*

Coolidge, F.L. (2000). *Statistics: A Gentle Introduction.* Thousand Oaks, CA: SAGE Publications.

Craven, P. & Wahba, G. (1979). Smoothing noisy data with spline functions. *Numerische Mathematik, 31*, 377-403.

DeGaetano, T. & Belcher, B.N. (2006). *Spatial interpolation of daily maximum and minimum air temperature based on meteorological model analyses and independent observations.* Retrieved July 16, 2008, from Web site: http://www.tc. cornell.edu/research/compag/interpolation_paper_final.pdf.

Dennett, M.D., Elston, J. & Diego, Q.R. (1998). Weather and yields of tobacco, sugar beet and wheat in Europe. *Agricultural Meteorology, 21*, 249-263.

Dietz, T.J., Put, M. & Subbiah, S. (1998). Drought risk assessment for dryland agricultural in semi-arid Telangana, Andhra Pradesh, India. In Bruins, H.J. (Ed.), *The Arid Frontier: Interactive management of Environment and Development* (pp. 143-161). Dordrecht, Netherlands: Kluwer Academic Publishers.

Dracup J.A., Lee, K.S. & Paulson, E.G. (1980). On a definition of droughts. *Water Resources Research, 16*, 297–302.

Drought Monitor. (2008). *Drought Monitor: State-of –the –art Blend of Science and Subjectivity.* Retrieved October 30, 2008, from Drought Monitor Web site: http://drought.unl.edu/dm/classify.htm.

Edwards, D.C. & McKee, T.B. (1997). Characteristics of 20th century drought in the United States at multiple time scales. *Climatology Report Number 97-2*, Colorado State University, Fort Collins, Colorado.

Einstein, N. (2005). *Palliser's Triangle*. Retrieved January 10, 2009, from Wikipedia Web site: http://en.wikipedia.org/wiki/Palliser's_Triangle.

Environment Canada. (2008a). *Snapshot of the Prairies ecozone.* Retrieved November 6, 2008, from Environment Canada Web site: http://www.ec.gc.ca/soer-eee/English /soer/1996Report/Doc/1-6-4-3-2-1.cfm.

Environment Canada. (2008b). *Flooding events in Canada-Prairie Provinces.* Retrieved November 6, 2008, from Environment Canada Web site: http://www.ec.gc.ca/ WATER/en/manage/floodgen/e_prair.htm#20.

Environmental System Research Institute. (2006). ArcGIS 9.2. Redlands, CA: Environmental System Research Institute.

Fang, X. (2007). Snow hydrology of Canadian prairie droughts: model development and application . *Msc Thesis.* University of Saskatchewan.

Fang, X. & Pomeroy, J.W. (2007). Snowmelt runoff sensitivity analysis to drought on the Canadian Prairies. *Hydrological Processes, 21*, 2594-2609.

Gray, D.M., Granger, R.J. & Landine, P.G. (1986). Modelling snowmelt infiltration and runoff in a prairie environment. In Kane, D.L (Ed.) *Proceedings of the Cold. Regions Hydrology Symposium* (pp.427-438). American Water Resources Association, Bethesda, MD.

Guttman, N.B. (1999). Accepting the standardized precipitation index: a calculation algorithm. *Journal of the American Water Resources Association, 35*, 311–322.

Hare, F.K. & Thomas, M.K. (1919). *Climate Canada.* Toronto: John Wiley & Sons Canada Limited.

Harwood, J., Heifner, R., Coble, K., Perry, J. & Somwary, A. (1999). Managing risk in farming: concepts, research, and analysis. *Agricultural Economic Report No. 774,* Economic Research Service, U.S. Department of Agricultural, Washington, DC.

Hayes, M.J. (2006). *Drought Indices.* Retrieved September 6, 2008, from NDMC (National Drought Mitigation Center) Web site: http://drought.unl.edu/whatis /indices.htm.

Heim, R.R. (2002). A review of twentieth-century drought indices used in the United States. *Bulletin of the American Meteorological Society, 83*(8), 1149–1165.

Herrington, R., Johnson, B.N. & Hunter, F.G. (1997). Responding to global climate change in the Prairies. *Canada Country Study: Climate Impacts and Adaptation, 3,* 75.

Hill, J.D., Strommen, N.D. Sakamoto, C.M. & Leduc, S.K. (1980). LACIE- an application of meteorology for United States and foreign wheat assessment. *Journal of Applied Meteorology and Climatology, 19*, 22-34.

Hu, Q. & Willson, G.D. (2000). Effects of temperature anomalies on the Palmer Drought Severity Index in the central Untied State. *International Journal of Climatology, 20*, 1899-1911.

Hubbard, K.G. & Wu, H. (2005). Modification of a crop-specific drought index for simulating corn yield in wet years. *Agronomy Journal, 97,* 1478-1484.

Hutchinson, M.F. & Bischof, R.J. (1983). A new method for estimating mean seasonal and annual rainfall for the Hunter Valley, New South Wales. *Australian Meteorological Magazine, 31*, 179-184.

Hutchinson, M.F. (1991). The application of thin plate smoothing splines to continent-wide data assimilation. In Jasper J.D. (Ed.) Data Assimilation Systems (pp. 104-113). BMRC Research Report No. 27. Melbourne: Bureau of Meteorology.

Hutchinson, M.F. & Gessler, P.E. (1994). Splines - more than just a smooth interpolator. *Geoderma, 62*, 45-67.

Hutchinson, M.F. (1995). Interpolating mean rainfall using thin plate smoothing splines. *International Journal of Geographical Information Systems, 9*(4), 385-403.

Hutchinson, M.F. (1998a). Interpolation of rainfall data with thin plate smoothing splines - part I: two dimensional smoothing of data with short-range correlation. *Journal of Geographic Information and Decision Analysis, 2*(2), 139-151.

Hutchinson, M.F. (1998b). Interpolation of rainfall data with thin plate smoothing splines-part II: analysis of topographic dependence. *Journal of Geographic Information and Decision Analysis 2*(2), 152-167.

Hutchinson, M.F. (2006). ANUSPLIN Version 4.3: User Guide, the Australian National University, Centre for Resource and Environmental Studies, Canberra, Australia.

Jarvis, C.H. & Stuart, N. (2001). A comparison among strategies for interpolating maximum and minimum daily air temperatures. Part I: the selection of " guiding" topographic and land cover variables. *Journal of Applied Meteorology, 40*(6), 1060-1074.

Jeffrey, S.J., Carter, J.O., Moodie, K.B. & Beswick, A.R. (2001). Using spatial interpolation to construct a comprehensive archive of Australian climate data. *Environmental Modelling & Software, 16*, 309-330.

Jolly, W.M., Graham, J.M., Michaelis, A., Nemani, R. & Running, S.W. (2005). A flexible, integrated system for generating metrological surfaces derived from point sources across multiple geographic scales. *Environmental Modelling & Software 20*, 873-882.

Kanwar, R.S., Baker, J.L. & Mukhtar, S. (1988). Excessive soil water effects at various stages of development on the growth and yield of corn. *Transactions of the American Society of Agricultural Engineers, 31*, 133–141.

Karl, T.R. (1986). The sensitivity of the Palmer Drought Severity Index and Palmer's Z-index to their calculation coefficients including potential evapotranspiration. *Journal of Climate and Applied Meteorology, 25*, 77-86.

Karl, T.R., Quilan, F. & Ezell, D.S. (1987). Drought termination and amelioration: its climatological probability. *Journal of Climate and Applied Meteorology, 26,* 1198-1209.

Kemp, D.D. (1982). The drought of 1804-1805 in central North America. *Weather, 37,* 34-41.

Khandekar, M.L. (2004). *Canadian Prairies drought: a climatologically assessment.* Retrieved November 8, 2008, from Government of Alberta Web site: http:// environment.gov.ab.ca/info/library/6673.pdf.

King, W.J. (1987). Irrigation of cereal crops. Saskatchewan Water Corporation, Outlook, Saskatchewan.

King, J.R. & Donald, A.J. (1999). Variable selection in large environmental data sets using principal components analysis. *Environmetrics, 10,* 67-77.

Kogan, F.N. (1995). Droughts of the late 1980s in the United States as derived from NOAA polar-orbiting satellite data. *Bulletin of the American Meteorological Society 76*(5), 655–668.

Kumar, V. (1999). Prediction of agricultural drought for the Canadian Prairies using climatic and satellite data, *Doctor Thesis*, Department of Geography, University of Manitoba.

Kumar, V. & Panu, U. (1997). Predictive assessment of severity of agricultural droughts based on agro-climatic factors. *Journal of American Water Resources Association, 33*(6), 1255–1264.

Kurtzman, D. & Kadmon, R. (1999). Mapping of temperature variable in Israel: a comparison of different interpolation methods. *Climate Research, 13*, 33-43.

Large, E.C. (1954). Growth stages in cereals. *Plant Pathology 3,* 128-129.

Loukas, A. & Vasiliades, L. (2004). Probabilistic analysis of drought spatiotemporal characteristics in Thessaly region, Greece, *Natural Hazards and Earth System Sciences, 4,* 719–731.

Luo, H., Skees, J.R. & Marchant, M.A. (1994). Weather information and the potential for intertemporal adverse selection in crop insurance. *Review of Agricultural Economics, 16*(3), 441-451.

Luo, Y. & Zhou, X. (2006). *Chapter 6. Temperature and spatial variations in soil respiration.* In Luo, Y. and Zhou, X. (Eds.), Soil respiration and the environment (pp.107-132). New York: Academic Press.

Manitoba Ag-Weather Program. (2001). *Average crop water demand to maturity for potatoes.* Retrieved March 2, 2009, from Manitoba Ag-Weather Program Web site: http://www.gov.mb.ca/agriculture/climate/pdf/wab00s10.pdf.

Mavromatis, T. (2007). Drought index evaluation for assessing future wheat production in Greece. *International of Journal Climatology, 27,* 911-924.

Maybank, J., Bonsal, B., Jones, K., Lawford, R., O'Brien, E.G., Ripley, E.A. & Wheaton E. (1995). Drought as a natural disaster. *Atmosphere-Ocean, 33,* 195-222.

McKee, T. B., Doesken, N. J. & Kleist, J. (1993). The relationship of drought frequency and duration to time scale. Preprints, *8th Conference on Applied Climatology,* 179–184. Anaheim, California.

McKee, T.B., Doesken, N.J. & Kleist, J. (1995). Drought monitoring with multiple time scales. Preprints, *9th Conference on Applied Climatology,* 233–236. Dallas, Texas.

McKenney, D.W., Kesteven, J.L., Hutchinson, M.F. & Venier, L.A. (2001). Canada's plant hardiness zones revisited using modern climate interpolation techniques. *Canadian Journal of Plant Science, 81,* 117-129.

McKenney, D.W., Pedlar, J.H., Papadopol, P. & Hutchinson, M.F. (2006). The development of 1901-2000 historical monthly climate models for Canada and the United States. *Agricultural and Forest Meteorology, 138,* 69-81.

Moreira, E.E., Paulo, A.A., Pereira, L.S. & Mexia, J.T. (2006). Analysis of SPI drought class transitions using loglinear models. *Journal of Hydrology, 331*(2), 349-359.

Morgan, R. (1985). The development and application of a drought early warning system in Botswana. *Disasters, 9*, 44-50.

Mota, F.S. (1983). Weather-technology models for corn and soybean in the south of Brazil. *Agricultural Meteorology, 28,* 49-64.

NDMC (National Drought Mitigation Center). (2006). *What is Drought?* Retrieved October 28, 2008, from NDMC Website: http://drought.unl.edu/whatis/concept/ htm.

Newlands, K.N., Davidson, A., Howard, A. & Hill, H. (2008). Agriclimatic data processing: 10km daily gridded climate datasets for Canada, 1961-2003. *GRIP-07MOA74817 Progress Report, 02,* 59-106.

Nkemdirim, L. & Weber, L. (1999). Comparison between the droughts of the 1930s and the 1980s in the southern prairies of Canada. *Journal of Climate, 12*, 2434-2450.

Palmer, W.C. (1965). Meteorological drought. *Research Paper No. 45.*

Palmer, W.C. (1968). Keeping track of crop moisture conditions nationwide: the new crop moisture index. *Weatherwise 21*, 156-161.

Paulo, A.A. & Pereira, L.S. (2007). Prediction of SPI Drought Class Transitions Using Markov Chains. *Water Resource Management, 21,* 1813-1827.

Pereira, L.S., Cordery, I. & Iacovides, I. (2002). Coping with Water Scarcity. *Technical Documents in Hydrology, 58,* 267.

Pomeroy, J.W. & Goodison, B.E. (1997). Winter and Snow. In Bailey, W.G., Oke, T.R. & Rouse, W.R. (Eds.) *The Surface Climates of Canada.* (pp. 68-100). Montreal: McGill-Queen's University Press.

Price, D.T., McKenney, D.W., Nalder, I.A., Hutchinson, M.F. & Kesteven, J.L. (2000). A comparison of two statistical methods for spatial interpolation of Canadian monthly mean data. *Agricultural and Forest Meteorology, 101*, 81-94.

Priestley, C.H.B. & Taylor, R.J. (1972). On the assessment of surface heat flux and evaporation using large-scale parameters. *Monthly Weather Review, 100*, 81-92.

Qian, B., Jong, R.D., Warren, R., Chipanshi., A. & Hill, H. (2009). Statistical spring wheat yield forecasting for the Canadian prairies provinces. *Agricultural and Forecast Meteorology.* Doi: 10.1016/j.agrformet.2008.12.006.

Quiring, S.M. (2001). The detection and prediction of agricultural drought in the Canadian Prairies. *Msc. Thesis*. University of Manitoba, Winnipge, Manitoba.

Quiring, S.M. & Papakryiskou, T.N. (2003). An evaluation of agricultural drought indices for the Canadian prairies. *Agricultural and Forest Meteorology, 118,* 49-62.

Quiring, S.M. & Papakryiskou, T.N. (2005). Characterizing the spatial and temporal variability of June-July moisture conditions in the Canadian Prairies. *International Journal of Climatology, 25*, 117-138.

R Development Core Team (2008). R: A language and environment for statistical computing. R Foundation for Statistical Computing, Vienna, Austria. ISBN 3-900051-07-0, URL http://www.R-project.org.

Raddatz, R.L. (1998). Anthropogenic vegetation transformation and the potential for deep convection on the Canadian prairies. *Canadian Journal of Soil Science, 78,* 657-666.

Rahmani, E., Khalili, A. & Liaghat, A. (2008). Quantitative survey of drought effects on barely yield in east Azerbaijan by classical statistical methods. *Journal of Science and Technology of Agriculture and Natural Resources, 12*(44), 37-50.

Richards, W. & Burridge, E. (2006). Historical drought detection and evaluation using the Standardized Precipitation Index and gridded data. Prepared for CCIAP A 932 "Canadian Agricultural Adaptations to 21st Century Droughts: Preparing for Climate Change". Environment Canada, Saskatoon, SK. 8pp.

Riha, S.J., Wilks, D.S. & Simoens, P. (1996). Impact of temperature and precipitation variability on crop model predictions. *Climatic Change, 32*, 293-311.

Rogerson, P.A. (2001). Chapter 10. Data reduction: factor analysis and cluster analysis. In Rogerson, P.A (Ed.) *Statistical methods for geography* (pp.192-197). London: SAG Publications Ltd.

Romesburg, H.C. (1984). Chapter 9. Clustering methods. In Romesburg, H.C. (Ed.). *Cluster analysis for researchers* (pp.119-140). Belmont, CA: Wadsworth.

Rosenberg, N.J. (1978). *North American Droughts.* American Association for the Advancement of Science, Symposium, Denver, Colorado, February 1977. Boulder, CO: Westview Press.

Sinha, C.P., Chaube, U.C. & Saxena, R.P. (1992). A critical analysis of drought indices for different regions. *Proc. World Congress on Natural Hazards,* New Delhi, January 10- 14.

Smakhtin, V.U. & Hughes, D.A. (2004). Review, automated estimation and analyses of drought indices in South Asia. *Working Paper 83.* Colombo, Sri Lanka: International Water Management Institute.

Smart, G.M. (1983). Drought analysis and soil moisture prediction. *Journal of the Irrigation and Drainage Engineering, American Society of Civil Engineers, 109*(2), 251-261.

Smith, D.I., Hutchinson, M.F. & McArthur, R.J. (1993). Australian climatic and agricultural drought: payments and policy. *Drought Network News, 5*(3), 11-12.

Stahl, K., Moore, R.D., Floyer, J.A., Asplin, M.G. & Mckendry, I.G. (2006). Comparison of approaches for spatial interpolation of daily air temperature in a large region with complex topography and highly variable station density. *Agricultural and forest Meteorology, 139*, 224-236.

Starr, T.B. & Kostrow, P.I. (1978). The response of spring wheat yield to anomalous climate sequences in the United States. *Journal of applied meteorology, 17*(8), 1101-1115.

Statistics Canada. (2007). *Census Agricultural Regions Boundary Files of the 2006 Census of Agriculture.* Retrieved November 20, 2008, from Statistics Canada Web site: http://www.statcan.gc.ca/pub/92-174-x/92-174-x2007000-eng.htm.

Statistics Canada. (2008). *Production of principal field crops.* Retrieved June 15, 2009, from Statistics Canada Web site: http://www.statcan.gc.ca/daily-quotidien/080822/dq080822a-eng.htm.

Steinemann, A.C., Hayes, M. & Cavalcanti, L. (2005). Drought indicators and triggers. In Wilhite, D.A. (Ed.), *Drought and water crises: Science, technology, and management issues* (pp. 71-92). New York: CRC.

Steinemann, A.C. & Luiz, F.N. (2006). Developing Multiple Indicators and Triggers for Drought Plans, *Journal of Water Resources Planning and Management, 132*(3), 164-174.

Strommen, N.D. & Motha, R.P. (1987). An operational early warning agricultural weather system. In Wilhite, D.A., Easterling, W.E. & Wood, D.A. (Eds.), *Planning for drought: Toward a reduction of societal vulnerability.* Boulder, CO: Westview Press.

Sullivan, P. (2002). *Drought resistant soil.* Retrieved June 13, 2009, from National Sustainable Agriculture Information Service Web site: http://attra.ncat.org/attra-pub/drought.html.

Sutton, D. (2003). *Agroclimatic atlas of Alberta: soil moisture conditions in Alberta.* Retrieved January 26, 2009, from Government of Alberta: Agriculture and Rural Development Web site: http://www1.agric.gov.ab.ca/$department/deptdocs.nsf/all/sag6302.

Svoboda, M., LeComte, D., Hayes, M., Heim, R., Gleason, K., Angel, J., Rippey, B., Tinker, R., Palecki, M., Stooksbury, D., Miskus, D. & Stephens, S. (2002). The drought monitor. *Bulletin of the American Meteorological Society, 83*(8), 1181-1190.

Thornthwaite, C.W. (1948). An approach toward a rational classification of climates. *Geophysical Review, 38,* 55-94.

Tsakiris, G. & Vangelis, H. (2004). Towards a drought watch system based on spatial SPI. *Water Resources Management, 18,* 1-12.

Wahba, G. (1990). Spline models for observational data. In *CBMS-NSF Regional Conference Series in Applied Mathematics*, Society for Industrial and Applied Mathematics (Philadelphia), 59, 169.

Wahba, G. & Wendelberger, J. (1980). Some new mathematical methods for variational objective analysis using splines and cross validation. *Monthly Weather Review, 108,* 122-1143.

Ward, J.H. (1963). Hierarchical grouping to optimize an objective function. *Journal of the American Statistical Association, 58,* 236-244.

Wenkert, W., Fausey, N.R. & Watters, H.D. (1981). Flooding responses in Zea mays L. Plant Soil 62, 351-366.

Wheaton, E.E., Arthur, L.M., Chorney, B., Shewchuk, S., Thorpe, J., Whiting, J. & Wittrock, V. (1992). The Prairies drought of 1988. *Climatological Bulletin, 26,* 188-205.

Wheaton, E.E., Kulshreshtha, S., Wittrock, V. & Koshida, G. (2008). Dry times: hard lessons from the Canadian drought of 2001 and 2002. *The Canadian Geographer, 52*(2), 241-262.

Wheaton, E.E., Wittrock, V., Kulshreshtha, S., Koshida, G., Grant, C., Chipanshi, A. & Bonsal, B. (2005). Lessons learned from the Canadian drought years of 2001 and 2002: synthesis report. Prepared for *Agricultural and Agri-Food Canada and the Canadian Drought Study Steering Committee*. Saskatchewan Research Council. Publication No. 11602-46E03. Retrieved November 19, 2008, from Agriculture and Agri-Food Canada Web site: http://www.agr.gc.ca/pfra/drought/info/11602-46E03.pdf.

Whitmore, J.S. (2000). Chapter 7. Hardy and drought – evasive cereal crops. In Whitmore, J.S (Ed.), *Drought Management on Farmland* (pp.79-97). London: Springer.

Wilhite, D.A. (1992). Drought. In Brekhovskikh, L., Turekian ,K.K., Emery, K., Tseng, C.K., LePichon, X., Curray, J.R., Seibold, E., Nasu, N. & Lisitzin, A.P (Eds.) *Encyclopedia of Earth System Science, 2* (pp. 81-92). San Diego, California: Academic Press.

Wilhite, D.A. & Buchanan-Smith, M. (2005). Drought as Hazard: understanding the natural and social context. In Whilhite, D.A. (Ed.) *Drought and Water Crises: Science, Technology, and Management Issues* (pp. 3-29). Boca Raton, Florida: CRC Press.

Wilhite, D.A. & Glantz, M.H. (1985). Understanding the drought phenomenon: The role of definitions, *Water International, 10*(3), 111–120.

Willeke, G., Hosking, J.R.M., Wallis, J.R. & Guttman, N.B. (1994). The National Drought Atlas. *Institute for Water Resources Report, 94–NDS–4.*

Wu, H., Hubbard, K.G. & Wilhite, D. (2004). An agricultural drought risk-assessment model for corn and soybeans. *International Journal of Climatology, 24,* 723–741.

APPENDIX A: R Code for the ADRA Model

```
Model = function(cluster, st, indices)
{

    tMBE=tRMSE=vMBE=vRMSE=tMBE1=tRMSE1=vMBE1=vRMSER1=R=R1
   =num=znum=vali_num=cali_num=0

   for (va in (1976:2003))
   {

       t1<-indices[indices$Year != va,]
       v1<-indices[indices$Year == va,]

        if (st=="Stage1 April")
        {pc<-princomp (~SPI_1_Sep+SPI_1_Oct+SPI_1_Nov+SPI_1_Dec+SPI_1_Jan
         +SPI_1_Feb+SPI_1_Mar+SPI_3_Nov+SPI_3_Dec+SPI_3_Jan +SPI_3_Feb
         +SPI_3_Mar+SPI_6_Feb+SPI_6_Mar+PDSI_Sep+PDSI_Oct+PDSI_Nov
         +PDSI_Dec+PDSI_Jan+PDSI_Feb+PDSI_Mar+Z_Sep+Z_Oct+Z_Nov+Z_Dec
         +Z_Jan+Z_Feb+Z_Mar, data=t1)}

        if (st=="Stage2 May")
        {pc<-princomp(~SPI_1_Sep+SPI_1_Oct+SPI_1_Nov+SPI_1_Dec+SPI_1_Jan
         +SPI_1_Feb+SPI_1_Mar+SPI_1_Apr+SPI_3_Nov+SPI_3_Dec+SPI_3_Jan
         +SPI_3_Feb+SPI_3_Mar+SPI_3_Apr+SPI_6_Feb+SPI_6_Mar+SPI_6_Apr
         +PDSI_Sep+PDSI_Oct+PDSI_Nov+PDSI_Dec+PDSI_Jan +PDSI_Feb
         +PDSI_Mar+PDSI_Apr+Z_Sep+Z_Oct+Z_Nov+Z_Dec+Z_Jan+Z_Feb
         +Z_Mar+Z_Apr, data=t1)}

        if (st=="Stage3 June")
        {pc<-princomp(~SPI_1_Sep+SPI_1_Oct+SPI_1_Nov+SPI_1_Dec+SPI_1_Jan
         +SPI_1_Feb+SPI_1_Mar+SPI_1_Apr+SPI_1_May+SPI_3_Nov+ SPI_3_Dec
         +SPI_3_Jan+SPI_3_Feb+SPI_3_Mar+SPI_3_Apr+SPI_3_May+SPI_6_Feb
         +SPI_6_Mar+SPI_6_Apr+SPI_6_May+PDSI_Sep+PDSI_Oct+PDSI_Nov
         +PDSI_Dec+PDSI_Jan+PDSI_Feb+PDSI_Mar+PDSI_Apr+PDSI_May +Z_Sep
         +Z_Oct+Z_Nov+Z_Dec+Z_Jan+Z_Feb+Z_Mar+Z_Apr+Z_May, data=t1)}

        if (st=="Stage4 July")
        {pc<-princomp(~SPI_1_Sep+SPI_1_Oct+SPI_1_Nov+SPI_1_Dec+SPI_1_Jan
         +SPI_1_Feb+SPI_1_Mar+SPI_1_Apr+SPI_1_May+SPI_1_Jun+SPI_3_Nov
         +SPI_3_Dec+SPI_3_Jan+SPI_3_Feb+SPI_3_Mar+SPI_3_Apr+SPI_3_May
         +SPI_3_Jun+SPI_6_Feb+SPI_6_Mar+SPI_6_Apr+SPI_6_May+SPI_6_Jun
         +PDSI_Sep+PDSI_Oct+PDSI_Nov+PDSI_Dec +PDSI_Jan+PDSI_Feb
         +PDSI_Mar+PDSI_Apr+PDSI_May+PDSI_Jun+Z_Sep+Z_Oct+Z_Nov+Z_Dec
         +Z_Jan+Z_Feb+Z_Mar+Z_Apr+Z_May+Z_Jun, data=t1)}
        if (st=="Stage5 August")
```

```
{pc<-princomp(~SPI_1_Sep+SPI_1_Oct+SPI_1_Nov+SPI_1_Dec+SPI_1_Jan
 +SPI_1_Feb+SPI_1_Mar+SPI_1_Apr+SPI_1_May+SPI_1_Jun+SPI_1_Jul
 +SPI_3_Nov+SPI_3_Dec+SPI_3_Jan+SPI_3_Feb+SPI_3_Mar+SPI_3_Apr
 +SPI_3_May+SPI_3_Jun+SPI_3_Jul+SPI_6_Feb+SPI_6_Mar+SPI_6_Apr
 +SPI_6_May+SPI_6_Jun+SPI_6_Jul +PDSI_Sep+PDSI_Oct+PDSI_Nov
+PDSI_Dec+PDSI_Jan+PDSI_Feb+PDSI_Mar+PDSI_Apr+PDSI_May
 +PDSI_Jun+PDSI_Jul+Z_Sep+Z_Oct+Z_Nov+Z_Dec +Z_Jan+Z_Feb
 +Z_Mar+Z_Apr+Z_May+Z_Jun+Z_Jul, data=t1)}

if (st=="Stage6 September")
{pc<-princomp(~SPI_1_Sep+SPI_1_Oct+SPI_1_Nov+SPI_1_Dec+SPI_1_Jan
 +SPI_1_Feb+SPI_1_Mar+SPI_1_Apr+SPI_1_May+SPI_1_Jun +SPI_1_Jul
 +SPI_1_Aug+SPI_3_Nov+SPI_3_Dec+SPI_3_Jan+SPI_3_Feb+SPI_3_Mar
 +SPI_3_Apr+SPI_3_May+SPI_3_Jun+SPI_3_Jul+SPI_3_Aug+SPI_6_Feb
 +SPI_6_Mar+SPI_6_Apr+SPI_6_May+SPI_6_Jun+SPI_6_Jul+SPI_6_Aug
 +PDSI_Sep+PDSI_Oct+PDSI_Nov+PDSI_Dec+PDSI_Jan+PDSI_Feb
 +PDSI_Mar+PDSI_Apr+PDSI_May+PDSI_Jun+PDSI_Jul+PDSI_Aug+Z_Sep
 +Z_Oct+Z_Nov+Z_Dec+Z_Jan+Z_Feb +Z_Mar+Z_Apr+Z_May +Z_Jun+Z_Jul
 +Z_Aug, data=t1)}

cum_var <- cumsum(pc$sdev^2)/sum(pc$sdev^2)

num = 1
while (num < length(cum_var))
{
   if (cum_var[num]> 0.9)
      break
  else
      num=num+1
}

z<-data.frame(z1=pc$score[,1])

for (znum in (2:num))
{
  z1=data.frame(z, zrow=pc$score[,znum])
  z=z1
 }

pc_t1<-data.frame(z,Y=t1$Yield)
zlm<-lm(Y~.,data=pc_t1)

Resummary<-summary(zlm)
R1<-Resummary$r.squared
tMBE1<-mean(predict.lm(zlm)-t1$Yield)
tRMSE1<-sqrt(mean((predict.lm(zlm)-t1$Yield)^2))
```

```
        cali_num=cali_num+1
        tMBE=tMBE+tMBE1
        tRMSE=tRMSE+tRMSE1
        R=R+R1

## validation ##

 if (nrow(v1)>0)
 {
    if (st=="Stage1 April")
    {validation<-data.frame(SPI_1_Sep=v1$SPI_1_Sep, SPI_1_Oct=v1$SPI_1_Oct,
    SPI_1_Nov=v1$SPI_1_Nov,SPI_1_Dec=v1$SPI_1_Dec,SPI_1_Jan=v1$SPI_1_Jan,
    SPI_1_Feb=v1$SPI_1_Feb,SPI_1_Mar=v1$SPI_1_Mar, SPI_3_Nov=v1$SPI_3_Nov,
    SPI_3_Dec=v1$SPI_3_Dec,SPI_3_Jan=v1$SPI_3_Jan,SPI_3_Feb=v1$SPI_3_Feb,
    SPI_3_Mar=v1$SPI_3_Mar,SPI_6_Feb=v1$SPI_6_Feb,SPI_6_Mar=v1$SPI_6_Mar,
    PDSI_Nov=v1$PDSI_Nov, PDSI_Dec=v1$PDSI_Dec,PDSI_Jan=v1$PDSI_Jan,
    PDSI_Feb=v1$PDSI_Feb,PDSI_Mar=v1$PDSI_Mar,Z_Sep=v1$Z_Sep,
    Z_Oct=v1$Z_Oct, Z_Nov=v1$Z_Nov, Z_Dec=v1$Z_Dec, Z_Jan=v1$Z_Jan,
    Z_Feb=v1$Z_Feb, Z_Mar=v1$Z_Mar)}

    if (st=="Stage2 May")
    {validation<-data.frame(SPI_1_Sep=v1$SPI_1_Sep, SPI_1_Oct=v1$SPI_1_Oct,
    SPI_1_Nov=v1$SPI_1_Nov,SPI_1_Dec=v1$SPI_1_Dec,SPI_1_Jan=v1$SPI_1_Jan,
    SPI_1_Feb=v1$SPI_1_Feb,SPI_1_Mar=v1$SPI_1_Mar, SPI_1_Apr=v1$SPI_1_Apr,
    SPI_3_Nov=v1$SPI_3_Nov, SPI_3_Dec=v1$SPI_3_Dec,SPI_3_Jan=v1$SPI_3_Jan,
    SPI_3_Feb=v1$SPI_3_Feb,SPI_3_Mar=v1$SPI_3_Mar,SPI_3_Apr=v1$SPI_3_Apr,
    SPI_6_Feb=v1$SPI_6_Feb, SPI_6_Mar=v1$SPI_6_Mar,SPI_6_Apr=v1$SPI_6_Apr,
    PDSI_Sep=v1$PDSI_Sep,PDSI_Oct=v1$PDSI_Oct, PDSI_Nov=v1$PDSI_Nov,
    PDSI_Dec=v1$PDSI_Dec, PDSI_Jan=v1$PDSI_Jan,PDSI_Feb=v1$PDSI_Feb,
    PDSI_Mar=v1$PDSI_Mar,PDSI_Apr=v1$PDSI_Apr,Z_Sep=v1$Z_Sep,
    Z_Oct=v1$Z_Oct,Z_Nov=v1$Z_Nov,Z_Dec=v1$Z_Dec ,Z_Jan=v1$Z_Jan,
    Z_Feb=v1$Z_Feb,Z_Mar=v1$Z_Mar,Z_Apr=v1$Z_Apr)}

    if (st=="Stage3 June")
    {validation<-data.frame(SPI_1_Sep=v1$SPI_1_Sep,SPI_1_Oct=v1$SPI_1_Oct,
    SPI_1_Nov=v1$SPI_1_Nov,SPI_1_Dec=v1$SPI_1_Dec,SPI_1_Jan=v1$SPI_1_Jan,
    SPI_1_Feb=v1$SPI_1_Feb,SPI_1_Mar=v1$SPI_1_Mar,SPI_1_Apr=v1$SPI_1_Apr,
    SPI_1_May=v1$SPI_1_May,SPI_3_Nov=v1$SPI_3_Nov,SPI_3_Dec=v1$SPI_3_Dec,
    SPI_3_Jan=v1$SPI_3_Jan,SPI_3_Feb=v1$SPI_3_Feb ,SPI_3_Mar=v1$SPI_3_Mar,
    SPI_3_Apr=v1$SPI_3_Apr,SPI_3_May=v1$SPI_3_May,SPI_6_Feb=v1$SPI_6_Feb,
    SPI_6_Mar=v1$SPI_6_Mar,SPI_6_Apr=v1$SPI_6_Apr,SPI_6_May=v1$SPI_6_May,
    PDSI_Sep=v1$PDSI_Sep,PDSI_Oct=v1$PDSI_Oct,PDSI_Nov=v1$PDSI_Nov,
    PDSI_Dec=v1$PDSI_Dec,PDSI_Jan=v1$PDSI_Jan,PDSI_Feb=v1$PDSI_Feb,
    PDSI_Mar=v1$PDSI_Mar,PDSI_Apr=v1$PDSI_Apr, PDSI_May=v1$PDSI_May
    Z_Sep=v1$Z_Sep,Z_Oct=v1$Z_Oct,Z_Nov=v1$Z_Nov,Z_Dec=v1$Z_Dec,
```

```
Z_Jan=v1$Z_Jan,Z_Feb=v1$Z_Feb,Z_Mar=v1$Z_Mar,Z_Apr=v1$Z_Apr,
Z_May=v1$Z_May)}

if (st=="Stage4 July")
{validation<-data.frame(SPI_1_Sep=v1$SPI_1_Sep,SPI_1_Oct=v1$SPI_1_Oct,
SPI_1_Nov=v1$SPI_1_Nov,SPI_1_Dec=v1$SPI_1_Dec,SPI_1_Jan=v1$SPI_1_Jan,
SPI_1_Feb=v1$SPI_1_Feb,SPI_1_Mar=v1$SPI_1_Mar,SPI_1_Apr=v1$SPI_1_Apr,
SPI_1_May=v1$SPI_1_May,SPI_1_Jun=v1$SPI_1_Jun,SPI_3_Nov=v1$SPI_3_Nov,
SPI_3_Dec=v1$SPI_3_Dec,SPI_3_Jan=v1$SPI_3_Jan,SPI_3_Feb=v1$SPI_3_Feb,
SPI_3_Mar=v1$SPI_3_Mar,SPI_3_Apr=v1$SPI_3_Apr,SPI_3_May=v1$SPI_3_May,
SPI_3_Jun=v1$SPI_3_Jun,SPI_6_Feb=v1$SPI_6_Feb,SPI_6_Mar=v1$SPI_6_Mar,
SPI_6_Apr=v1$SPI_6_Apr,SPI_6_May=v1$SPI_6_May ,SPI_6_Jun=v1$SPI_6_Jun,
PDSI_Sep=v1$PDSI_Sep,PDSI_Oct=v1$PDSI_Oct,PDSI_Nov=v1$PDSI_Nov,
PDSI_Dec=v1$PDSI_Dec,PDSI_Jan=v1$PDSI_Jan,PDSI_Feb=v1$PDSI_Feb,
PDSI_Mar=v1$PDSI_Mar,PDSI_Apr=v1$PDSI_Apr,PDSI_May=v1$PDSI_May,
PDSI_Jun=v1$PDSI_Jun,Z_Sep=v1$Z_Sep,Z_Oct=v1$Z_Oct,Z_Nov=v1$Z_Nov,
Z_Dec=v1$Z_Dec,Z_Jan=v1$Z_Jan,Z_Feb=v1$Z_Feb,Z_Mar=v1$Z_Mar,
Z_Apr=v1$Z_Apr,Z_May=v1$Z_May,Z_Jun=v1$Z_Jun)}

if (st=="Stage5 August")
{validation<-data.frame(SPI_1_Sep=v1$SPI_1_Sep,SPI_1_Oct=v1$SPI_1_Oct,
 SPI_1_Nov=v1$SPI_1_Nov,SPI_1_Dec=v1$SPI_1_Dec,SPI_1_Jan=v1$SPI_1_Jan,
 SPI_1_Feb=v1$SPI_1_Feb,SPI_1_Mar=v1$SPI_1_Mar,SPI_1_Apr=v1$SPI_1_Apr,
 SPI_1_May=v1$SPI_1_May,SPI_1_Jun=v1$SPI_1_Jun,SPI_1_Jul=v1$SPI_1_Jul,
 SPI_3_Nov=v1$SPI_3_Nov,SPI_3_Dec=v1$SPI_3_Dec,SPI_3_Jan=v1$SPI_3_Jan,
 SPI_3_Feb=v1$SPI_3_Feb,SPI_3_Mar=v1$SPI_3_Mar,SPI_3_Apr=v1$SPI_3_Apr,
 SPI_3_May=v1$SPI_3_May,SPI_3_Jun=v1$SPI_3_Jun,SPI_3_Jul=v1$SPI_3_Jul,
 SPI_6_Feb=v1$SPI_6_Feb,SPI_6_Mar=v1$SPI_6_Mar,SPI_6_Apr=v1$SPI_6_Apr,
 SPI_6_May=v1$SPI_6_May,SPI_6_Jun=v1$SPI_6_Jun,SPI_6_Jul=v1$SPI_6_Jul,
 PDSI_Sep=v1$PDSI_Sep,PDSI_Oct=v1$PDSI_Oct,PDSI_Nov=v1$PDSI_Nov,
 PDSI_Dec=v1$PDSI_Dec,PDSI_Jan=v1$PDSI_Jan,PDSI_Feb=v1$PDSI_Feb,
 PDSI_Mar=v1$PDSI_Mar,PDSI_Apr=v1$PDSI_Apr, PDSI_May=v1$PDSI_May,
 PDSI_Jun=v1$PDSI_Jun,PDSI_Jul=v1$PDSI_Jul,Z_Sep=v1$Z_Sep,
 Z_Oct=v1$Z_Oct, Z_Nov=v1$Z_Nov,Z_Dec=v1$Z_Dec ,Z_Jan=v1$Z_Jan,
 Z_Feb=v1$Z_Feb,Z_Mar=v1$Z_Mar,Z_Apr=v1$Z_Apr ,Z_May=v1$Z_May,
 Z_Jun=v1$Z_Jun,Z_Jul=v1$Z_Jul)}

if (st=="Stage6 September")
{validation<-data.frame(SPI_1_Sep=v1$SPI_1_Sep,SPI_1_Oct=v1$SPI_1_Oct,
 SPI_1_Nov=v1$SPI_1_Nov,SPI_1_Dec=v1$SPI_1_Dec,SPI_1_Jan=v1$SPI_1_Jan,
 SPI_1_Feb=v1$SPI_1_Feb,SPI_1_Mar=v1$SPI_1_Mar,SPI_1_Apr=v1$SPI_1_Apr,
 SPI_1_May=v1$SPI_1_May,SPI_1_Jun=v1$SPI_1_Jun,SPI_1_Jul=v1$SPI_1_Jul,
 SPI_1_Aug=v1$SPI_1_Aug,SPI_3_Nov=v1$SPI_3_Nov,SPI_3_Dec=v1$SPI_3_Dec,
 SPI_3_Jan=v1$SPI_3_Jan,SPI_3_Feb=v1$SPI_3_Feb,SPI_3_Mar=v1$SPI_3_Mar,
 SPI_3_Apr=v1$SPI_3_Apr,SPI_3_May=v1$SPI_3_May,SPI_3_Jun=v1$SPI_3_Jun,
 SPI_3_Jul=v1$SPI_3_Jul,SPI_3_Aug=v1$SPI_3_Aug ,SPI_6_Feb=v1$SPI_6_Feb,
```

```
SPI_6_Mar=v1$SPI_6_Mar,SPI_6_Apr=v1$SPI_6_Apr,SPI_6_May=v1$SPI_6_May,
SPI_6_Jun=v1$SPI_6_Jun,SPI_6_Jul=v1$SPI_6_Jul,SPI_6_Aug=v1$SPI_6_Aug,
PDSI_Sep=v1$PDSI_Sep,PDSI_Oct=v1$PDSI_Oct,PDSI_Nov=v1$PDSI_Nov,
PDSI_Dec=v1$PDSI_Dec,PDSI_Jan=v1$PDSI_Jan,PDSI_Feb=v1$PDSI_Feb,
PDSI_Mar=v1$PDSI_Mar,PDSI_Apr=v1$PDSI_Apr, PDSI_May=v1$PDSI_May,
PDSI_Jun=v1$PDSI_Jun,PDSI_Jul=v1$PDSI_Jul,PDSI_Aug=v1$PDSI_Aug,
Z_Sep=v1$Z_Sep,Z_Oct=v1$Z_Oct,Z_Nov=v1$Z_Nov,Z_Dec=v1$Z_Dec,
Z_Jan=v1$Z_Jan,Z_Feb=v1$Z_Feb,Z_Mar=v1$Z_Mar,Z_Apr=v1$Z_Apr,
Z_May=v1$Z_May,Z_Jun=v1$Z_Jun,Z_Jul=v1$Z_Jul,Z_Aug=v1$Z_Aug)}

        pred<-predict(pc,newdata=validation)

        z<-data.frame(z1=pred[,1])
        for (znum in (2:num))
        {
          z1=data.frame(z, zrow=pred[,znum])
          z=z1
        }

        newpredict<-data.frame(z)
        valm<-predict.lm(zlm, newdata=newpredict)

        vMBE1<-mean(valm-v1$Yield)
        vRMSE1<-sqrt(mean((valm-v1$Yield)^2))

        vMBE=vMBE+vMBE1
        vRMSE=vRMSE+vRMSE1
        vali_num=vali_num+1
      }
  }

       t_MBE=round(tMBE/cali_num,2)
       t_RMSE=round(tRMSE/cali_num,2)
      v_MBE=round(vMBE/vali_num,2)
      v_RMSE=round(vRMSE/vali_num,2)
      R_2=round(R/cali_num,2)

      results<-data.frame(stage=st, R2=R_2,cali_MBE=t_MBE, vali_MBE=v_MBE,
                          vali_RMSE=v_RMSE)

      setwd("F:\\ADRA Model\\Model Development\\results")
      name=paste(cluster, st, sep="_")
      name=paste(name, ".csv", sep="")
      write.table(results, name, col.names=T, append=F, na = "NA", row.names = F, sep=",")
}
```

```
for (cluster in (1:9))
{
        setwd("F:\\ADRA Model\\Model Preparation")
        name = paste("c", cluster, sep="")
        infile_name = paste(name, "_without outlier.csv", sep="")
        stage<-read.table(infile_name, sep=",", head=T)
        pre<-data.frame(CAR=stage$CAR, Year=stage$Year, Month=stage$Month,
            SPI_1=stage$SPI_1, SPI_3=stage$SPI_3, SPI_6=stage$SPI_6,
            PDSI=stage$PDSI, Z=stage$Z, Yield=stage$zdYield)

        indices<-data.frame(SPI_1_Sep=pre$SPI_1[pre$Month==9],
        SPI_1_Oct=pre$SPI_1[pre$Month==10], SPI_1_Nov=pre$SPI_1[pre$Month==11],
        SPI_1_Dec=pre$SPI_1[pre$Month==12], SPI_1_Jan=pre$SPI_1[pre$Month==1],
        SPI_1_Feb=pre$SPI_1[pre$Month==2], SPI_1_Mar=pre$SPI_1[pre$Month==3],
        SPI_1_Apr=pre$SPI_1[pre$Month==4], SPI_1_May=pre$SPI_1[pre$Month==5],
        SPI_1_Jun=pre$SPI_1[pre$Month==6], SPI_1_Jul=pre$SPI_1[pre$Month==7],
        SPI_1_Aug=pre$SPI_1[pre$Month==8], SPI_3_Nov=pre$SPI_3[pre$Month==11],
        SPI_3_Dec=pre$SPI_3[pre$Month==12], SPI_3_Jan=pre$SPI_3[pre$Month==1],
        SPI_3_Feb=pre$SPI_3[pre$Month==2], SPI_3_Mar=pre$SPI_3[pre$Month==3],
        SPI_3_Apr=pre$SPI_3[pre$Month==4], SPI_3_May=pre$SPI_3[pre$Month==5],
        SPI_3_Jun=pre$SPI_3[pre$Month==6], SPI_3_Jul=pre$SPI_3[pre$Month==7],
        SPI_3_Aug=pre$SPI_3[pre$Month==8], SPI_6_Feb=pre$SPI_6[pre$Month==2],
        SPI_6_Mar=pre$SPI_6[pre$Month==3], SPI_6_Apr=pre$SPI_6[pre$Month==4],
        SPI_6_May=pre$SPI_6[pre$Month==5], SPI_6_Jun=pre$SPI_6[pre$Month==6],
        SPI_6_Jul=pre$SPI_6[pre$Month==7], SPI_6_Aug=pre$SPI_6[pre$Month==8],
        PDSI_Sep=pre$PDSI[pre$Month==9], PDSI_Oct=pre$PDSI[pre$Month==10],
        PDSI_Nov=pre$PDSI[pre$Month==11], PDSI_Dec=pre$PDSI[pre$Month==12],
        PDSI_Jan=pre$PDSI[pre$Month==1], PDSI_Feb=pre$PDSI[pre$Month==2],
        PDSI_Mar=pre$PDSI[pre$Month==3], PDSI_Apr=pre$PDSI[pre$Month==4],
        PDSI_May=pre$PDSI[pre$Month==5], PDSI_Jun=pre$PDSI[pre$Month==6],
        PDSI_Jul=pre$PDSI[pre$Month==7], PDSI_Aug=pre$PDSI[pre$Month==8],
        Z_Sep=pre$Z[pre$Month==9], Z_Oct=pre$Z[pre$Month==10], Z_Nov=pre$Z
        [pre$Month==11], Z_Dec=pre$Z[pre$Month==12], Z_Jan=pre$Z[pre$Month==1],
        Z_Feb=pre$Z[pre$Month==2], Z_Mar=pre$Z[pre$Month==3], Z_Apr=pre$Z
        [pre$Month==4], Z_May=pre$Z[pre$Month==5], Z_Jun=pre$Z[pre$Month==6],
        Z_Jul=pre$Z[pre$Month==7], Z_Aug=pre$Z[pre$Month==8], CAR=pre$CAR
        [pre$Month==6], Year=pre$Year[pre$Month==6], Yield=pre$Yield[pre$Month==6])

        model(name,"Stage1 April", indices)
        model(name,"Stage2 May", indices)
        model(name,"Stage3 June", indices)
        model(name,"Stage4 July", indices)
        model(name,"Stage5 August", indices)
        model(name,"Stage6 September", indices)

}
```

APPENDIX B: Confusion Matrices for Predictions of Nine Clusters

C1		Predicted				
Stage1		Normal	Mild	Moderate	Severe	Extreme
Actual	Normal	66	23	4	1	0
	Mild	11	5	2	0	0
	Moderate	8	5	2	0	0
	Severe	2	0	0	0	0
	Extreme	5	0	0	0	0
Stage 2		Normal	Mild	Moderate	Severe	Extreme
Actual	Normal	66	21	7	0	0
	Mild	11	4	3	0	0
	Moderate	6	7	2	0	0
	Severe	2	0	0	0	0
	Extreme	5	0	0	0	0
Stage 3		Normal	Mild	Moderate	Severe	Extreme
Actual	Normal	73	11	8	2	0
	Mild	11	4	3	0	0
	Moderate	9	5	1	0	0
	Severe	0	2	0	0	0
	Extreme	5	0	0	0	0
Stage 4		Normal	Mild	Moderate	Severe	Extreme
Actual	Normal	72	13	9	0	0
	Mild	12	4	2	0	0
	Moderate	4	6	5	0	0
	Severe	1	0	1	0	0
	Extreme	1	4	0	0	0
Stage 5		Normal	Mild	Moderate	Severe	Extreme
Actual Category	Normal	73	13	7	1	0
	Mild	10	5	3	0	0
	Moderate	2	8	4	1	0
	Severe	0	1	0	1	0
	Extreme	0	1	4	0	0
Stage 6		Normal	Mild	Moderate	Severe	Extreme
Actual	Normal	73	15	5	1	0
	Mild	6	9	3	0	0
	Moderate	3	7	4	1	0

	Severe	0	1	0	1	0
	Extreme	0	1	4	0	0

C2		Predicted				
Stage1		Normal	Mild	Moderate	Severe	Extreme
Actual	Normal	21	7	5	0	0
	Mild	6	2	0	0	0
	Moderate	3	1	1	0	0
	Severe	2	0	1	0	0
	Extreme	2	0	1	0	0
Stage 2		Normal	Mild	Moderate	Severe	Extreme
Actual	Normal	20	9	4	0	0
	Mild	7	1	0	0	0
	Moderate	2	3	0	0	0
	Severe	2	0	1	0	0
	Extreme	1	1	1	0	0
Stage 3		Normal	Mild	Moderate	Severe	Extreme
Actual	Normal	22	9	2	0	0
	Mild	6	2	0	0	0
	Moderate	2	1	1	1	0
	Severe	1	1	1	0	0
	Extreme	0	2	0	1	0
Stage 4		Normal	Mild	Moderate	Severe	Extreme
Actual	Normal	25	5	3	0	0
	Mild	5	3	0	0	0
	Moderate	1	1	3	0	0
	Severe	0	3	0	0	0
	Extreme	0	1	1	1	0
Stage 5		Normal	Mild	Moderate	Severe	Extreme
Actual Category	Normal	26	6	1	0	0
	Mild	3	3	2	0	0
	Moderate	1	0	4	0	0
	Severe	0	2	1	0	0
	Extreme	0	0	2	1	0
Stage 6		Normal	Mild	Moderate	Severe	Extreme
Actual	Normal	24	7	2	0	0
	Mild	3	3	2	0	0

	Moderate	1	0	4	0	0
	Severe	0	2	1	0	0
	Extreme	0	1	1	1	0

C3		Predicted				
Stage1		Normal	Mild	Moderate	Severe	Extreme
Actual	Normal	25	9	2	0	0
	Mild	1	2	2	0	0
	Moderate	5	2	0	0	0
	Severe	1	1	2	0	0
	Extreme	0	3	0	0	0
Stage 2		Normal	Mild	Moderate	Severe	Extreme
Actual	Normal	28	6	2	0	0
	Mild	2	1	2	0	0
	Moderate	2	3	2	0	0
	Severe	1	0	3	0	0
	Extreme	0	1	2	0	0
Stage 3		Normal	Mild	Moderate	Severe	Extreme
Actual	Normal	28	7	1	0	0
	Mild	2	1	2	0	0
	Moderate	2	3	2	0	0
	Severe	1	0	1	2	0
	Extreme	0	1	2	0	0
Stage 4		Normal	Mild	Moderate	Severe	Extreme
Actual	Normal	31	4	1	0	0
	Mild	2	0	3	0	0
	Moderate	1	4	2	0	0
	Severe	0	2	1	1	0
	Extreme	0	0	1	2	0
Stage 5		Normal	Mild	Moderate	Severe	Extreme
Actual	Normal	29	6	1	0	0
	Mild	1	1	2	1	0
	Moderate	0	3	3	1	0
	Severe	0	0	2	2	0
	Extreme	0	1	0	2	0
Stage 6		Normal	Mild	Moderate	Severe	Extreme
Actual	Normal	30	6	0	0	0

	Mild	1	3	1	0	0
	Moderate	0	3	4	0	0
	Severe	0	0	2	2	0
	Extreme	0	1	0	2	0

C4		Predicted				
Stage1		Normal	Mild	Moderate	Severe	Extreme
Actual	Normal	73	16	10	0	0
	Mild	7	4	2	0	0
	Moderate	8	2	3	0	0
	Severe	3	2	0	0	0
	Extreme	3	3	2	0	0
Stage 2		Normal	Mild	Moderate	Severe	Extreme
Actual	Normal	76	16	6	1	0
	Mild	6	4	2	1	0
	Moderate	7	3	1	2	0
	Severe	2	3	0	0	0
	Extreme	3	3	2	0	0
Stage 3		Normal	Mild	Moderate	Severe	Extreme
Actual	Normal	79	13	6	1	0
	Mild	6	3	4	0	0
	Moderate	7	3	2	1	0
	Severe	2	1	2	0	0
	Extreme	1	2	1	4	0
Stage 4		Normal	Mild	Moderate	Severe	Extreme
Actual	Normal	75	21	3	0	0
	Mild	4	5	3	1	0
	Moderate	5	3	3	2	0
	Severe	2	0	0	3	0
	Extreme	0	1	3	4	0
Stage 5		Normal	Mild	Moderate	Severe	Extreme
Actual Category	Normal	77	17	5	0	0
	Mild	4	4	5	0	0
	Moderate	2	4	4	3	0
	Severe	0	2	1	2	0
	Extreme	0	0	1	7	0
Stage 6		Normal	Mild	Moderate	Severe	Extreme

Actual	Normal	73	19	7	0	0
	Mild	4	2	7	0	0
	Moderate	2	5	5	1	0
	Severe	0	1	4	0	0
	Extreme	0	0	1	5	2

C5

Stage1		Predicted				
		Normal	Mild	Moderate	Severe	Extreme
Actual	Normal	33	12	4	1	0
	Mild	12	1	0	0	0
	Moderate	6	2	0	0	0
	Severe	4	0	0	0	0
	Extreme	4	0	0	0	0
Stage 2		Normal	Mild	Moderate	Severe	Extreme
Actual	Normal	28	20	2	0	0
	Mild	13	0	0	0	0
	Moderate	7	1	0	0	0
	Severe	4	0	0	0	0
	Extreme	4	0	0	0	0
Stage 3		Normal	Mild	Moderate	Severe	Extreme
Actual	Normal	27	19	4	0	0
	Mild	12	1	0	0	0
	Moderate	7	0	1	0	0
	Severe	4	0	0	0	0
	Extreme	4	0	0	0	0
Stage 4		Normal	Mild	Moderate	Severe	Extreme
Actual	Normal	35	9	5	1	0
	Mild	7	5	1	0	0
	Moderate	3	3	2	0	0
	Severe	3	0	1	0	0
	Extreme	3	1	0	0	0
Stage 5		Normal	Mild	Moderate	Severe	Extreme
Actual Category	Normal	38	6	5	1	0
	Mild	7	5	1	0	0
	Moderate	4	2	2	0	0
	Severe	2	1	1	0	0
	Extreme	1	3	0	0	0

Stage 6		Normal	Mild	Moderate	Severe	Extreme
Actual	Normal	37	6	4	3	0
	Mild	7	4	1	1	0
	Moderate	4	0	4	0	0
	Severe	2	1	1	0	0
	Extreme	2	2	0	0	0

C6		Predicted				
Stage1		Normal	Mild	Moderate	Severe	Extreme
Actual	Normal	67	22	7	2	0
	Mild	8	5	3	0	0
	Moderate	4	1	1	0	0
	Severe	2	3	0	0	0
	Extreme	7	3	0	0	0
Stage 2		Normal	Mild	Moderate	Severe	Extreme
Actual	Normal	68	19	7	4	0
	Mild	9	5	2	0	0
	Moderate	5	0	1	0	0
	Severe	2	3	0	0	0
	Extreme	7	3	0	0	0
Stage 3		Normal	Mild	Moderate	Severe	Extreme
Actual	Normal	69	20	7	2	0
	Mild	7	4	4	1	0
	Moderate	4	2	0	0	0
	Severe	1	2	2	0	0
	Extreme	5	5	0	0	0
Stage 4		Normal	Mild	Moderate	Severe	Extreme
Actual	Normal	73	15	10	0	0
	Mild	7	2	7	0	0
	Moderate	3	1	2	0	0
	Severe	0	1	4	0	0
	Extreme	0	6	4	0	0
Stage 5		Normal	Mild	Moderate	Severe	Extreme
Actual Category	Normal	79	16	3	0	0
	Mild	5	6	4	1	0
	Moderate	0	3	2	1	0
	Severe	0	0	3	2	0

	Extreme	0	1	6	3	0
Stage 6		Normal	Mild	Moderate	Severe	Extreme
Actual	Normal	80	13	5	0	0
	Mild	6	4	5	1	0
	Moderate	1	2	2	1	0
	Severe	0	0	3	2	0
	Extreme	0	0	8	2	0

C7		Predicted				
Stage1		Normal	Mild	Moderate	Severe	Extreme
Actual	Normal	46	17	4	0	0
	Mild	15	2	1	0	0
	Moderate	6	1	1	0	0
	Severe	7	2	0	0	0
	Extreme	3	0	1	0	0
Stage 2		Normal	Mild	Moderate	Severe	Extreme
Actual	Normal	48	13	5	1	0
	Mild	12	6	0	0	0
	Moderate	5	2	1	0	0
	Severe	6	3	0	0	0
	Extreme	3	0	1	0	0
Stage 3		Normal	Mild	Moderate	Severe	Extreme
Actual	Normal	49	11	4	3	0
	Mild	11	5	2	0	0
	Moderate	4	2	2	0	0
	Severe	6	3	0	0	0
	Extreme	3	1	0	0	0
Stage 4		Normal	Mild	Moderate	Severe	Extreme
Actual	Normal	54	6	7	0	0
	Mild	8	9	1	0	0
	Moderate	0	3	4	1	0
	Severe	5	2	2	0	0
	Extreme	1	2	1	0	0
Stage 5		Normal	Mild	Moderate	Severe	Extreme
Actual Category	Normal	54	10	3	0	0
	Mild	6	7	5	0	0
	Moderate	0	2	6	0	0

	Severe	1	3	4	1	0
	Extreme	1	1	2	0	0
Stage 6		Normal	Mild	Moderate	Severe	Extreme
Actual	Normal	55	9	3	0	0
	Mild	5	9	4	0	0
	Moderate	0	3	5	0	0
	Severe	1	1	6	1	0
	Extreme	1	1	2	0	0

C8		Predicted				
Stage1		Normal	Mild	Moderate	Severe	Extreme
Actual	Normal	36	6	4	0	0
	Mild	8	2	0	0	0
	Moderate	3	0	2	0	0
	Severe	0	1	1	0	0
	Extreme	3	1	0	0	0
Stage 2		Normal	Mild	Moderate	Severe	Extreme
Actual	Normal	37	6	1	2	0
	Mild	10	0	0	0	0
	Moderate	3	1	1	0	0
	Severe	1	1	0	0	0
	Extreme	3	1	0	0	0
Stage 3		Normal	Mild	Moderate	Severe	Extreme
Actual	Normal	33	10	3	0	0
	Mild	7	2	1	0	0
	Moderate	4	0	1	0	0
	Severe	0	0	1	0	1
	Extreme	4	0	0	0	0
Stage 4		Normal	Mild	Moderate	Severe	Extreme
Actual	Normal	41	4	1	0	0
	Mild	7	3	0	0	0
	Moderate	3	1	0	1	0
	Severe	0	0	0	0	2
	Extreme	2	2	0	0	0
Stage 5		Normal	Mild	Moderate	Severe	Extreme
Actual Category	Normal	39	6	1	0	0
	Mild	6	4	0	0	0

	Moderate	2	2	0	1	0
	Severe	0	0	0	0	2
	Extreme	1	3	0	0	0
Stage 6		Normal	Mild	Moderate	Severe	Extreme
Actual	Normal	39	4	3	0	0
	Mild	5	4	1	0	0
	Moderate	2	1	2	0	0
	Severe	0	0	0	1	1
	Extreme	1	2	1	0	0

C9		Predicted				
Stage1		Normal	Mild	Moderate	Severe	Extreme
Actual	Normal	66	13	1	0	0
	Mild	12	4	0	0	0
	Moderate	9	0	0	0	0
	Severe	4	0	0	0	0
	Extreme	3	0	0	0	0
Stage 2		Normal	Mild	Moderate	Severe	Extreme
Actual	Normal	69	8	3	0	0
	Mild	14	2	0	0	0
	Moderate	9	0	0	0	0
	Severe	4	0	0	0	0
	Extreme	3	0	0	0	0
Stage 3		Normal	Mild	Moderate	Severe	Extreme
Actual	Normal	71	9	0	0	0
	Mild	14	2	0	0	0
	Moderate	8	1	0	0	0
	Severe	2	2	0	0	0
	Extreme	3	0	0	0	0
Stage 4		Normal	Mild	Moderate	Severe	Extreme
Actual	Normal	66	12	2	0	0
	Mild	13	2	1	0	0
	Moderate	7	1	1	0	0
	Severe	1	1	2	0	0
	Extreme	2	1	0	0	0
Stage 5		Normal	Mild	Moderate	Severe	Extreme
Actual	Normal	65	13	2	0	0

Category	Mild	15	0	1	0	0
	Moderate	6	2	0	1	0
	Severe	1	1	1	1	0
	Extreme	1	2	0	0	0
Stage 6		Normal	Mild	Moderate	Severe	Extreme
Actual	Normal	70	6	4	0	0
	Mild	14	1	1	0	0
	Moderate	7	1	0	1	0
	Severe	1	3	0	0	0
	Extreme	0	2	1	0	0